Role of ABA-induced Ca^{2+} signals, and the Ca^{2+}-controlled protein kinase CIPK23, in regulation of stomatal movements

(Rolle von ABA-abhängigen Ca^{2+} Signalen, und der Ca^{2+}-gesteuerten Proteinkinase CIPK23, bei der Regulation der Spaltöffnungsbewegungen)

Dissertation on the attainment of a doctorate in natural sciences
Julius-Maximilians-Universität Würzburg,

submitted by

Shouguang Huang

from

Guangxi, People's Republic of China

Würzburg 2020

Submitted on: …….……..

Office stamp

Members of the *Promotions committee*:

Chairperson: …….....

Primary referee: PD. Dr. M. Rob G. Roelfsema

Second referee: PD. Dr. Frank Waller

Date of Public Defence: …….……

Date of Receipt of Certificates: …….

Contents

Summary IV

Zusammenfassung VI

Glossary VIII

List of figures and tables X

1. Introduction 1

1.1 Function of stomata 1

1.2 Ion fluxes cause stomatal movements 2

1.3 H^+-ATPase 4

1.4 K^+ transport across the plasma membrane of guard cells 7

1.4.1 Inward K^+ channels 8

1.4.2 Outward K^+ channels 10

1.5 Anion transport in the plasma membrane of guard cells 12

1.5.1 S-type anion channels 12

1.5.2 R-type anion channels 15

1.6 Ca^{2+} transport in guard cells 17

1.7 ABA signaling transduction in guard cells 19

1.7.1 ABA receptors 21

1.7.2 Type 2C protein phosphatases 22

1.7.3 Ca^{2+}-independent protein kinases 23

1.7.4 Ca^{2+}-dependent protein kinases 26

1.7.5 The agricultural application 29

2. Material and methods 32

2.1 Plant material and growth conditions 32

2.2 Electrophysiological recording in guard cells 33

2.2.1 The two-electrode voltage clamp technique 33

2.2.2 Voltage clamp recordings in guard cells 33

2.3 Current ejection technique 35

2.3.1 Application of ABA to single guard cell in intact leaves 36

2.3.2 Estimation of the ABA concentration on the guard cell wall after current ejection37

2.4 Live-cell imaging of guard cell Ca^{2+} signals in intact leaves 38

2.4.1 Acquisition of Ca^{2+} signals from R-GECO1-mTurquoise 38

2.4.2 Calibration of R-GECO1-mTurquoise 39

2.4.3 Calibration of FURA2 39

2.5 Estrogen-induced guard cell specific expression system 40

2.5.1 The inducible constructs 40

2.5.2 *Arabidopsis* transformation and screening 42

2.5.3 Induction of gene expression with estrogen 42

2.5.4 Quantification of transcript levels in estrogen-treated guard cells 43

2.5.5 Confocal microscopy 44

2.6 Stomatal aperture assays and gas exchange measurements 44

2.7 The heterologous expression system of *Xenopus laevis* oocyte 45

2.7.1 cRNA generation for expression studies with oocytes 45

2.7.2 Oocyte voltage clamp recordings 45

3. Results 47

3.1 ABA-induced Ca^{2+} signals accelerate stomatal closure 47

3.1.1 Current-ejected ABA triggers single guard cell movement 47

3.1.2 Quantification of ABA concentrations evoked by current ejection. 48

3.1.3 Calibration of R-GECO1-mTurquoise in guard cells 50

3.1.4 ABA-induced guard cell responses split up in three groups 53

3.1.5 ABA-induced Ca^{2+} signals speed up stomatal closure 55

3.1.6 Elevated cytosolic Ca^{2+} levels activate the S-type anion channels SLAC1 and SLAH3 56

3.1.7 Loss of OST1 impairs ABA-induced stomatal closure and -Ca^{2+} signals 58

3.1.8 Cytosolic Ca^{2+} signals trigger rapid activation of anion channels in *ost1-3* 59

3.2 CIPK23 inhibits stomatal closure 62

3.2.1 Expression of CIPK23 variants in guard cells 62

3.2.2 CIPK23 alters stomatal movements in response to light/darkness and ABA 64

3.2.3 CIPK23 enhances guard cell inward K^+ channel activity 67

3.2.4 Activation of AKT1 by CIPK23 does not depend on its protein kinase activity..... 70

3.2.5 CIPK23 inhibits guard cell S-type anion channel activity 72

3.2.6 $CIPK23^{T190D}$ fails to activate SLAC1 and SLAH3 in oocytes 75

3.2.7 $CIPK23^{T190D}$ suppresses CPK23- and CIPK11-activated SLAC1 78

4. Discussion 80

4.1 ABA-induced Ca^{2+} signals and stomatal closure 80

4.1.1 ABA-evoked Ca^{2+} signals are mainly caused by fast changes in osmotic content of guard cells 80

4.1.2 Ca^{2+} signals accelerate ABA-induced stomatal closure 82

4.1.3 Ca^{2+}-dependent activation of SLAC1 and SLAH3 anion channels 83

4.1.4 Outlook of Ca^{2+} signals in stomatal movements 84

4.2 The role of CIPK23 in stomatal movements 86

4.2.1 CIPK23 regulation of AKT1 does not affect stomatal movements 86

4.2.2 The activation of AKT1 by CIPK23 is independent of its kinase activity 87

4.2.3 CIPK23 inhibits the activity of S-type anion channels and stimulates stomatal opening 88

4.2.4 Inhibition of S-type anion channel activity in guard cells 89

4.2.5 Outlook of Ca^{2+}-dependent protein kinases and stomatal movements 92

5. References 94

6. Acknowledgments 109

7. Appendix 110

7.1 Primers 110

7.2 Publications 111

7.3 Affidavit 112

Summary

Stomata are pores in the leaf surface, formed by pairs of guard cells. The guard cells modulate the aperture of stomata, to balance uptake of CO_2 and loss of water vapor to the atmosphere. During drought, the phytohormone abscisic acid (ABA) provokes stomatal closure, via a signaling chain with both Ca^{2+}-dependent and Ca^{2+}-independent branches. Both branches are likely to activate SLAC1-type (Slow Anion Channel Associated 1) anion channels that are essential for initiating the closure of stomata. However, the importance of the Ca^{2+}-dependent signaling branch is still debated, as the core ABA signaling pathway only possesses Ca^{2+}-independent components. Therefore, the aim of this thesis was to address the role of the Ca^{2+}-dependent branch in the ABA signaling pathway of guard cells.

In the first part of the thesis, the relation between ABA-induced Ca^{2+} signals and stomatal closure was studied, with guard cells that express the genetically encoded Ca^{2+}-indicator R-GECO1-mTurquoise. Ejection of ABA into the guard cell wall rapidly induced stomatal closure, however, only in ¾ of the guard cells ABA evoked a cytosolic Ca^{2+} signal. A small subset of stomata (¼ of the experiments) closed without Ca^{2+} signals, showing that the Ca^{2+} signals are not essential for ABA-induced stomatal closure. However, stomata in which ABA evoked Ca^{2+} signals closed faster as those in which no Ca^{2+} signals were detected. Apparently, ABA-induced Ca^{2+} signals enhance the velocity of stomatal closure. In addition to ABA, hyperpolarizing voltage pulses could also trigger Ca^{2+} signals in wild type guard cells, which in turn activated S-type anion channels. However, these voltage pulses failed to elicit S-type anion currents in the *slac1/slah3* guard cells, suggesting that SLAC1 and SLAH3 contribute to Ca^{2+}-activated conductance. Taken together, our data indicate that ABA-induced Ca^{2+} signals enhance the activity of S-type anion channels, which accelerates stomatal closure.

The second part of the thesis deals with the signaling pathway downstream of the Ca^{2+} signals. Two types of Ca^{2+}-dependent protein kinase modules (CPKs and CBL/CIPKs) have been implicated in guard cells. We focused on the protein kinase CIPK23 (CBL-Interacting Protein Kinase 23), which is activated by the Ca^{2+}-dependent protein CBL1 or 9 (Calcineurin B-Like protein 1 or 9) via interacting with the NAF domain of CIPK23. The

CBL1/9-CIPK23 complex has been shown to affect stomatal movements, but the underlying molecular mechanisms remain largely unknown. We addressed this topic by using an estrogen-induced expression system, which specifically enhances the expression of wild type CIPK23, a phosphomimic CIPK23^{T190D} and a kinase dead CIPK23^{K60N} in guard cells. Our data show that guard cells expressing CIPK23^{T190D} promoted stomatal opening, while CIPK23^{K60N} enhanced ABA-induced stomatal closure, suggesting that CIPK23 is a negative regulator of stomatal closure. Electrophysiological measurements revealed that the inward K^+ channel currents were similar in guard cells that expressed CIPK23, CIPK23^{T190D} or CIPK23^{K60N}, indicating that CIPK23-mediated inward K^+ channel AKT1 does not contribute to stomatal movements. Expression of CIPK23^{K60N}, or loss of CIPK23 in guard cells enhanced S-type anion activity, while the active CIPK23^{T190D} inhibited the activity of these anion channels. These results are in line with the detected changes in stomatal movements and thus indicate that CIPK23 regulates stomatal movements by inhibiting S-type anion channels. CIPK23 thus serves as a brake to control anion channel activity. Overall, our findings demonstrate that CIPK23-mediated stomatal movements do not depend on CIPK23-AKT1 module, instead, it is achieved by regulating S-type anion channels SLAC1 and SLAH3.

In sum, the data presented in this thesis give new insights into the Ca^{2+}-dependent branch of ABA signaling, which may help to put forward new strategies to breed plants with enhanced drought stress tolerance, and in turn boost agricultural productivity in the future.

Zusammenfassung

Stomata sind Poren in der Blattoberfläche, die von einem Paar von Schließzellen gebildet werden. Die Schließzellen kontrollieren den Öffnungsweite der stomatären Pore, um die Aufnahme von CO_2 und den Verlust von Wasserdampf in die Atmosphäre auszubalancieren. Während Trockenperioden bewirkt das Phytohormon Abscisinsäure (ABA) einen Stomaschluss über eine Signalkaskade, welche über Ca^{2+}-abhängige und Ca^{2+}-unabhängige Pfade verfügt. Beide Pfade aktivieren wahrscheinlich Anionenkanäle aus der SLAC1 Familie (Slow Anion Channel Associated 1), welche essentiell sind um den Stomaschluss einzuleiten. Allerdings wird über die Wichtigkeit des Ca^{2+}-abhängigen Pfades noch immer diskutiert, da der ABA-Hauptsignalweg ausschließlich Ca^{2+}-unabhängige Komponenten beinhaltet. Aus diesem Grund war das Ziel dieser Thesis, die Rolle des Ca^{2+}-abhängigen Pfades im ABA-Signalweg aufzulösen.

Im ersten Teil der Thesis wurde mit Schließzellen, die den genetisch kodierten Ca^{2+}-Sensor R-GECO1-mTurquoise exprimierten, der Zusammenhang zwischen ABA-induzierten Ca^{2+} Signalen und dem Stomaschluss untersucht. Die Injektion von ABA in die Zellwand von Schließzellen bewirkte einen schnellen Stomaschluss, jedoch wurde nur bei drei Vierteln der Zellen auch ein zytosolisches Ca^{2+} Signal erzeugt. Ein kleiner Teil der Stomata (in einem Viertel der Experimente) schloss sich ohne Ca^{2+} Signal, was zeigt, dass die Ca^{2+} Signale nicht essentiell für den ABA-induzierten Stomaschluss sind. Es schlossen sich jedoch Stomata schneller, in deren Schließzellen ABA-induzierte Ca^{2+} Signale detektiert wurden. ABA-induzierte Ca^{2+}-Signale verbesserten also offenbar die Geschwindigkeit des Stomaschlusses. Neben ABA konnten Ca^{2+} Signale in wildtypischen Schließzellen auch durch hyperpolarisierende Spannungspulse erzeugt werden, welche daraufhin S-Typ Anionenkanäle aktivierten. Diese Spannungspulse konnten jedoch in *slac1/slah3* Schließzellen keine S-typischen Anionenströme hervorrufen, was darauf hindeutet, dass SLAC1 und SLAH3 zur Ca^{2+}-aktivierten Leitfähigkeit beitragen. Zusammengefasst deuten unsere Daten darauf hin, dass ABA-induzierte Ca^{2+} Signale die Aktivität von S-Typ Anionenkanälen verbessern und somit den Stomaschluss beschleunigen.

Der zweite Teil der Thesis befasst sich mit dem Signalweg, der den Ca^{2+}-Signalen nachgeschaltet ist. Es wurden zwei Typen Ca^{2+}-abhängiger Proteinkinase-Module (CPKs

und CBL/CIPKs) in Schließzellen nachgewiesen. Wir haben uns auf die Proteinkinase CIPK23 (CBL-Interacting Protein Kinase 23) konzentriert, welche von den Ca^{2+}-abhängigen Proteinen CBL1 und CBL9 (Calcineurin B-Like Protein 1 oder 9) über Interaktion mit der NAF Domäne des CIPK23 aktiviert wird. Es konnte bereits gezeigt werden, dass der CBL1/CIPK23 Komplex die stomatäre Bewegung beinflusst, jedoch sind die zugrunde liegenden molekularen Mechanismen bisher weitgehend unbekannt geblieben. Wir haben dieses Thema mit einem Östrogen-induzierten Expressionssystem untersucht, welches spezifisch in Schließzellen die Expression von wildtypischem CIPK23 erhöhte. Hinzu kamen Experimente mit einer phosphomimetischen $CIPK23^{T190D}$ und einer $CIPK23^{K60N}$ mit disfunktionaler Kinasedomäne. Unsere Daten zeigen, dass $CIPK23^{T190D}$ exprimierende Schließzellen eine verbesserte Stomaöffnung aufwiesen, während $CIPK23^{K60N}$ den ABA-induzierten Stomaschluss förderte, was auf eine negativ regulierende Rolle von CIPK23 beim Stomaschluss hindeutet. Elektrophysiologische Messungen zeigten, dass die einwärtsgerichteten K^+-Ströme in CIPK23-, $CIPK23^{T190D}$- oder $CIPK23^{K60N}$-exprimierenden Schließzellen vergleichbar waren, was darauf hindeutet, dass die Aktivierung von AKT1 durch CIPK23 nicht zur stomatären Bewegung beiträgt. Allerdings führte die Expression von $CIPK23^{K60N}$, wie auch der Verlust von CIPK23, in Schließzellen zu einer erhöhten S-typischen Anionenkanalaktivität, während eine $CIPK23^{T190D}$-Expression diese Anionenkanalaktivität inhibierte. Diese Ergebnisse stimmen mit den Beobachtungen zu den gezeigten Veränderungen der stomatären Bewegung überein und deuten daher auf eine regulierende Rolle von CIPK23 für die stomatäre Bewegung durch die Inhibierung von S-Typ Anionenkanälen hin. Insgesamt beweisen unsere Befunde, dass die CIPK23-vermittelte stomatäre Bewegung nicht durch eine Interaktion von CIP23 mit AKT1, sondern durch die Regulierung der S-Typ Anionenkanäle SLAC1 und SLAH3 vermittelt wird.

Zusammengefasst ergeben die in dieser Thesis präsentierten Daten neue Einblicke in den Ca^{2+}-abhängigen Pfad des ABA-Signalwegs. Dies könnte in Zukunft helfen neue Strategien zur Zucht von Pflanzen mit verbesserter Trockenstresstoleranz zu entwickeln und somit die agrarwirtschaftliche Produktivität zu erhöhen.

Translated by Jan Rathje (Molecular Plant Physiology and Biophysics, University of Wuerzburg)

Glossary

Abbr.	*Full name*
ABF3	ABA Responsive Elements Binding Factors 3
ABI1	ABA Insensitive 1
ACAs	Autoinhibited Ca^{2+}-ATPases
AHAs	Autoinhibited H^+-ATPase isoforms
AKT1	Arabidopsis K^+ Transporter 1
ALMTs	Aluminum-activated Malate Transporters
AREB1	ABA Responsive Elements-Binding Protein 1
AtKC1	*Arabidopsis* K^+ Channel 1
CAXs	Ca^{2+} Exchangers
CBLs	Calcineurin B-Like proteins
CDPKs/CPKs	Ca^{2+}-Dependent Protein Kinases
CIPKs	CBL-Interacting Protein Kinases
CNGCs	Cyclic Nucleotide-Gated Channels
CspB	Cold shock protein B RNA chaperone
CSC	Calcium permeable Stress-gated cation Channel
ECAs	ER-type Ca^{2+}-ATPases
GHR1	Guard Cell Hydrogen Peroxide-Resistant 1
GLRs	Glutamate-Like Receptors
GORK1	Guard cell Outward Rectifier K^+ Channel 1
HAB1	Homology to ABA Insensitive 1
KAT1	K^+ channel from *Arabidopsis thaliana*1
LKS1	Low K^+ Stress 1
MAP3K	Mitogen-Activated Protein Kinase Kinase Kinase
MAPKK	Mitogen-Activated Protein Kinase Kinase
MAPK	Mitogen-Activated Protein Kinase
OSCA1	Osmolality Sensitive Ca^{2+} Channel 1
OST1	Open Stomata 1
PKS5	SOS2-like Protein Kinase 5 (CIPK11)
PMA2	Plasma Membrane H^+-ATPase isoform 2
PP2CA	Protein Phosphatase 2CA
PP2Cs	Type 2C Protein Phosphatases

PYR/PYL	Pyrabactin Resistance/PYR-Like
QUAC1	Quick Anion Channel
RCAR	Regulatory Components of ABA Receptors
SKOR1	Stelar K^+ Outward Rectifying Channel 1
SLAC1	Slow Anion Channel Associated 1
SLAH3	SLAC1 Homolog 3
SnRK2	Sucrose nonfermenting 1-Related protein Kinases 2
SPIK	Shaker Pollen Inward K^+ Channel
ABA	abscisic acid
AD/DA	analog to digital and vice versa
ATP	adenosine triphosphate
ADP	adenosine diphosphate
BAPTA	1,2-bis(o-aminophenoxy)ethane-N,N,N',N'-tetraacetic acid
BTP	1,3-bis(tris(hydroxymethyl) methylamino) propane
DMSO:	dimethyl sulfoxide
E_m	free running membrane potential
I_m	membrane current
K_d	dissociation constant
MES	2-(N-morpholino) ethanesulfonic acid
MS	Murashige and Skoog medium
pGC1	Guard cell protomer 1
R-type	Rapid type
S-type	Slow type
V_m	experimental controlled membrane potential
WT	wild type

List of figures and tables

Fig. 1.1 The "Watergate", a stoma of *Arabidopsis* can open and close its pore reversibly 2

Fig. 1.2 P-type H^+-ATPases energize the plasma membrane. 5

Fig. 1.3 K^+ channels in guard cells are activated upon voltage stimulation. 8

Fig. 1.4 S-type anion channels recorded in guard cells of Col-0. 13

Fig. 1.5 A working model of the ABA signaling pathway in guard cells. 20

Fig. 1.6 The 2D structure of ABA and its agonists, antagonists. 31

Fig. 2.1 Two electrode voltage clamp technique applied to guard cells. 34

Fig. 2.2 Microelectrodes used for guard cells impalement or current ejection. 35

Fig. 2.3 Setup for guard cell impalement and current ejection experiments 36

Fig. 2.4 The schematic illustration of the estrogen-induced pLB12 vector. 41

Fig. 2.5 The schematic illustration of modified pLB12. 42

Fig. 2. 6 The estrogen dependent induction of gene expression in guard cells. 43

Fig. 3.1 Stimulation of a single guard cell in an intact leaf by current ejection of ABA. 48

Fig. 3.2 Estimation of ABA concentration in the guard cell wall, imposed by current ejection. 49

Fig. 3.3 Dose-response curve of ABA-induced stomatal closure. 50

Fig. 3.4 Calibration of RG-mT with FURA2 in *Arabidopsis* guard cells. 52

Fig. 3.5 ABA-induced Ca^{2+} signals occur either before or during the stomatal closing. 54

Fig. 3.6 ABA-induced Ca^{2+} signals in guard cells accelerate stomatal closure. 55

Fig. 3.7 Cytosolic Ca^{2+} signals activate S-type anion channels in guard cells. 57

Fig. 3.8 ABA evoked Ca^{2+} signals are strongly impaired in *ost1-3* guard cells. 59

Fig. 3.9 Ca^{2+}-dependent activation of S-type anion channels in *ost1-3*. 60

Fig. 3.10 Fluorescence of Venus, and expression of CIPK23 variants in guard cells with or without estrogen treatment. 63

Fig. 3.11 Phosphomimic $CIPK23^{T190D}$ stimulates stomatal opening, while $CIPK23^{K60N}$ enhances stomatal closure. 65

Fig. 3.12 CIPK23 stimulates stomatal opening. 66

Fig. 3.13 CIPK23 variants increase inward K^+ channel conductance in guard cells. 68

Fig. 3.14 CIPK23 enhances the expression of *AKT1* in guard cells. 69

Fig. 3.15 CIPK23 stimulates guard cell inward K^+ channels. 69

Fig. 3.16 CIPK23-activation of AKT1 does not require the kinase activity of CIPK23. 71

Fig. 3.17 The C terminus of CIPK23 is important for the activation of AKT1 72

Fig. 3.18 CIPK23 suppresses the S-type anion channel conductance of guard cells. 73

Fig. 3.19 CIPK23 attenuates S-type anion conductance in guard cells. 74

Fig. 3.20 Transcript levels of S-type anion channels in guard cells. 75

Fig. 3.21 CIPK23^{T190D} and CIPK23^{K60N} fail to activate SLAC1 and SLAH3 in oocytes. 76

Fig. 3.22 CIPK23 variants, denoted as constitutively active forms, cannot activate SLAC1 in oocytes. 77

Fig. 3.23 CIPK23^{T190D} disrupts the activation of SLAC1 by CPK23 and CIPK11. 79

Fig. 4.1 Fast changes in the osmotic content of guard cells elicit Ca^{2+} signals. 81

Fig. 4.2 Ca^{2+}-dependent signaling stimulates anion channels in guard cells. 84

Fig. 4.3 Regulation of S-type anion channel activity in guard cells. 90

Table 2. 1 The description of plants used in this study 32

1. Introduction

1.1 Function of stomata

The tiny pores called stomata located on the surface of aerial plant tissues are of great importance for our planet. The opening of these microscopic pores enables plants to absorb atmospheric carbon dioxide (CO_2), which is the starting material for photosynthesis and gives rise to the carbohydrates and oxygen (O_2), the indispensable resources for life on Earth. Moreover, the assimilation of enormous CO_2 quantities by plants through stomata efficiently reduces the greenhouse effect and global warming (Roelfsema & Kollist, 2013). In addition to CO_2 uptake, the open stomata also transpire vast amounts of water to the atmosphere, which is of major importance for worldwide biogeochemical water cycles.

In nature, water is frequently a limiting resource for plants due to their sessile nature. Plants are thus vulnerable to water deficit, or drought stress. Given that water is so important for plant life, one may ask why plants evolved the stomata to “waste” water? The answer to this question may relate to the evolution when plants colonized the terrestrial environment. During this transition, they had to develop an impermeable cuticle on the plant surface, to prevent excessive water loss. However, the cuticle also presents a barrier against the CO_2 uptake, an essential substrate for photosynthesis. Stomata provide openings in the cuticle, which enable CO_2 uptake for photosynthesis. Moreover, transpiration allows plants to sustain water uptake and drives nutrient transport. These evolutionary adaptations, therefore, allowed plants to colonize terrestrial lands, from wetland to desert (Chater *et al.*, 2017; Sussmilch *et al.*, 2019).

Water and CO_2 are indispensable compounds for plant growth and stomata therefore must be accurately controlled. The fine-tuning of this process ensures that plants can survive under rapidly changing environmental conditions. A pair of specialized epidermal cells, the guard cells, which form stomata, are responsible for regulating the aperture of the stomatal pore (**Fig. 1.1**). It is well known that a multitude of receptors have evolved in guard cells for sensing the intracellular and extracellular signals, such as phytohormones, CO_2 concentration, pathogenic effectors, light quality and intensity, temperature and the hydration status of plant tissues, in which phytohormone ABA plays

an important role (Roelfsema & Hedrich, 2005; Melotto *et al.*, 2006; Marten *et al.*, 2007a; Hu *et al.*, 2010; Bauer *et al.*, 2013; Guzel Deger *et al.*, 2015). These signals are sensed by a number of receptors and propagated to the final targets, via second messengers, or post-translation modification within the guard cells. These signaling pathways interact and give rise to a complex network, which finally determines the stomatal movement.

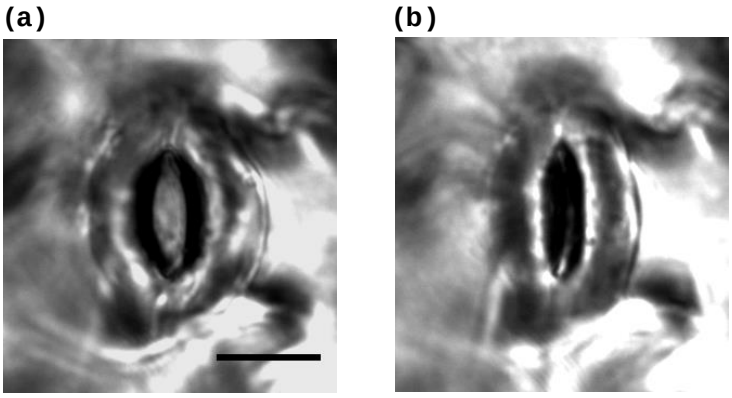

Fig. 1.1 The "Watergate", a stoma of *Arabidopsis* can open and close its pore reversibly.

(a) Open stomata provide a portal for CO_2 uptake which supports photosynthesis, while water is inevitably lost. Scale bar=10 µm.

(b) Stomata close in response to drought stress hormone ABA, which avoids dehydration.

Guard cells are highly specialized cells that lack plasmodesmata connection within the stomata complex, or with adjacent epidermal cells (Wille & Lucas, 1984). However, stomata in ferns and mosses seem to be an exception, as they have plasmodesmata connection between the guard cells (Voss *et al.*, 2018). Because of their isolation from other leaf cells, guard cells are an attractive model system for electrophysiological and cell signaling research. The results of these studies have made important contributions to our understanding of ABA signaling, which is likely to be beneficial for future plant breeding.

1.2 Ion fluxes cause stomatal movements

Stomatal movements are provoked by the changes in guard cell volume (Roelfsema & Hedrich, 2005), which in turn are determined by ion fluxes in the cells. Ion uptake from the apoplast causes a decrease in the osmotic potential, which will trigger a flow of water into the guard cells and thus cause cell expansion. As a result, both guard cells will bend

and force the stomatal pore to open. In contrast, the efflux of ions is accompanied with water loss from the cells, which will cause the cells to shrink and stomata to close.

Even though the stomatal movements have been studied since the 19th century, only in the 1960s it was realized that the stomatal opening is mediated by K^+ ion uptake into guard cells (Willmer & Fricker, 1996). Initially, stomatal opening and closure were explained by several hypotheses, including a theory of photosynthesis in guard cells, a theory of glycolate metabolism, and starch sugar inter-conversion theory (Willmer & Fricker, 1996). The theory of photosynthesis in guard cells was proposed by Von Mohl (1856), which suggested that chloroplasts in guard cells can photosynthesize carbohydrates under light, leading to osmotic pressure increase in guard cells and thereby triggers stomatal opening. However, whether guard cell chloroplasts can conduct photosynthesis is still in a fierce debate over decades (Lawson, 2009; Morison, 2010). Moreover, an increase in CO_2 concentration, which promotes photosynthesis, induces stomatal closure rather than opening. The theory of glycolate metabolism suggested that glycollate-glyoxyllate system in guard cells not only can generate ATP, but also raises the osmotic pressure, both of which promote stomatal opening (Zelitch, 1963; Zelitch & Walker, 1964). However, this hypothesis lacks experimental support. The starch sugar inter-conversion theory was popular in the scientific communities from 1895 to the mid-1960s (Willmer & Fricker, 1996). In this theory, starch is degraded during the daytime which causes the accumulation of osmotically active sugars, and leads to stomatal opening. During the night starch synthesis occurs and leads to a reduction in the osmotic content, which promotes stomatal closure (Lloyd, 1908; Loftfield, 1921; Steward, 1967). However, later studies demonstrated that stomatal movements do not match with starch synthesis and sugar transport (Stadler *et al.*, 2003), but instead strongly depends on K^+ ion flux into guard cells (Fujino, 1967; Fischer, 1968). Fujino (1967) was the first to show stomatal opening in association with the uptake of K^+ ion. A year later, the independent work of Fischer (1968) confirmed this finding and showed that the accumulation of K^+ in *Vicia faba* guard cells was essential to increase the osmotic pressure, which can drive stomatal opening. Later on, the changes in K^+ levels and osmotic pressure required for stomatal opening were also quantified (MacRobbie & Lettau, 1980). These early studies were mainly carried out with *V. faba* and *C.communis*, while the importance of K^+ in

stomatal movement was further addressed in the model plants of molecular biology *Arabidopsis* and *Oryza sativa* (Dayanandan & Kaufman, 1975; Roelfsema & Prins, 1995).

It has been estimated that guard cells maintain a cytoplasm K^+ concentration of approximately 100 – 160 mM, which was calculated from the K^+ reversal potential (Clint & Blatt, 1989). The electrical charges of the accumulated K^+ ions need to be compensated by anions. Counter anions are either taken up from the apoplast, or synthesized in the cytosol. It is supposed that Cl^- is transported into the cytosol from apoplast by a H^+/Cl^- symporter, while the organic ions, such as malate, are synthesized in guard cells during stomatal opening (Raschke & Schnabl, 1978).

The lipid bilayer of the plasma membrane serves as a diffusion barrier for many solvents, including ions. Thus, transport of ion across the plasma membrane of guard cells requires specific ion transport proteins. These proteins, classified as electrogenic pumps, ion channels, or transporters, allow K^+ and other anions to quickly redistribute between the cytosol and apoplastic surrounding. Pioneering studies indicate that the activity of H^+-ATPases, K^+ channels, anion channels, and Ca^{2+} channels in guard cells play specific roles in regulation of stomatal movements (Hedrich, 2012; Kollist *et al.*, 2014), which will be introduced below.

1.3 H^+-ATPase

In early studies, scientists realized that guard cell K^+ uptake was activated by light (Fischer, 1968), and H^+ was released from guard cells under (blue) light stimulation (Raschke & Humble, 1973; Gepstein *et al.*, 1982; Shimazaki *et al.*, 1986). By using gas exchange and patch-clamp techniques, Assmann *et al.*, (1985) showed that blue light stimulated stomatal opening is correlated with the activation of H^+-pumps (H^+-ATPases) in the plasma membrane of guard cells. The activation of plasma membrane H^+-ATPases extrudes H^+ from the cytosol to the apoplast by consuming the ATP, which generates the chemical gradient of H^+ and the electrical gradient (**Fig. 1.2**). The activity of H^+-ATPases shifts the membrane potential to values that are more negative as K^+ equilibrium potential (also called hyperpolarization), leading to the activation of inward K^+ channels (Schroeder *et al.*, 1984). As a result, K^+ accumulates in guard cells and induces stomatal

opening. Thus, the plasma membrane H^+-ATPases are the energizers for stomatal opening.

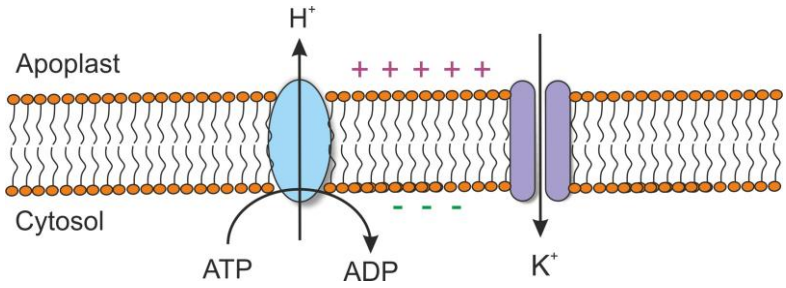

Fig. 1.2 P-type H^+-ATPases energize the plasma membrane.

Plasma membrane/P-type ATPases couple ATP hydrolysis and H^+ transport, which generate a H^+ gradient, and electrical charge difference across the plasma membrane. The chemoelectrical gradient can activate voltage-gated inward K^+ channels, which enable the uptake of K^+ ions. The increase in osmotic pressure will drive H_2O flow into the cell and thereby cause stomatal opening.

The function of H^+-ATPases in stomatal opening

In *Arabidopsis*, guard cells express all genomically encoded H^+-ATPase isoforms (a total of 11 AHA genes), of which AHA1, AHA2, and AHA5 (Autoinhibited H^+-ATPase isoform 1, 2 and 5) show highest expression levels (Ueno *et al.*, 2005). However, the first genetic evidence for the importance of the AHA encoded pump was obtained with *ost2* (Open Stomata2). Mutants of *ost2* with constitutively opened stomata were screened by using the infrared thermal imaging technique (Merlot *et al.*, 2002). Genetic mapping revealed that the mutant *ost2-1D* carries a single point mutation of Pro-68 to Ser (P68S) in the AHA1 gene, while *ost2-2D* harbors two missense mutations (Leu-169 to Phe (L169F); Gly-867 to Ser (G867S)) in the coding region (Merlot *et al.*, 2007). Both *ost2-1D* and *ost2-2D* possess the constitutively active forms of AHA1, which leads to an open stomata phenotype, indicating that the active form of the PM H^+-ATPase energizes the plasma membrane and causes stomatal opening. In addition to AHA1, studies with plants that overexpress AHA2 in guard cells (*GC1:AHA2*) show that this PM H^+-ATPase also enhances light-induced stomatal opening, while it promotes plant photosynthesis and growth (Wang *et al.*, 2014). Intriguingly, plants that express the $AHA2^{P68S}$ variant in guard cells (*GC1:* $AHA2^{P68S}$), which harbors the same mutation as AHA1 *ost2-1D,* do not show an

enhanced plant growth, even though they exhibit more opened-stomata (Wang *et al.*, 2014). A difference in the nighttime water loss may result in the distinct growth phenotypes, since stomata remain open in the darkness in AHA2^{P68S} expressing plants, whereas they close in plants that express with wild type form of AHA2 (Wang *et al.*, 2014).

Regulation of H^+-ATPase activity

The AHA2 encoded H^+-ATPase has been studied in most detailed and consists of 10 transmembrane segments (M1–M10), of which the N- and C-terminal domains are exposed to the cytosolic side of the membrane (Falhof *et al.*, 2016). In an autoinhibited state, the catalytic domains on the cytoplasmic side (formed by the A, N, and P domain) are inhibited by the C-terminal domain (Palmgren *et al.*, 1991). ATP hydrolysis is only loosely coupled to H^+ transport in this state, whereas a tight coupling between ATP hydrolysis and H^+ pumping takes place in the active state (Falhof *et al.*, 2016), after releasing the C-terminal domain from the catalytic domain (Venema & Palmgren, 1995; Baunsgaard *et al.*, 1996). This indicates that the C-terminal domain is important for H^+-ATPase regulation. The substitutions of P68S and G867S in *ost2* may cause the prevention of intramolecular contacts between the C-terminal domain and the cytoplasmic sites, leading to the ATPase in a permanently open conformation, and therefore forming constitutively active state. However, by using the split ubiquitin system, Merlot *et al.*, (2007) did not find that the P68S or G867S mutations obstruct the interaction between the C-terminal domain and the catalytic domain. Possibly other mechanisms are involved in regulation of *ost2* ATPase activity.

PM H^+-ATPases in guard cells are activated by light, especially by blue light at 460 nm, which can efficiently induce the acidification of apoplast (Shimazaki *et al.*, 1986; Roelfsema *et al.*, 1998) and stomatal opening (Sharkey & Raschke, 1981) via the receptors PHOT-1 and PHOT-2 (Kinoshita *et al.*, 2001). In the presence of blue light, PHOT receptors become active and phosphorylate the protein kinase BLUS1 (Blue light Signaling1). BLUS1 may indirectly activate an unidentified protein kinase, which can phosphorylate Thr-947 in AHA2, or Thr-948 in AHA1, and this phosphorylation triggers release of the autoinhibitory C-terminal domain, and creates a binding site for 14-3-3

protein (Falhof *et al.*, 2016). Binding of 14-3-3 protein to the H^+-ATPase stabilizes the active state of the pump (Kinoshita & Shimazaki, 1999; Svennelid *et al.*, 1999; Duby *et al.*, 2009; Takemiya *et al.*, 2013; Falhof *et al.*, 2016). Evidence also shows that multiple phosphorylation sites in AHAs are important for their activation. Phosphorylation of AHA2 at Ser-931 by CIPK11 (PKS5) inhibits the interaction between AHA2 and an activating 14-3-3 proteins (Fuglsang *et al.*, 2007). Using a mass spectrometric analysis, Duby *et al.*, (2009) identified a Thr-938 phosphorylation site of PMA2 (Plasma Membrane H^+-ATPase isoform 2) in *Nicotiana tabacum* (corresponding to Thr-931 of AHA2 in *Arabidopsis*) which negatively regulates the H^+-ATPase activity, regardless of whether Thr-947 is phosphorylated. In contrast, phosphorylation of AHA2 Thr-881 in *Arabidopsis* or Thr-889 in tobacco PMA2 leads to H^+-ATPase activation (Niittyla *et al.*, 2007; Fuglsang *et al.*, 2014).

1.4 K^+ transport across the plasma membrane of guard cells

During stomatal opening, guard cells utilize not only the driving forces provided by H^+-ATPases, but also the inward K^+ channels, which provide a selective pathway for K^+ through the biological membrane. Likewise, the outward K^+ channels in guard cells function during stomatal closure. These K^+ channels in the plasma membrane are enabling a rapid redistribution of K^+ between guard cell cytosol and apoplast. The efflux of positively charged ions at the plasma membrane generates outward current, while the influx produces inward current.

In *Arabidopsis*, a total of 15 genes have been identified to encode K^+ channels, 9 of which belong to the voltage-dependent, Shaker-like, K^+ channels and localize to the plasma membrane (Hedrich, 2012). Based on the channel gating properties, the Shaker-like K^+ channels are further divided into three subgroups: inward, outward and weak K^+ rectifiers (Very & Sentenac, 2002; Hedrich, 2012). The activity of Shaker-like K^+ channels is regulated by a voltage-sensing region, which causes opening of the channel pore at a certain voltage across the plasma membrane.

The hallmark of inward K^+ channels is that they are normally activated by hyperpolarization, which the membrane potentials are more negative than Ek (the Nernst potential of K^+) (Kollist *et al.*, 2014). The Ek can be calculated by the formula:

$$Ek = -58\,mV * log_{10}\frac{[K^+]_i}{[K^+]_o}$$

In which $[K^+]_i/[K^+]_o$ is the concentration ratio of K^+ across the membrane. The Ek is approximately -70 mV in guard cells of intact plants (Roelfsema *et al.*, 2001). Inward K^+ channels transport K^+ from the apoplast to the cytosol, and thus generate the inward direction current (**Fig. 1.3**). The accumulation of K^+ in cytosol increases the osmotic pressure in the guard cells, leading to stomatal opening.

In contrast with inward K^+ channels, the outward K^+ channels are responsible for extruding K^+ from the cytosol to the apoplast, producing an outward directed current (**Fig. 1.3**). These channels are activated when guard cell plasma membrane potential is more positive than Ek (Roelfsema *et al.*, 2001).

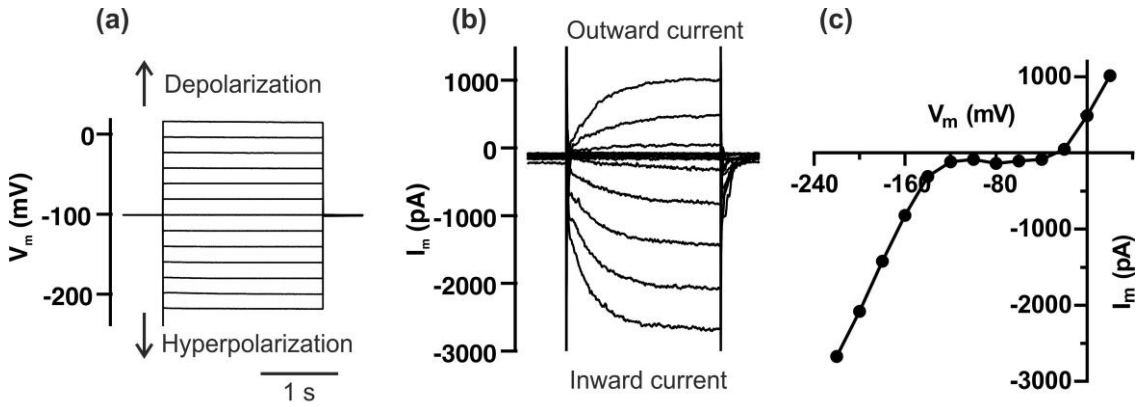

Fig. 1.3 K^+ channels in guard cells are activated upon voltage stimulation.

(a) A guard cell in an intact leaf of Col-0 was impaled with a double-barreled electrode, and the plasma membrane was held at -100 mV. The cell was stimulated with 2 s depolarizing and hyperpolarizing pulses, which ranged from 20 to -220 mV with 20 mV decrements.

(b) Outward and inward K^+ channels in the plasma membrane of guard cells were activated by the depolarizing and hyperpolarizing pulses, respectively.

(c) Steady-state K^+ currents were plotted against the voltages from the same cell as in (b). Note that the outward and inward K^+ activity became pronounced at -20 and -140 mV, respectively.

1.4.1 Inward K^+ channels

Features of inward K^+ channels

The first inward K^+ channel, KAT1 (K$^+$ channel from *Arabidopsis thaliana*1), was identified by heterologous expression of plant transporter genes in *Saccharomyces cerevisiae*. KAT1

was able to rescue a K^+ transport-defective yeast mutant (Anderson *et al.*, 1992). In the same year, another inward K^+ channel, AKT1 (*Arabidopsis* K^+ Transporter1), was cloned from *Arabidopsis* (Sentenac *et al.*, 1992). Years later, KAT2 (a homolog of KAT1), AKT2/3 (also named AKT2 or AKT3), SPIK (Shaker Pollen Inward K^+ Channel, or AKT6) and AtKC1 (*Arabidopsis* K^+ Channel 1) were identified (Cao *et al.*, 1995; Marten *et al.*, 1999; Pilot *et al.*, 2001; Mouline *et al.*, 2002; Reintanz *et al.*, 2002). In spite of being in the same subgroup, the features of inward K^+ channels are distinct, for instance, KAT1 and KAT2 are strict inward rectifiers and are stimulated by the hyperpolarization and sensitive to pH (Hedrich *et al.*, 1995; Pilot *et al.*, 2001), whereas AKT2/3 represents a weak K^+ inward channel, and is sensitive to Ca^{2+}, expressed in the phloem networks and guard cells (Marten *et al.*, 1999; Ivashikina *et al.*, 2005). AtKC1 represents a silent K^+ channel (Reintanz *et al.*, 2002), which does not form functional channels, but instead modulates the properties of the AKT1·AtKC1 heterocomplex (Geiger *et al.*, 2009a). In general, the inward K^+ channels can assemble to heterologous complexes to achieve their function (Pilot *et al.*, 2001).

The function of inward K^+ channels in stomatal opening

Since inward K^+ channels are capable of facilitating K^+ uptake into guard cells, it was speculated that the inward K^+ channel is essential for stomatal opening. As KAT1 is specifically expressed in guard cells, loss of function KAT1 was expected to disrupt stomatal opening. However, stomatal movement in response to light, CO_2, and ABA, as well as K^+ uptake was not affected in KAT1-deficient plants. This shows that KAT1 is not required for stomatal opening (Szyroki *et al.*, 2001). In line with these loss of function mutants, overexpression of KAT1 driven by GC1 promoter (Yang *et al.*, 2008) in guard cells does not influence stomatal opening (Wang *et al.*, 2014). Similarly, the knock-out mutant *kat2-1* or *domneg-1* (expressing a dominant negative *kat2* construct in WT background) does not affect stomatal opening, whereas *kincless* mutant (expressing a dominant negative *kat2* construct in *kat2-1* background), which has completely lost all inward K^+ channel activity, is impaired in stomatal responsiveness to light, VPD (vapor pressure difference), and CO_2 (Lebaudy *et al.*, 2008). This suggests that guard cell inward K^+ channel activity is crucial for plants to adapt the harsh environments. Intriguingly,

though AKT1 is a dominant channel for the K^+ uptake in roots, it also seems to be involved in stomatal movement regulation, based on the evidences that the AKT1 knock-out mutants have a less water transpiration under long-term water stress in soil, and their stomata are more sensitive to ABA, compared to wild type (Nieves-Cordones *et al.*, 2012).

Regulation of inward K^+ channel activity

K^+ is not only important for K^+ uptake during the stomatal movement, but also for the maintenance of the membrane potential. The inward K^+ channels therefore must be regulated finely. Recently, it was reported that the constitutively active CPK3 (CPK3CA, deleting the EF hand domain) strongly inhibits KAT1, and the C terminus of KAT1 is essential for this inhibition (Qi *et al.*, 2018). Moreover, another CPK, CPK13, suppresses KAT1- and KAT2-derived currents in oocytes via the phosphorylation (Ronzier *et al.*, 2014). Unlike KAT1 and KAT2, expression of AKT1 solely in oocytes cannot obtain K^+ conductance, suggesting that the channel activation requires an activator. By employing the forward-genetic screening, Xu *et al.*, (2006) found out an activator of AKT1, CIPK23 (also named LKS1, Low K^+ Stress 1). Coexpression of CIPK23 (LKS1) and CBL1 (or CBL9), together with AKT1 in oocytes, resulted in inward currents conducted by AKT1 (Li *et al.*, 2006; Xu *et al.*, 2006). In addition, AKT1 is regulated by the electrically silent Shaker-like channel AtKC1, which modulates the voltage dependence of AKT1 and prevents the K^+ leaking from the channel (Geiger *et al.*, 2009a; Wang *et al.*, 2016). AKT2/3, the homolog of AKT1, is also regulated by phosphorylation events, since the phosphorylation sites at Ser-210 and Ser-329 in the voltage sensor domain (S4) are important for the channel voltage regulation (Michard *et al.*, 2005).

1.4.2 Outward K^+ channels

Features of GORK

GORK (Guard cell Outward Rectifier K^+ channel) encodes the major voltage-gated outward K^+ channel in the plasma membrane of guard cells (Ache *et al.*, 2000; Hosy *et al.*, 2003). Unlike KAT1, the activity of GORK is strongly influenced by the external K^+ concentration (Blatt & Gradmann, 1997; Roelfsema & Prins, 1997; Ache *et al.*, 2000; Eisenach *et al.*, 2014). In addition, a decrease in the external pH (acidification) suppresses

GORK activity (Ache *et al.*, 2000). Heterologous expression of GORK in oocytes showed that the channel exhibits sigmoidal activation kinetics upon the depolarization stimulation, in other words, GORK needs a few seconds to reach the full activation (Ache *et al.*, 2000), which is in line with the delayed outward rectifier in intact guard cells and protoplasts (Roelfsema & Prins, 1997; Ache *et al.*, 2000). SKOR (Stelar K^+ Outward Rectifying channel) was also identified as outward-rectifying K^+ channel, but it expresses only in the xylem parenchyma cells of roots (Gaymard *et al.*, 1998).

The function of GORK in stomatal closure

The function of GORK in stomatal closure was characterized with the *gork-1* mutant or dominant-negative mutant *gork-dn1* and *gork-dn2* (Hosy *et al.*, 2003). Patch-clamp experiments on guard cell protoplasts reveal that the outward K^+ currents are strongly disrupted in these mutants, but the inward K^+ currents are similar to those in wild-type. Despite of the absence of an obvious growth phenotype in this mutant, fast stomatal movement in response to darkness and ABA is significantly impaired in *gork1-1*. Under long-term drought conditions, these mutants increase water consumption compared to control plants. These data provide the proof that GORK is required for K^+ release from guard cells during stomatal closure and is important for plants to adapt to drought (Hosy *et al.*, 2003). Interestingly, ABA, which can trigger stomatal closure, does not up-regulate the GORK expression in guard cells. ABA also fails to activate GORK-mediated outward K^+ channels in guard cells (Becker *et al.*, 2003), implying that GORK is mainly regulated by voltage in guard cells. Upon an ABA-induced depolarization, GORK gets activated in a voltage-dependent manner and releases K^+ from the guard cells (Roelfsema *et al.*, 2004).

Regulation of GORK

Recently, Corratge-Faillie *et al.*, (2017) reported that CPK33, but not the kinase-dead $CPK33^{K102M}$, enhances GORK activity in oocytes. In addition, three phosphorylation sites, Thr-344, Ser-518 and Ser-649, in the C terminal of GORK protein are determined as the phosphorylation target of CPK21 (van Kleeff *et al.*, 2018). 14-3-3, which directly interacts with CPK21 but not with GORK, increases GORK phosphorylation after binding to CPK21. It suggests that 14-3-3 proteins regulate GORK activity via binding with and activation of CPK21 (van Kleeff *et al.*, 2018). In contrast to the positive regulation of protein kinases,

the protein phosphatase PP2CA inhibits the GORK activity (Lefoulon *et al.*, 2016). In addition to PP2CA, the ABI2, but not ABI1, is able to suppress GORK as well, but the effect is counteracted by CIPK5-CBL1 (Forster *et al.*, 2019). Despite of these findings in oocyte system, it is still not clear if CPKs, or PP2Cs, regulate GORK in guard cells, since a study showed that the ABA has little impact on GORK activity in *V.faba* guard cells (Roelfsema *et al.*, 2004).

Voltage-dependent gating of inward and outward K^+ channels

In spite of the structural similarity between the outward-rectifying GORK-type and the inward-rectifying KAT1- and AKT1-type channels, they display a distinct property in the gating. The activity of GORK is affected by both voltage and the extracellular K^+ concentration, resulting in its activation that can only be detected under the depolarization condition. In contrast, KAT1 and AKT1 channels open their gate at hyperpolarization and are not influenced by the external K^+ ion (Hedrich, 2012). Though the crystal structure of Kvs is available (Long *et al.*, 2005), which is a homolog of plant Shaker channels, it remains poorly understood what determines the gating properties for inward and outward rectifiers.

1.5 Anion transport in the plasma membrane of guard cells

The outward K^+ channels are capable of releasing K^+ in guard cells, however, these channels can only be activated if the plasma membrane becomes depolarized. In guard cells, a depolarization can be accomplished via activation of anion channels, which release anions into apoplast and thereby shift the membrane potential to more positive values (Roelfsema *et al.*, 2004; Roelfsema *et al.*, 2012). Anion channel currents were initially recorded in *Vicia faba* guard cells with patch-clamp technique (Keller *et al.*, 1989; Schroeder & Hagiwara, 1989), and classified as R-type (Rapid) and S-type (Slow) channels, according to the differences in the velocity of their voltage-dependent activation and deactivation (Hedrich *et al.*, 1990; Schroeder & Keller, 1992).

1.5.1 S-type anion channels

Features of S-type anion channels

The membrane potentials of guard cells in intact plants can get negative of -140 mV (Roelfsema *et al.*, 2001; Roelfsema *et al.*, 2002). In this voltage range, R-type anion channels are not able to initiate a depolarization of the cell, instead, a depolarization can be achieved by activating the S-type anion channels, which display a relatively weak voltage-dependency (Keller *et al.*, 1989; Schroeder & Hagiwara, 1989; Roelfsema & Hedrich, 2005). As shown in **Fig. 1.4**, S-type anion channels are activated when the voltages step from +20 to -120 mV (Schmidt *et al.*, 1995; Roelfsema *et al.*, 2004; Roelfsema & Hedrich, 2005).

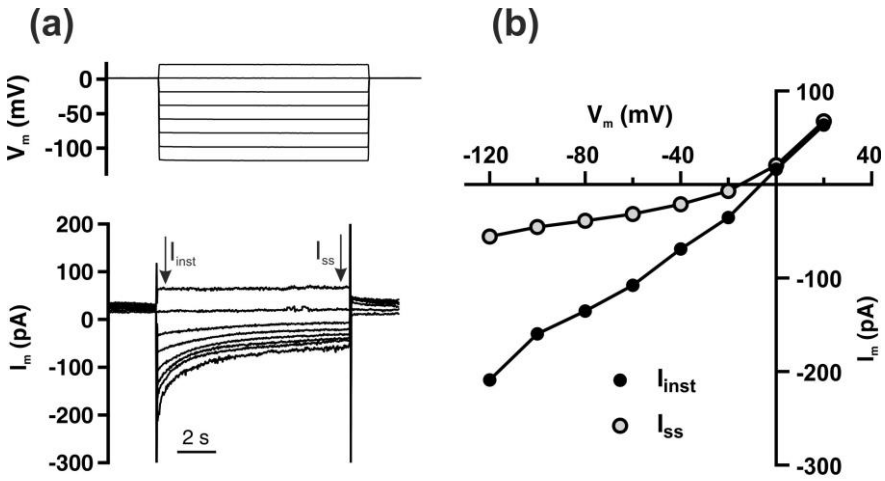

Fig. 1.4 S-type anion channels recorded in guard cells of Col-0.

(a) S-type anion currents (bottom panel) of a Col-0 guard cell in an intact leaf were activated from a holding potential of 0 mV to test potentials of 20 to -120 mV with 20 mV decrements (top panel). Note that the activation and deactivation of S-type anion channels are slow.

(b) Instantaneous (I_{inst}) and steady state (I_{ss}) currents (shown by arrows in a) plotted against the test voltage.

The function of SLAC1 in stomatal closure

An ozone-sensitive *Arabidopsis* mutant *rcd3* (*radical-induced cell death* 3) was isolated in 2008, exhibiting constitutively high stomatal conductance (Vahisalu *et al.*, 2008). An independent research group isolated *cdi3* (*carbon dioxide insensitive* 3) mutant in which the CO_2-dependent leaf temperature change was impaired (Negi *et al.*, 2008). The mutant in *cdi3* turned out to have a mutation in the same gene locus (At1g12480) as *rcd3,* but both mutations had occurred at different positions in the gene. Guard cell *RCD3* was shown to encode an S-type anion channel, which was named SLAC1 (Slow Anion Channel

Associated 1) (Negi *et al.*, 2008; Vahisalu *et al.*, 2008). Gas exchange measurements and stomatal aperture assay revealed that the *slac1* mutant is impaired in stomatal closure in response to various stimuli, including ozone, high atmospheric CO_2 concentration, ABA, low air humidity, Ca^{2+} ions, H_2O_2, whereas they close slowly in the darkness (Vahisalu *et al.*, 2008). In agreement with these stomatal phenotypes, neither the cytosolic Ca^{2+}, nor ABA can activate S-type anion channels in *slac1* guard cells, however, the R-type anion channels and Ca^{2+} channels are not affected (Vahisalu *et al.*, 2008). Recently, it was reported that SLAC1 can inhibit KAT1, but not KAT2, and thereby suppress stomatal opening (Zhang *et al.*, 2016). However, these findings are not in line with the previous finding that inward K^+ channel currents are inhibited in guard cells of *slac1* loss of function mutant (Laanemets *et al.*, 2013).

Although SLAC1 is homologous to the yeast malate transporter MAE1, heterologous expression of SLAC1 in yeast *mae1* mutant does not rescue the malate-uptake-deficient phenotype (Negi *et al.*, 2008). SLAC1 preferentially transports Cl^- and NO_3^-, whereas the conductivity for malate, sulfate, and HCO_3^- are negligible (Geiger *et al.*, 2009b). Patch-clamp experiments with wild type guard cell protoplasts showed that HCO_3^- can stimulate S-type anion channels (Xue *et al.*, 2011; Tian *et al.*, 2015a; Hsu *et al.*, 2018; Zhang *et al.*, 2018a). HCO_3^- is in equilibrium with CO_2 in H_2O and thus SLAC1 may be important for CO_2 signaling in guard cells.

Regulation of SLAC1

Initially, SLAC1 could not be functionally expressed in *Xenopus* oocytes, which implies that the activation of SLAC1 depends on the presence of appropriate regulators (Negi *et al.*, 2008). Indeed, SLAC1 currents can be recorded when the channel is coexpressed with several protein kinases in oocytes, including members of the gene families SnRK2 (Sucrose non-fermenting-Related Kinase), LRR-RLK (leucine-rich repeat kinase), MPK (mitogen-activated protein kinase), CPK/CDPKs, and CBL/CIPKs (Roelfsema *et al.*, 2012; Kollist *et al.*, 2014; Hedrich & Geiger, 2017; Saito & Uozumi, 2019) (**See 1.7.3** and **1.7.4**).

SLAC1 is homologous to the TehA gene of *Haemophilus influenzae,* and the crystal structure of TehA has been revealed (Chen *et al.*, 2010a). Based on the data of Chen *et al.,* (2010a), SLAC1 encoded protein forms a symmetrical trimer, consisting of subunits with

ten transmembrane helices that arrange from helical hairpin pairs to form a central five-helix transmembrane pore (Chen *et al.*, 2010a). In the narrowest part of the pore, a conserved phenylalanine (F450) residue locates at the central position of the transmembrane helix 9 (Chen *et al.*, 2010a). It is speculated that the orientation of F450 residue gates the channel. The orientation of F450 may be affected by the phosphorylation status of the N terminal domain, which is the interaction target of protein kinases (Chen *et al.*, 2010a; Roelfsema *et al.*, 2012).

Features and function of SLAH3

In *Arabidopsis,* the SLAC/SLAH family is divided into three groups: SLAC1 and SLAH3, SLAH1 and 4, and SLAH2 and 3 (Dreyer *et al.*, 2012). SLAH1, 2 and 4 are expressed in roots and the xylem, but not in guard cells (Maierhofer *et al.*, 2014b; Cubero-Font *et al.*, 2016). In guard cells, apart from SLAC1, SLAH3 (SLAC1 homolog 3) is also expressed. Though the loss of function SLAH3 mutant does not display a pronounced phenotype in gas exchange experiments, S-type anion channel currents in guard cells are attenuated (Geiger *et al.*, 2011). Moreover, SLAH3 can rescue the CO_2-insensitive phenotype of the *slac1* mutant (Negi *et al.*, 2008). In contrast to SLAC1, SLAH3 requires NO_3^- to prime the channel opening, and it also mainly conducts NO_3^-. Furthermore, SLAH3 acts an outward rectifier at positive voltages (Geiger *et al.*, 2011; Hedrich, 2012). SLAH3 can be activated by CPKs, CIPKs, low pH and SLAH1, but not by OST1 (Geiger *et al.*, 2011; Maierhofer *et al.*, 2014a; Cubero-Font *et al.*, 2016). Both SLAC1 and SLAH3 are likely to contribute to the Cl^- and NO_3^- efflux during stomatal closure.

1.5.2 R-type anion channels

Features of R-type anion channels

The hallmark of R-type anion channels is that they activate rapidly, within 50 ms, which is approximately 1000 times faster than that of S-type (Schroeder & Keller, 1992). The strong voltage-dependent activation is a characteristic of R-type anion channels (Keller *et al.*, 1989; Schroeder & Keller, 1992). Moreover, the voltage at which R-type channels become active is affected by the extracellular anions concentration and species (Dietrich & Hedrich, 1998). R-type anion channels permeate a large range of anions, including NO_3^-, Br^-, Cl^-, HCO_3^- and SO_4^{2-} (Dietrich & Hedrich, 1998; Frachisse *et al.*, 1999; Diatloff *et al.*,

2004). Intriguingly, the organic anion malate stimulates the activity of R-type anion channels in guard cells, suggesting that R-type anion channels play a role in malate transport and/or malate dependent CO_2 sensing (Hedrich & Marten, 1993; Hedrich *et al.*, 1994).

The function of R-type anion channels in stomatal closure

Although S-type anion channels seem to be of major importance for ABA-induced stomatal closure, the drought stress hormone also can activate R-type anion channels (Roelfsema *et al.*, 2004). The first R-type anion channel in guard cells, ALMT12 (Aluminum-Activated Malate Transporter 12) was identified by Meyer *et al.*, in 2010. R-type anion currents have a reduced in an ALMT12 loss of function mutant, and this mutant is impaired in stomatal closure in response to various stimuli, including high CO_2 levels (800 ppm), darkness, and ABA (Meyer *et al.*, 2010; Sasaki *et al.*, 2010). ALMT12 not only can transport malate but also sulfate (Meyer *et al.*, 2010; Malcheska *et al.*, 2017). As the accumulation of sulfate in the xylem sap can stimulate ABA synthesis in guard cells or/and trigger stomatal closure in an ABA-dependent manner, Poplar and *Arabidopsis* lacking ALMT12 are strongly impaired in stomatal close in response to sulfate and ABA (Malcheska *et al.*, 2017). In spite of its name of Aluminum-activated Malate Transporter 12, the ALMT12 channel is not sensitive to aluminum (Meyer *et al.*, 2010). It was therefore proposed to change the original name of AtALMT12 to Quick Anion Channel 1 (QUAC1) (Linder & Raschke, 1992; Meyer *et al.*, 2010).

Regulation of R-type anion channels

The electrophysiological nature of QUAC1/ALMT12 was characterized in oocytes by Mumm *et al.*, (2013), who found that the gating of this channel is not only affected by the extracellular, but also the intracellular malate concentration. The activity of QUAC1 is enhanced by the increasing cytosolic malate concentrations, leading to a shift of the peak inward current to more negative membrane potentials. The voltage-dependent gating of QUAC1 is dependent on the C-terminus, since the fusion of YFP to C-terminus of QUAC1 completely abolishes the voltage-dependency of this channel, while site-directed mutation G276Q at the C-terminus impairs channel activation.

Although the crystal of ALMT12 is not available, its secondary structure is likely to consist of six transmembrane domains and a large C terminus (Roelfsema *et al.*, 2012), according to the TaALMT1 model (Motoda *et al.*, 2007). However, a new model has been proposed in which the large C-terminus is spanning the membrane twice and the N-terminal may contain an additional membrane spanning region (Dreyer *et al.*, 2012). In *Arabidopsis* the 13 members of the ALMT family are phylogenetically divided into four clades: clade I (ALMT1, 2, 7, 8), clade II (ALMT3, 4, 5, 6, 9), clade III (ALMT12/QUAC1, 13, 14), and clade IV (ALMT10) (Dreyer *et al.*, 2012). The R-type anion channel currents in QUAC1 mutants are not abolished completely (Meyer *et al.*, 2010), suggesting redundant ALMTs (probably ALMT13 and 14) exist together with QUAC1 in guard cells. In addition, the vacuolar anion channels, ALMT4, 6 and 9 are also important for stomatal movements (De Angeli *et al.*, 2013; Eisenach *et al.*, 2017).

1.6 Ca^{2+} transport in guard cells

In guard cells, the Ca^{2+} concentration gradient between the cytosol and apoplast is approximately 10^4 fold. The large chemical gradient of Ca^{2+} and an inside negative membrane potential provide a large driving force for Ca^{2+} influx across the plasma membrane. In response to various stimuli, the cytosolic Ca^{2+} concentration increases immediately, or after a lag time, to generate a Ca^{2+} signature, of which spatio-temporal patterns, amplitude and frequency are hypothesized to be specific for a particular stimulus (Westlake *et al.*, 2015). The elevated cytosolic Ca^{2+} concentration is a ubiquitous second messenger which is likely to play an important role in a wide-range of physiological responses. Because of the influx of cations, activation of Ca^{2+} channels can cause the plasma membrane to depolarize. Moreover, an increase in the cytosolic Ca^{2+} concentration stimulates both R- and S-type anion channels (Keller *et al.*, 1989; Schroeder & Hagiwara, 1989), which will further depolarize the guard cell and trigger stomatal closure. De Silva *et al.,* (1985) were the first to link Ca^{2+} signals to ABA-induced stomatal closure. They found a synergistic effect of ABA and external Ca^{2+} on preventing stomatal opening in the epidermal strips of *C. communis*. A few years later, McAinsh *et al.,* (1990) used the Ca^{2+} sensitive fluorescence dye FURA2 to visualize and quantitatively analyze the Ca^{2+} signals in guard cells, and found that ABA-triggered Ca^{2+} signals, which

preceded the stomatal closure. It was therefore speculated that Ca^{2+} signals were required for ABA-induced stomatal movements (McAinsh *et al.*, 1990; Allen *et al.*, 1999b; Keinath *et al.*, 2015; Ye *et al.*, 2015).

Features of Ca^{2+} channels in guard cells

In general, the cytosolic free Ca^{2+} concentration in guard cells is maintained at approximately 100 nM, via the Ca^{2+} transport mechanisms, which include Ca^{2+} efflux as well as influx proteins (Sanders *et al.*, 2002). In plant cells, the known Ca^{2+} efflux transporters include ACAs (Autoinhibited Ca^{2+}-ATPases), ECAs (ER-type Ca^{2+}-ATPases), and CAXs (Ca^{2+} Exchangers) (Bose *et al.*, 2011; Manohar *et al.*, 2011; Spalding & Harper, 2011), while Ca^{2+} channels represent the Ca^{2+} influx components. Unlike the Ca^{2+} channels in animal cells, which are activated by depolarizing voltages or binding of a ligand, the Ca^{2+} channels in *V. faba* guard cells are stimulated by hyperpolarization (Cosgrove & Hedrich, 1991; Grabov & Blatt, 1998; Hamilton *et al.*, 2000). Similar results were also observed with guard cells of tobacco (Stange *et al.*, 2010). Interestingly, a transient increase in the cytosolic free Ca^{2+} concentration is also recorded when membrane potential returns to -100 mV, after a long depolarization (0 mV for 100 s). This indicates that a prolonged depolarization alters the activity of Ca^{2+} transport proteins, leading to an overshoot of $[Ca^{2+}]_{cyt}$ after returning the membrane potential to -100 mV (Stange *et al.*, 2010).

OSCA1 represents a Ca^{2+} channel in guard cells

Electrophysiological recordings and Ca^{2+} imaging experiments indicate that OSCA1 (Osmolality Sensitive Ca^{2+} Channel 1. later named as OSCA1.1; 15 members in *Arabidopsis*) represents a hyperosmolality gated, Ca^{2+}-permeable channel (Hou *et al.*, 2014; Yuan *et al.*, 2014). Guard cells of *osca1* are impaired in osmolality-induced Ca^{2+} signals, and their stomata fail to closure in response to PEG-induced osmotic stress (Yuan *et al.*, 2014). Heterologous expression of the channel OSCA1.2/AtCSC1 (Calcium permeable Stress-gated cation Channel) in oocytes revealed that OSCA1.2 conducts Na^+, K^+ and Ca^{2+}. The channel is activated by Ca^{2+}-free hyperosmotic buffers, but Ca^{2+} is required for the inactivation/closure of the channel (Hou *et al.*, 2014). The OSCA1.2 channel expressed in oocytes does not display any rectification upon voltages stimulation

(Hou *et al.*, 2014), which agrees with the results obtained with HEK293 cells (Yuan *et al.*, 2014). Homologs of OSCA1.2 are found in most eukaryotes, including yeast, fruit flies, and humans (Hou *et al.*, 2014; Yuan *et al.*, 2014). The OSCA1.2 homologs, ScYLR241W from *Saccharomyces cerevisiae* and HsTM63C from humans, also exhibits osmotically gated Ca^{2+} conductance and similar electrophysiological properties to OSCA1.2 (Hou *et al.*, 2014). Recently, the crystal structure of these channels revealed that OSCA belongs to a new class of mechanosensitive ion channels (Jojoa-Cruz *et al.*, 2018; Zhang *et al.*, 2018b), which show structural similarity to the mammalian TMEM16 family proteins. Based on these data, OSCA forms symmetric dimers, each consists of 11 transmembrane helixes (from M0 to M10), and the channel activation involves conformational changes of M0 and M6 helices (Zhang *et al.*, 2018b).

GLR and CNGC channels

In addition to OSCA1, two families of putative Ca^{2+} channels are found in plants, which are homologs to animal glutamate receptor channels (GLR, 20 members in *Arabidopsis*) and cyclic nucleotide-gated channels (CNGC, 20 members in *Arabidopsis*) (Hedrich, 2012). However, the specific functions of these putative Ca^{2+} channels in stomatal movements are still uncovered. For example, GLR3.1 and 3.5 have been identified as L-methionine-activated Ca^{2+} channels, however, the double loss-of-function mutant is only defective in Ca^{2+}-induced, but not in ABA-induced stomatal closure (Kong *et al.*, 2016). Likewise, CNGC5 and 6 were showed to serve as cGMP-activated channels, but both channels are not required for ABA, CO_2 or darkness-induced stomatal closure (Wang *et al.*, 2013b). Recently, the CNGC2 and CNGC4 proteins were reported only to form functional Ca^{2+} channels, if heterologous of both units are formed. These channels are important for plant immunity (Tian *et al.*, 2019), but it is not known yet whether they are involved in regulation of stomatal movements.

1.7 ABA signaling transduction in guard cells

Guard cells can be regarded as electrically isolated units, which makes them as an ideal system for the investigation of ion channels. In addition, guard cells harbor a large number of receptors which can sense environmental stimuli, such as changes in light quality and quantity, humidity, CO_2 concentration, and ABA (Kollist *et al.*, 2014). ABA is a

small molecule that functions in plant stress responses, such as rapid stomatal closure, which is evoked by changes in channel/transporter activity in the plasma membrane of guard cells. ABA activates the R- and S-type anion channels in a Ca^{2+} dependent and independent way (Roelfsema *et al.*, 2004; Roelfsema & Hedrich, 2005). The anion efflux from anion channels depolarizes the plasma membrane, which will stimulate outward K^+ channels to release K^+ from guard cells. ABA also attenuates the plasma membrane H^+-ATPase activity (Goh *et al.*, 1996; Zhang *et al.*, 2004; Hayashi *et al.*, 2011), so that enhances the depolarization. In addition, ABA also enhances the outward K^+ channels (Blatt, 1990; Roelfsema *et al.*, 2004). The effect of ABA on inward K^+ channels is still in debate, since ABA was reported to suppress inward K^+ channels in guard cells (Schwartz *et al.*, 1994; Acharya *et al.*, 2013), whereas other studies showed that the inward conductance of guard cells is similar in the presence or absence of ABA (Pei *et al.*, 1997; Roelfsema *et al.*, 2004). The dramatical changes in the plasma membrane conductance of guard cells result in K^+ efflux and water loss, which leads to stomatal closure. In the past two decades, the core ABA signaling pathway has been uncovered. The pathway comprises a group of ABA receptors, protein phosphatases and protein kinases, and anion channels. **Fig. 1.5** presents a simplified working model of the ABA signaling pathway in guard cells of *Arabidopsis*.

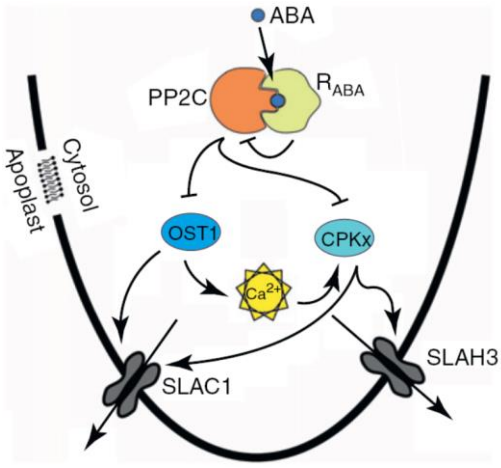

Fig. 1.5 A working model of the ABA signaling pathway in guard cells

In the absence of ABA, the co-receptors of ABI1/2 protein phosphatases (PP2C) are active and inhibit the protein kinase OST1. Upon binding of ABA to PYR/PYL/RCAR proteins (R_{ABA}), PP2Cs are recruited and suppressed by R_{ABA}, which leads to the activation of OST1 and CPKs. As a result, these protein kinases activate the S-type anion channels SLAC1 and SLAH3. OST1 may also crosstalk with CPKs by influencing the cytosolic free Ca^{2+} concentration. Figure adapted from Roelfsema *et al.*, Trends in Plant Science, 2012.

1.7.1 ABA receptors

In 2009, a family of STAR-related lipid transfer (START) proteins (called Pyrabactin Resistance/PYR-Like, 14 members in *Arabidopsis*, PYR1/PYL1-13) was identified with an elegant chemical genetic strategy (Park *et al.*, 2009), in which the synthetic pyrabactin was used to conduct a mutant screen. Pyrabactin is an ABA agonist, which selectively mimics ABA-inhibited seed germination. In a screening experiment, if the mutated seeds (after ethyl methanesulfonate treatment) can germinate in pyrabactin containing agar plates, it is likely due to loss of function in pyrabactin-binding protein, namely the ABA receptor that control seed germination. A second independent research group employed the yeast two-hybrid approach and identified proteins that interact with ABI1 and ABI2, which were named Regulatory Components of ABA Receptors (RCARs) (Ma *et al.*, 2009). RCARs and PYR1/PYLs are turned out to encode the same ABA receptors in *Arabidopsis*. Both groups found that PYR1 inhibits the phosphatase activity of HAB1 in the presence of ABA (Park *et al.*, 2009), or binding of (S)-ABA to RCAR1(PYL9) is required for inhibition of the phosphatases ABI1 and 2 (Ma *et al.*, 2009). In line with these results, it was shown that ABI1 interacts with several members of the RCAR/PYR/PYL family *in vivo,* by analysis of YFP-tagged ABI1 complexes with mass-spectrometry technique (Nishimura *et al.*, 2010). PYR/PYL and RCAR receptors are encoded by 14 genes, rather than a single entity, which may explain that previous screening approaches for ABA receptors had failed. Because of the redundancy by which PYR/PYLs act in ABA signaling, only the quadruple mutant *pyr1;pyl1;pyl2;pyl4* exhibits ABA insensitivity in root growth and seed germination, but not double mutant *pyr1;pyl4* (Park *et al.*, 2009). In addition, the quadruple mutant also impairs in ABA-regulated stomatal movements (Nishimura *et al.*, 2010).

The crystal structures of PYR1, PYL1, and PYL2 reveal that a gate-latch-lock mechanism underlies ABA signaling (Melcher *et al.*, 2009; Miyazono *et al.*, 2009; Nishimura *et al.*, 2009; Yin *et al.*, 2009). In the absence of ABA, a pocket structure at the surface of receptors is exposed, and two highly conserved ß-loops that function as a gate and latch are located at the pocket entrance. Binding ABA to this pocket causes conformational changes in the ß-loops, and triggers the gate closure and lock the ABA into the pocket. The pocket creates a novel binding surface that enables the receptor to dock to the

active site of PP2Cs, which stabilizes the closed conformation of receptors, resulting in full activation of the ABA signaling pathway. Several groups were successful to reconstitute the ABA signaling pathway *in vitro* by using the ABA receptor PYR1, the protein phosphatase ABI1, the serine/threonine protein kinase SnRK2.6/OST1 (or CPKs) and the transcription factor ABF2/AREB1, or SLAC1 (Fujii *et al.*, 2009; Geiger *et al.*, 2010; Brandt *et al.*, 2012). Recently, the core ABA signaling pathway was also rebuilt in yeast (Ruschhaupt *et al.*, 2019).

1.7.2 Type 2C protein phosphatases

Type 2C protein phosphatases (PP2Cs) are evolutionarily conserved in archaea, bacteria, fungi, plants and animals, and play a crucial role in stress signaling (Rodriguez, 1998; Fuchs *et al.*, 2013). In *Arabidopsis*, a total of eighty PP2Cs are found and divided into ten subgroups from A to K (Fuchs *et al.*, 2013). In clade A of PP2Cs, ABI1, ABI2, HAB1, HAB2 function as co-receptors of ABA, and thus negatively regulate ABA signaling via inhibiting the downstream protein kinases (Umezawa *et al.*, 2009). The inhibition of the protein kinases by clade A PP2Cs is released when it forms a trimeric complex with ABA and PYR/PLR/RCAR proteins (Melcher *et al.*, 2009; Miyazono *et al.*, 2009; Nishimura *et al.*, 2009; Yin *et al.*, 2009). Biochemical and protein interaction experiments indicate that ABA receptors can interact with several members of the clade A PP2Cs to activate the downstream targets (Joshi-Saha *et al.*, 2011; Fuchs *et al.*, 2013). The multiple combinations between the ABA receptors and these co-receptors may provide specific modules, which enable plants to deal with diverse stress stimulation (Joshi-Saha *et al.*, 2011).

Mutations in PP2Cs strongly affect stomatal movement. The gain-of-function mutants *abi1-1* ($ABI1^{G180D}$) and *abi2-1* ($ABI2^{G168D}$) display severe wilting phenotype because of an impaired stomatal closure (Koornneef *et al.*, 1984; Roelfsema & Prins, 1995; Gosti *et al.*, 1999). Moreover, *abi1-1* and *abi2-1* disrupt the ability of ABA to inhibit blue light-induced H^+-ATPase activity (Hayashi *et al.*, 2011) and to activate S-type anion currents in guard cells (Pei *et al.*, 1997; Roelfsema *et al.*, 1998; Roelfsema *et al.*, 2004). In contrast, the loss-of-function PP2C single mutants, *hab1-1* and *pp2ca-1* show a hypersensitive inhibition of seed germination by ABA (Saez *et al.*, 2004; Kuhn *et al.*, 2006), and double

mutants of *hab1-1/pp2ca-1* and *abi1-2/pp2ca-1* show a reduced water loss from leaves and enhance drought stress resistance (Rubio *et al.*, 2009). These data thus are in line with a function of PP2Cs as negative regulators in ABA signaling.

The negative role of PP2Cs in ABA signaling is achieved by inhibition of positive regulators. Biochemical experiments revealed that ABI1 is able to interact with and suppress the kinase activity of OST1/SRK2E, CPKs and CIPKs (Yoshida *et al.*, 2006; Fujii *et al.*, 2009; Hedrich & Geiger, 2017). Moreover, Brandt *et al* (2015) reported that ABI1 and PP2CA rapidly remove the phospho-groups of SLAC1 added by CPK21, CPK23, and OST1, so that the anion channels are maintained in their closed state.

1.7.3 Ca^{2+}-independent protein kinases

OST1/SnRK2.6

The protein kinases involved in ABA signaling are divided into two groups, according to their ability to sense cytosolic Ca^{2+}. The first group OST1/SnRK2.6/SRK2E (Sucrose nonfermenting 1-Related protein Kinases 2.6), together with its homologous SnRK2.2/SRK2D, SnRK2.3/SRK2I, are Ca^{2+}-independent protein kinases which are strongly activated by ABA (Umezawa *et al.*, 2004; Umezawa *et al.*, 2009). OST1/SnRK2.6/SRK2E plays a key role in guard cells and has been studied intensively.

OST1/SnRK2.6 (Open Stomata 1) was initially isolated in an infrared thermography screen (Merlot *et al.*, 2002) and identified as an ABA-activated protein kinase which is similar to the AAPK in *V. faba*. (Li & Assmann, 1996; Li *et al.*, 2000; Mustilli *et al.*, 2002; Yoshida *et al.*, 2002). Both OST1 and AAPK are ABA-activated, Ca^{2+}-independent, protein kinases. The role of AAPK in guard cells was supported by expression of a kinase-dead variant ($AAPK^{K43A}$, Lys-43 replaced by Ala-43) to wild-type *V. faba.* This nonfunctional AAPK prevented ABA-induced stomatal closure and disrupted ABA-activation of anion channels (Li *et al.*, 2000). Likewise, *ost1* mutants exhibit higher stomatal conductance and do not close in response to ABA (Mustilli *et al.*, 2002; Yoshida *et al.*, 2002; Acharya *et al.*, 2013). In contrast, stomata in OST1 overexpression plants are hypersensitive to ABA (Acharya *et al.*, 2013; Liang *et al.*, 2015). Mutation in OST1/SnRK2.6 mainly impacts the ABA-sensitivity of guard cells, whereas the double mutant *snrk2.2/2.3* affects seed germination, dormancy and seedling growth. Mutants that have lost the OST1 protein

kinase, as well as the homologous SnRK2.2 and 2.3 proteins, show severe defects in plant growth, and their tiny leaves have high transpiration rates. The *snrk2.2/2.3/ost1* mutant only produces few seeds, which do not display any dormancy (Fujii & Zhu, 2009; Fujita *et al.*, 2009). Overall, these studies provide strong evidence for the protein kinases OST1, SnRK2.2 and 2.3 are key positive regulators in ABA signaling.

The activity of OST1 is strongly suppressed in the gain-of-function *abi1-1* mutant (Yoshida *et al.*, 2006; Umezawa *et al.*, 2009), whereas it has higher activity in the loss-of-function *abi1, abi2*, and *hab1* mutants (Vlad *et al.*, 2009). This indicates that OST1 is negatively regulated by PP2Cs in ABA signaling. Biochemical experiments showed that OST1 physically interacts with ABI1 via its Domain II (ABA box) at C terminal (Yoshida *et al.*, 2006). PP2Cs inhibits the OST1 activity via dephosphorylation of Ser176, which is located in the activation loop and is essential for OST1 autoactivation (Ng *et al.*, 2011; Yunta *et al.*, 2011).

The positive role of OST1 is accomplished by regulation of several downstream targets, which are important for stomatal closure. Patch-clamp recording revealed that the S-type anion channel currents are strongly reduced in *ost1-2* guard cells (Geiger *et al.*, 2009b), while the overexpression lines of OST1 enhance the activity of ABA-activated S-type anion channels (Acharya *et al.*, 2013). By employing experiments with *Xenopus* oocytes, Geiger *et al.,* (2009b) revealed that OST1 interacts with and activates SLAC1. However, OST1 fails to stimulate the SLAC1^{S120A} mutant, indicating that S120 of SLAC1 is a crucial phosphorylation site of OST1. Apart from S120, several other phosphorylation sites in SLAC1 have been identified as the targets for OST1 *in vitro*, but *in vivo* verification has yet to be conducted (Vahisalu *et al.*, 2010; Brandt *et al.*, 2012; Maierhofer *et al.*, 2014a). In addition to SLAC1, OST1 appears to regulate the R-type anion channel QUAC1 (Imes *et al.*, 2013), since the loss of OST1 attenuates R-type anion channel currents in guard cell protoplasts. In *Xenopus* oocytes, OST1 interacts with QUAC1 and stimulates the activity of the channel. Activation of QUAC1 by OST1 is due to a change in the QUAC1 voltage-dependent gating of the channel (Imes *et al.*, 2013). Besides the regulation of anion channels, OST1 was reported to interact with the C-terminus of KAT1, and phosphorylate the residue of Thr-306, which is essential for channel activity. This suggests that OST1 can also inactivate KAT1 via phosphorylating the Thr-306 in KAT1 (Sato *et al.*, 2009). However,

a recent study could not configure this role of OST1, since KAT1 currents cannot be inhibited by OST1 in *Xenopus* oocytes (Zhang *et al.*, 2016). In addition to its role in regulating ion channels, OST1 also regulates several transcription factors including AREB1 (ABA responsive elements-binding protein or -binding factors1), AREB2, and ABF3. These transcription factors can alter stress-responsive gene expression and thus affect plant drought stress resistance (Yoshida *et al.*, 2010). Overall, OST1 has a dual impact on both anion channels and the inward K^+ channel KAT1, while OST1 also mediates changes in gene transcription, which will affect stomatal movement in a long-time frame.

GHR1

The receptor-like kinase GHR1 (Guard cell Hydrogen peroxide-Resistant 1) is likely to play an important role in stomatal responses to apoplastic ROS, and also implicated in response to ABA, high CO_2 concentrations, and diurnal light/dark transitions (Hua *et al.*, 2012; Horak *et al.*, 2016; Sierla *et al.*, 2018). Just as OST1, GHR1 interacts with and activates SLAC1 (Hua *et al.*, 2012), but the activation mechanism was shown to not dependent on the kinase activity of GHR1 (Sierla *et al.*, 2018). Instead, GHR1 was regarded as a pseudokinase, based on the finding that it lacks key residues in its kinase domain. Moreover, neither wild type GHR1 nor the putative phosphomimic $GHR1^{N897D}$ can phosphorylate the artificial substrate myelin-basic protein (MBP) or the physiologically relevant SLAC1 N-terminal domain in the *in vitro* kinase assays (Sierla *et al.*, 2018). Instead of phosphorylation, the activation of SLAC1 by GHR1 relies on the interaction, since the $GHR1^{G108D}$ and $GHR1^{D293N}$, which cannot interact with SLAC1, fail to activate SLAC1 in oocytes. It was proposed that the interaction between GHR1 and SLAC1 could trigger a conformational change in the channel and thus modulates the channel properties (Sierla *et al.*, 2018).

MAPK kinases

The role of MAPK kinases in ABA-signaling has been proposed (Jammes *et al.*, 2009). It was shown that ABA enhances the activity of MPK12 in guard cells, and that ABA-activated S-type anion channels are impaired in the *mpk9-1/12-1* mutant (Jammes *et al.*, 2009). It was suggested that the homologous MPK9 and MPK12 protein kinases function upstream of anion-channels but downstream of ROS signals in the ABA signaling pathway

that triggers stomatal closure (Jammes *et al.*, 2009). Other components of MAPK cascade, including MAP3K17/18, MKK3, and MPK1/2/7/14, are also shown to modulate ABA signaling by the phosphorylation of the AREB/ABF transcription factors (Danquah *et al.*, 2015; Matsuoka *et al.*, 2015; Mitula *et al.*, 2015; de Zelicourt *et al.*, 2016). These data suggest that MAPK kinases represent important regulators in ABA-induced stomatal movements.

1.7.4 Ca^{2+}-dependent protein kinases

A central role for Ca^{2+} signals in ABA-induced stomatal closure has been suggested in several reviews (Schroeder *et al.*, 2001; Hetherington & Brownlee, 2004; Kim *et al.*, 2010). However, several studies showed that ABA-induced stomatal closure can also occur without elevation of cytosolic Ca^{2+} (McAinsh *et al.*, 1990; Macrobbie, 1992; Grabov & Blatt, 1998; Staxen *et al.*, 1999; Hamilton *et al.*, 2000; Levchenko *et al.*, 2005; Marten *et al.*, 2007b; Stange *et al.*, 2010). Overall, these studies thus indicate that guard cell ABA signaling pathway possesses a Ca^{2+}-dependent and an -independent branch (Roelfsema & Hedrich, 2005; Cutler *et al.*, 2010). Both branches share the same initial components of the PYR/PYL/RCAR-type ABA receptor(s) and the PP2Cs co-receptors (Hedrich & Geiger, 2017). The components of the Ca^{2+}-dependent branch include Ca^{2+} channels and Ca^{2+}-dependent protein kinases, which can bind and translate the Ca^{2+} signals into physiology function. In *Arabidopsis*, CPKs (Ca^{2+}-dependent Protein Kinases) and CBL/CIPKs (Calcineurin B-Like protein/CBL-Interacting Protein Kinases) have been implicated as the Ca^{2+}-dependent protein kinases that are important for ABA-induced stomatal closure.

CPKs

CPKs have a unique structure that combines a Ca^{2+}-sensor domain and a protein kinase effector domain within one molecule (Wernimont *et al.*, 2011). The structure of CPKs comprises a variable N-terminal domain, a serine/threonine protein kinase domain tethered to a CLD (C-terminal CaM-like domain) via an autoinhibitory junction. CLD contains Ca^{2+} binding domain EF-hands (Harper *et al.*, 2004; Bender *et al.*, 2018). In the inactive conformation, the autoinhibitory junction binds to the kinase domain, preventing substrate binding. Upon Ca^{2+} binding, the CLD triggers a conformational

change, releasing the autoinhibitory junction from the kinase domain to get its active state (Liese & Romeis, 2013).

The CPK family (34 members in *Arabidopsis*) have multiple functions in aspects of plant growth and development, defense responses and adaptation (Curran *et al.*, 2011; Boudsocq & Sheen, 2013; Westlake *et al.*, 2015). Recent work has identified several CPKs that are able to regulate SLAC1 (Hedrich & Geiger, 2017). By applying split YFP-based protein interaction assays, Geiger *et al.,* (2010) found out that CPK21 and its close homolog CPK23 are the major interacting partners of SLAC1 in guard cells. Both CPK21 and CPK23 are capable of activating SLAC1 in oocytes, but the current amplitude of SLAC1 induced by CPK23 is larger than that provoked by CPK21. However, this distinction is lost if the constitutively active forms of CPKs are made, of which the autoinhibitory C-terminus (EF-hands) is deleted. *In vitro* phosphorylation assays revealed that the Ca^{2+}-sensitivity differs between CPK21 and 23. The activity of CPK21 is tightly regulated by the cytosolic Ca^{2+} concentration, whereas CPK23 has already 60% of maximum activity at Ca^{2+} concentration of non-excited cells (~100 nM). These results demonstrated that SLAC1 can be regulated by CPKs with distinct Ca^{2+} affinity (Geiger *et al.*, 2010).

In line with the oocyte data, S-type anion channel currents are reduced in guard cells of *cpk23* mutant (Geiger *et al.*, 2010). A reduction in the activity of S-type anion channels is supposed to cause more open stomata, but the mutant exhibits less water transpiration and enhances drought stress resistance (Ma & Wu, 2007). These controversial data may be explained by the up-regulated level of ABI1 in *cpk23* mutant, which ABI1 interacts with and inhibits protein kinases, thus preventing SLAC1 activation (Geiger *et al.*, 2010). For CPK21, the impact on guard cell S-type anion channel currents has not been reported. The *cpk21* mutant has a wild type like stomatal conductance (Merilo *et al.*, 2013), even though CPK21 is able to activate SLAC1 and GORK in oocytes (Geiger *et al.*, 2010; van Kleeff *et al.*, 2018), which both are important for stomatal closure. The role of CPK21 in stomatal closure regulation thus still needs to be investigated.

In addition to CPK21 and CPK23, CPK3 and its homolog CPK6 have been shown to affect ABA signaling in guard cells (Mori *et al.*, 2006). The double mutant *cpk3/6* was partially impaired in ABA- and Ca^{2+}-induced stomatal closure, which may be due to the inability of ABA and Ca^{2+} to activate S-type anion channels (Mori *et al.*, 2006). In line with this

hypothesis, both CPK3 and CPK6 were shown to activate SLAC1 and SLAH3 in oocytes (Brandt *et al.*, 2012; Scherzer *et al.*, 2012). CPK3-activated SLAC1 is in a Ca^{2+} dependent manner; whereas CPK6 activity does not depend on the cytosolic Ca^{2+} concentration (Ca^{2+}-independent) (Scherzer *et al.*, 2012). Moreover, CPK6 phosphorylates SLAC1 at Ser-59, a position that differs from the target site of OST1 (Ser-120). Taken together, CPK3 and CPK6 seem to regulate stomatal movements by phosphorylating and activating SLAC1 and SLAH3.

CBL/CIPKs

The model of action of CBL/CIPKs is unique, since the Ca^{2+} sensor (CBL) and effector (CIPK) are separated into separate proteins (Kudla *et al.*, 2018). The modular structure of CIPKs contains a short N-terminal domain, followed by a serine/threonine protein kinase domain, a junction region and a C-terminal regulatory domain (Edel & Kudla, 2015). An auto-inhibitory NAF domain (with the conserved amino acids N, A and F) and the phosphatase interaction (PPI) motif are found in the regulatory domain (Ohta *et al.*, 2003). Upon binding of Ca^{2+} to the EF-hands of CBLs, these proteins interact with CIPKs, which leads to a release of the kinase domain from inhibition of the autoinhibitory NAF domain (Chaves-Sanjuan *et al.*, 2014). The interaction between CBLs and CIPKs is also important for targeting to their substrate and changing their subcellular localization (Hashimoto *et al.*, 2012).

In *Arabidopsis*, numerous CIPKs (26 members) and CBLs (10 members) provide a large number of sensor-responder combinations, which may facilitate the versatile functions. In guard cells, CIPK23 and CIPK11 have an important role in regulating stomatal movements (Maierhofer *et al.*, 2014a; Saito *et al.*, 2018). CIPK23-CBL1 (or CBL9) module is able to activate SLAC1 in the oocytes. Like CPKs, the activation of SLAC1 by CIPK23 requires the interaction and phosphorylation of the N-terminus of SLAC1, and the activation is suppressed by ABI1. Just as the CPKs, CIPK23 can also activate SLAH3 (Maierhofer *et al.*, 2014a). The activation of SLAC1 and SLAH3 anion channels by CIPK23 is supposed to lead to stomatal closure. Based on this assumption, loss of CIPK23 function thus should cause stomatal opening and hyposensitivity to ABA. However, the *cipk23* knock-out mutant, as well as the double mutant *cbl1/9,* displayed less

transpiration and an improved drought stress tolerance (Cheong *et al.*, 2007). Apparently, the oocyte data (activation of SLAC1/SLAH3 by CIPK23) do not match with the *cipk23* phenotype, and the mechanism by which CIPK23 regulates stomatal movements needs to further study.

Recently, Saito *et al.,* (2018) demonstrated that the modification of N-myristoylation and S-acylation at N-terminus of CPKs or CBLs are essential for CIPK11/CBL5 and CPK6 to activate SLAC1. Protein sequence analysis revealed that these motifs are conserved among the CBLs and CPKs, which implies that the modification of N-myristoylation and S-acylation is a common requirement for these kinases to modulate the activity of ion channels (Saito *et al.*, 2018). In *planta*, CIPK11/PKS5 is a negative regulator of the plasma membrane proton pump AHA2 (Fuglsang *et al.*, 2007). However, it has so far not been reported that CIPK11 affects stomatal movements.

1.7.5 The agricultural application

The increasing worldwide population and climate change are challenges for global food security (Lesk *et al.*, 2016). The improvement of crop productivity is an urgent task for population dense countries, such as China, which has a population of 1.4 billion people. Drought periods, which frequently occur in agricultural areas, cause significant reductions in crop yield (Lesk *et al.*, 2016). In order to cope with the drought stress, plants employ the phytohormone ABA to reduce stomatal conductance and loss less water from leaves. In the past two decades, the core components of the ABA signaling cascade were found to consist of receptor PYR/PYLs/RCARs, co-receptors PP2Cs, and Ca^{2+}-independent and dependent protein kinases, and anion channels. Even though most of these studies have been conducted with the model plant *Arabidopsis*, they provide a blueprint to modify ABA signaling in commercial crops and help to improve their yields and drought tolerance.

Based on the current ABA signaling model, overexpression of positive regulators will result in ABA hypersensitive plants. For example, overexpression of the ABA receptors or SnRK2s should confer drought stress tolerance, whereas the accumulation of PP2Cs (negative regulators) is likely to weaken the ability of plants to deal with water deficiency (Ben-Ari, 2012; Miao *et al.*, 2018). Indeed, many transgenic crops, including rice (Kim *et*

al., 2014; Tian *et al.*, 2015b; Verma *et al.*, 2019), maize (He *et al.*, 2018), wheat (Zhang *et al.*, 2012; Tong *et al.*, 2017), soybean (Barbosa *et al.*, 2013), tomato (Park *et al.*, 2015) and cabbage (Yuan *et al.*, 2013), have enhanced the drought stress responses by changing their ABA signaling. To date, DroughtGard^{TM} Hybrids, which overexpress CspB (cold shock protein B RNA chaperone from *Bacillus subtilis*) in maize, is the only commercially available crop that improves drought stress tolerant and improves approximately 10% yield under water-deficit conditions compared to non-transgenic plants (Castiglioni *et al.*, 2008) (https://www.genuity.com/corn/Pages/DroughtGard-Hybrids.aspx).

Alternatively, drought tolerance can be induced by application of commercial ABA agonists or antagonists (**Fig. 1.6**). The synthetic ABA agonist, pyrabactin has been pivotal for the identification of the ABA receptors PYR1/PYL/RCAR family (Park *et al.*, 2009). Just as pyrabactin, quinabactin (also known as AM1) can induce stomatal closure and enhance crop drought stress resistance (Cao *et al.*, 2013; Okamoto *et al.*, 2013). The commercial agrochemical of mandipropamid functions as a selective agonist of engineered PYR1^{MANDI} to control the transpiration and drought tolerance in transgenic plants (Park *et al.*, 2015). Apart from agonist, ABA antagonists DFPM and AS6 have been designed and tested (Kim *et al.*, 2011; Takeuchi *et al.*, 2014). Recently, AA1 (ABA Antagonist 1), the first broad-spectrum antagonist of ABA receptors in *Arabidopsis,* is reported and functions to delay leaf senescence and fruit ripening in tomato (Ye *et al.*, 2017).

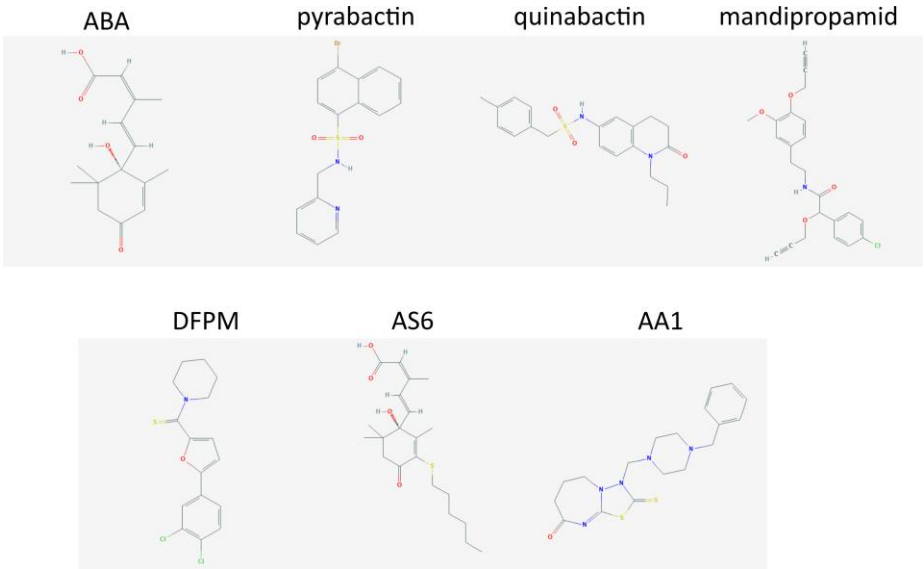

Fig. 1.6 The 2D structure of ABA and its agonists, antagonists.
(The structures are downloaded from https://pubchem.ncbi.nlm.nih.gov)

It is no doubt that the core ABA signaling pathway established in guard cells can be used to improve plant drought stress tolerance. However, many species specific aspects of ABA signaling remain to be addressed in the future, before agricultural application can be realized. Firstly, ABA signaling in the dicot *Arabidopsis* may differ from agriculturally important monocot crop plants (e.g. rice, corn, wheat, sorghum, barley). One example is that ABA-induced stomatal closure in barley (*Hordeum vulgare*) is NO_3^--dependent, whereas it is not required for *Arabidopsis*. This difference is due to a tandem amino acid residue motif of SLAC1 channels in monocots, which is distinct from that in dicots (Schafer *et al.*, 2018). Thus, it is important to dissect the ABA signaling in detail in crop plants. Secondly, improvement of drought stress tolerance in crop plants, by modifying ABA signaling, will raise concerns about the safety of genetically modified organism (GMO), which is still in a fierce debate. Therefore, the procedures that used to evaluate the safety of GMOs and address public concern, are critical steps to be taken, before such plants can be used in agriculture. Thirdly, application of ABA agonists, or antagonists provides an alternative strategy to improve plant drought stress tolerance, but the safety of these chemicals for human consumption and biodiversity still has to be tested. Overall, the new knowledge about ABA signaling provides us new strategies to improve plant drought stress tolerance, which will help to improve agricultural productivity.

2. Material and methods

2.1 Plant material and growth conditions

All *Arabidopsis thaliana* lines used in this study were in Col-0 background and are listed in **Table 2.1**. Seeds were sown on sterilized soil and plants were grown in a climate cabinet, with equal day and night length (day/night cycle of 12/12 h, temperatures of 21/18 °C). The photon flux density and relative humidity were maintained 100 µmol m^{-2} s^{-1}, and 60%, respectively. After 2 weeks, the seedlings were carefully transferred to new pots (diameter 6 cm) and grown for another 2-3 weeks, at the same conditions.

Table 2. 1 The description of plants used in this study

Line	Description	Reference
Col-0	Wild type, Columbia-0	-
ost1-3 (SALK_008068)	OST1 T-DNA insertion line	(Yoshida *et al.*, 2002)
slac1-3 (SALK_099139)	SLAC T-DNA insertion line	(Negi *et al.*, 2008; Vahisalu *et al.*, 2008)
slah3-1 (GABI Kat371G03)	SLAH3 T-DNA insertion line	(Geiger *et al.*, 2011)
slac1-3/slah3-1	Double mutant	(Guzel Deger *et al.*, 2015)
R-GECO-mTurquoise	Cytosolic Ca^{2+} indicator in Col-0	(Waadt *et al.*, 2017)
ost1-3 (R-GECO-mTurquoise)	Cytosolic Ca^{2+} indicator in *ost1-3*	**Generated in this study**
LKS,OE	CIPK23 overexpression line	(Xu *et al.*, 2006)
lks1-3 (SALK_036154)	CIPK23 T-DNA insertion line	(Xu *et al.*, 2006)
cipk23-1 (SALK_032341)	CIPK23 T-DNA insertion line	(Cheong *et al.*, 2007)
Venus	Estrogen-induced Venus	**Generated in this study**
CIPK23	Estrogen-induced *CIPK23*	**Generated in this study**
$CIPK23^{T190D}$	Estrogen-induced $CIPK23^{T190D}$	**Generated in this study**
$CIPK23^{K60N}$	Estrogen-induced $CIPK23^{K60N}$	**Generated in this study**

Experiments were either performed on stomata in intact leaves, or with isolated epidermal strips. The intact leaves were detached from 4-5 weeks old plants with a sharp razor blade, and the adaxial side was gently fixed in a petri dish (diameter 35 mm) with

double-sided adhesive tape. The leaves were immediately submerged in a bath solution (10 mM KCl, 1 mM $CaCl_2$ and 10 mM K/citrate, pH 5) and illuminated with 100 µmol m^{-2} s^{-1} white light for at least 2 h before the start of the experiment.

Epidermal strips were gently peeled from the abaxial side with a tweezer. The strips were fixed on round cover slips (diameter 18 mm) with medical adhesive (Medical Adhesive B, Aromando, http://www.amt-med.de) and kept in the following bath solution: 10 mM KCl, 1 mM $CaCl_2$, 10 mM MES-BTP, pH 6.0.

2.2 Electrophysiological recording in guard cells

2.2.1 The two-electrode voltage clamp technique

The electrical conductance of the plasma membrane was recorded with the two-electrode voltage clamp technique (**Fig. 2.1**). The conventional voltage clamp consists of two separate microelectrodes, which can be used to impale the large cells, such as *Xenopus* oocyte. However, for the small cells, like *Arabidopsis* guard cells, the double-barreled electrode as shown (**Fig. 2.2b**) in can reduce membrane damage, and is easier to manipulate under the microscope. The electrodes are filled with a conductive solution (normally KCl). The voltage recording barrel (M1) is recording the membrane potential, which can be clamped to a command value with the current injection barrel (M2). The magnitude of injection current is equal to the net current caused by ions that move across the cell membrane. Based on these recordings, the ion conductance of the membrane potential can be determined. The voltage clamp system relies on at least two amplifiers. The input amplifier (A_1) measures the membrane potential (V_{in}), while the differential amplifier (A_2) compares the difference between the value from A1 with the command voltage V_{cmd}. A compensation current is injected into the cell by the current-injection amplifier, so that V_{in} approaches to V_{cmd}. The efflux of positively charged ions at the plasma membrane is designed as an outward current, while the influx is regarded as an inward current.

2.2.2 Voltage clamp recordings in guard cells

The plasma membrane conductance of guard cells was recorded with the voltage clamp technique using double-barreled microelectrodes (**Fig. 2.2b**). These microelectrodes were prepared from two borosilicate capillaries (inner diameter, 0.58 mm; outer diameter, 1.0

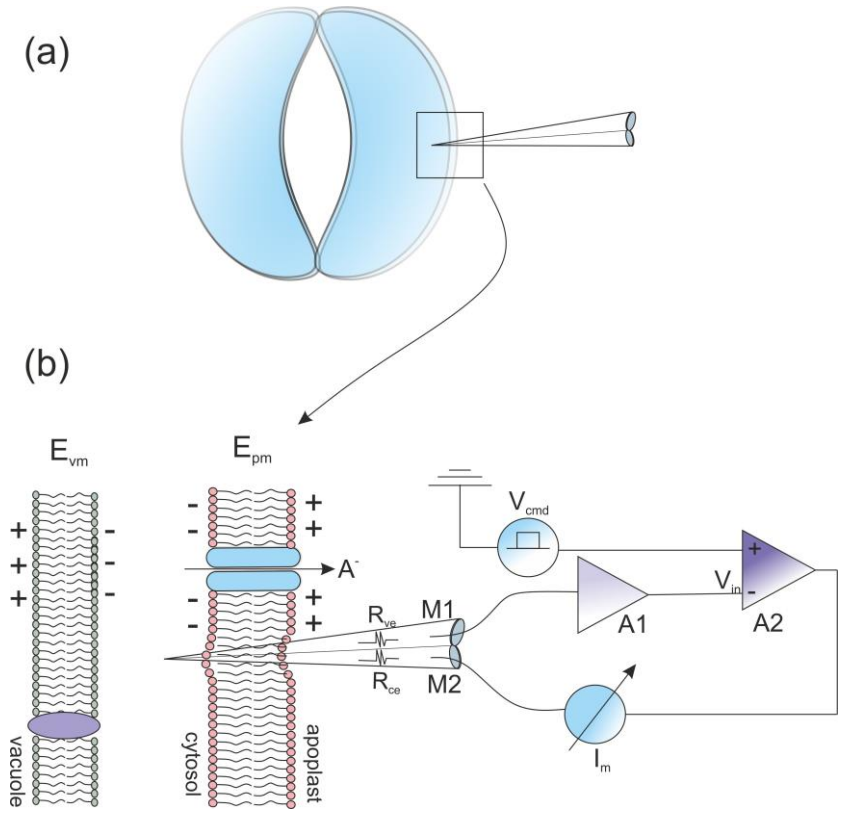

Fig. 2.1 Two electrode voltage clamp technique applied to guard cells.

(a) Schematic representation of a guard cell that is impaled with a double-barreled electrode. The rectangle area is enlarged in b.

(b) The double-barreled electrode penetrates the plasma membrane of a guard cell and the tip is positioned in the cytosol of the cell. The voltage recording barrel M1, is connected to an input amplifier A1, which monitors the membrane potential. A differential amplifier A2 is used to compare input voltage V_{in} and the command voltage V_{cmd}. A current will be injected into the guard cell through the current injection barrel M2, if the value of V_{in} differs from V_{cmd}. Abbreviation, M1: voltage recording barrel; M2: current injection barrel; R_{ve}: the resistance of the voltage recording barrel; R_{ce}: the resistance of the current injection barrel; A1: the input amplifier; A2: the differential amplifier; V_{cmd}: command voltage; I_m: membrane current; E_{pm}or V_{in}: the membrane potential of plasma membrane; E_{vm} the membrane potential of vacuole membrane.

mm; Hilgenberg) in two steps. First, the capillaries were aligned, heated, twisted 360 degrees, and pre-pulled by a vertical puller (L/M-3P-A, Heka). Subsequently, the pre-pulled capillaries were pulled on a horizontal laser puller (P 2000; Sutter Instruments Co., http://www.sutter.com). The resistance of electrodes is ranged from 200 to 280 MΩ when filled with 300 mM KCl. The electrodes were backfilled with 300 mM KCl to study the activity of K^+ channels, while they were filled with 300 mM CsCl to record S-type

anion channels (Guzel Deger *et al.*, 2015). A reference electrode, which was made from a capillary filled with 300 mM KCl and sealed with 2% agarose (prepared in 300 mM KCl solution), was placed in the bath solution (**Fig. 2.3**). Ag/AgCl half-cells were used to connect the electrodes to a custom-made amplifier (Ulliclamp01) equipped with headstages with an input impedance of 10^{11} Ω. Guard cells were impaled with the electrodes by using a piezo-driven micromanipulator (MM3A, Kleindiek Nanotechnik) (**Fig. 2.3**). Voltage clamp pulses were applied with WinWCP software (Dempster, 1997) (University of Strathclyde, https://www.strath.ac.uk). The electrical signals were first low-pass filtered at 0.5 kHz with a dual low-pass Bessel Filter (LPF 202A; Warner Instruments Corp., United States, www.warneronline.com), and recorded at 1 kHz with the National Instruments interfaces (USB-6002, http://www.ni.com).

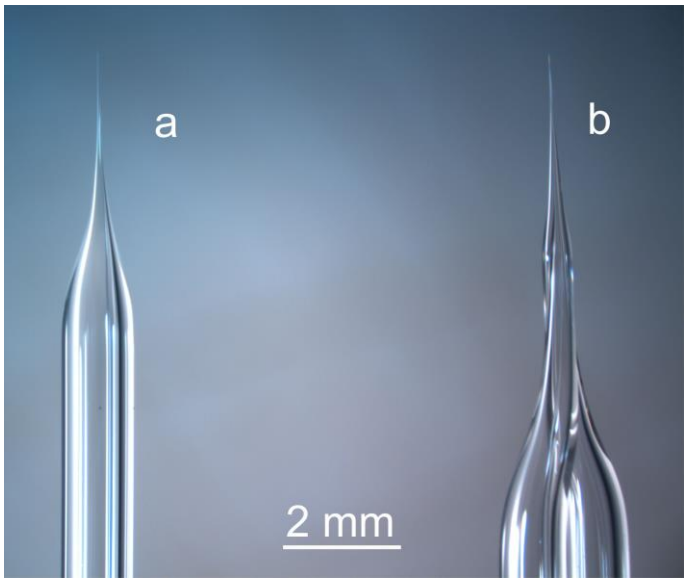

Fig. 2.2 Microelectrodes used for guard cells impalement or current ejection

Single- (a) and double- (b) barreled electrodes used for guard cell electrophysiological measurements. Scale bar=2 mm.

2.3 Current ejection technique

The cuticle on the surface of intact leaves prevents solutes from entering the leaves. To overcome this physical obstacle, an electrode filled with ABA solution is slowly moved and touched/connected to the guard cell wall. Subsequently, ABA is ejected to the cell wall by applying a negative current (**Fig. 2.3**). This method was named the current ejection technique.

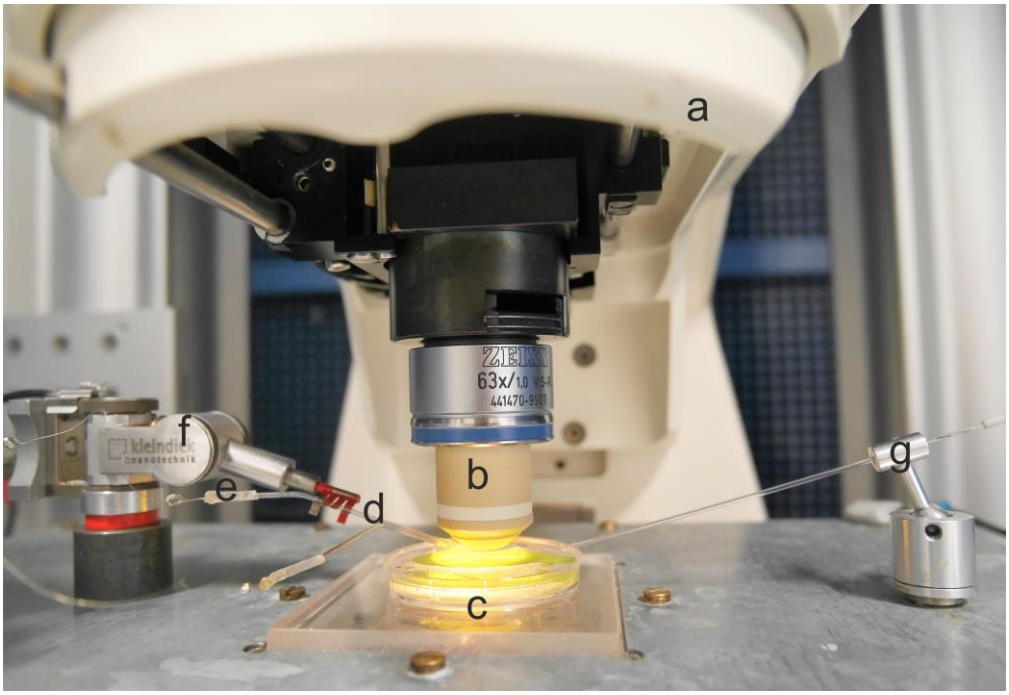

Fig. 2.3 Setup for guard cell impalement and current ejection experiments

Image of the experimental setup with an upright microscope (Axioskop 2FS, ZEISS) (a), 63x/1.0w objective (ZEISS) (b), intact leaf fixed on a Petri dish (c), double-barreled electrode (d), half-cell (e), micromanipulator (Kleindiek) (f), reference electrode (g).

2.3.1 Application of ABA to single guard cell in intact leaves

The current ejection technique was applied to guard cells in the abaxial epidermis of intact leaves. Open stomata were visualized with an upright microscope (Axioskop 2FS, Zeiss) equipped with a water immersion objective (W Plan-Apochromat, 63x/1.0, Zeiss, http://www.zeiss.com). The tip of a single-barreled electrode was filled with either 50 µM ABA, or 50 µM benzoic acid as control, while the remaining of the barrel was filled with 300 mM KCl. For the dose-response experiments, concentrations ranging from 0.5 to 100 µM of ABA were used. The electrodes were connected via Ag/AgCl half-cells to a headstage (with an input impedance of 10^{11} Ω) of a custom-made amplifier (Ulliclamp01). A reference electrode filled with 300 mM KCl and sealed with 2% agarose in 300 mM KCl was placed into the bath solution. The microelectrode was slowly moved towards the cell wall of guard cells with the piezo-driven micro-manipulator. The tip potential changed from a value of approximately 0 mV to voltages in the range -8 to -15 mV after the electrode got in contact with the guard cell wall. Subsequently, a current of -0.8 nA, for a period of 20-30 s, was applied via the electrodes, which forces the negatively charged

ABA, or benzoic acid as control, to move out from the tip into the cell wall. After the current ejection, the microelectrode was rapidly removed from the guard cell wall.

2.3.2 Estimation of the ABA concentration on the guard cell wall after current ejection

The ABA concentration achieved in the guard cell wall, after current ejection, was estimated with the fluorescent dye Lucifer Yellow CH (LY) (Stewart, 1978). Firstly, the fluorescence signal of LY was calibrated to its concentration with the following procedure. Single-barreled microelectrodes (**Fig. 2.2a**) were pulled from borosilicate glass capillaries (inner diameter, 0.58 mm; outer diameter, 1.0 mm; Hilgenberg, http://www.hilgenberg-gmbh.com) on a horizontal laser puller (P2000; Sutter Instruments Co., Novato, CA, USA). The tip of microelectrodes was broken to an opening of 0.5 µm, and filled with a range of LY concentrations (0; 1; 2.5; 5 and 10 µM). LY was pressure injected into the standard bath solution with 1 s pulses (at 30 psi) using a Picospritzer II microinjection system (General Valve). Simultaneously, the LY signal was acquired with a charge multiplying CDD camera (QuantEM, Photometrics, http://www.photometrics.com) mounted to the fluorescence microscope. The following filter setting was used: λ_{Ex}= 430/24 nm (ET 430/24 Chroma Technologies, www.chroma.com); λ_{Em}=520/30 nm (520/30 nm, Brightline, Semrock, http://www.semrock.com); dichroic mirror=499 nm.

In the next step, the tip of a single barrel microelectrode was filed with 50 µM LY and current-ejected into the guard cell wall, using the same conditions as for ABA. The amount of ABA that was current injected into guard cell was estimated based on the LY data. The ratio between the flux of ABA and LY, injected into the guard cell wall, is given by Eq. 1;

$$\frac{J_{ABA}}{J_{LY}} = \frac{[ABA]\, Vd_{ABA}}{[LY]\, Vd_{LY}} \qquad (Eq.1)$$

the concentration of dissociated ABA^- is 21 µM, assuming a pKa of 4.8 (www.chemicalbook.com), while LY will be fully dissociated at a concentration of 50 µM (Stewart, 1978) and Vd_{ABA} and Vd_{LY} represent the drift velocity of ABA and LY. The drift velocity can be calculated with Eq. 2;

$$Vd = \mu_q\, E \qquad (Eq.2)$$

in which μ_q is the electrical mobility of an ion and E the electrical field that acts on the ion. If an identical electrical field is assumed to act on ABA and LY, the ratio in drift velocity will be given by Eq. 3.

$$\frac{\mu_{q(ABA)}}{\mu_{q(LY)}} = \frac{q_{(ABA)}\ \mu_{(ABA)}}{q_{(LY)}\ \mu_{(LY)}} \qquad (Eq.3)$$

in which q represents the number of elementary charges (q=1 for ABA and q=2 for LY), and μ the chemical mobility that can a from the diffusion constants of ABA ($6x10^{-10}$ m^2 s^{-1}) (Slovik *et al.*, 1992) and LY ($5x10^{-10}$ m^2 s^{-1}) (Imanaga *et al.*, 1987) using Eq. 4;

$$\mu = \frac{D}{K_b\ T} \qquad (Eq.4)$$

in which K_b is Boltzmann's constant and T the absolute temperature.

Based on these considerations, a ratio J_{ABA}/J_{LY} = 0.25 was calculated and this value was used to estimate the ABA concentration that was applied in the guard cell wall.

2.4 Live-cell imaging of guard cell Ca^{2+} signals in intact leaves

Live cell Ca^{2+} imaging was performed on Col-0 or *ost1-3* plants that were transformed with the genetically encoded Ca^{2+} indicator R-GECO1-mTurquoise (Waadt *et al.*, 2017).

2.4.1 Acquisition of Ca^{2+} signals from R-GECO1-mTurquoise

Guard cells expressing the Ca^{2+} indicator R-GECO1-mTurquoise were visualized with an upright microscope (Axioskop 2FS, Zeiss), which was equipped with a CARV confocal spinning disc unit (CARV II, Crest Optics, http://www.crestopt.com) and a charge multiplying CDD camera (QuantEM, Photometrics, http://www.photometrics.com). The CARV unit was equipped with excitation, emission and dichroic filter wheels, which enables a rapid change of filter settings. During the measurements, the spinning disc was moved out of the light path in the CARV. An LED illumination system (pE-4000, CoolLED, https://www.coolled.com), connected to the CARV unit, was used to excite R-GECO1 and mTurquoise with the wavelengths of 435 and 580 nm, respectively. The emission signals from the specimens were first passed through dichroic mirrors with cut off frequencies of 450 nm (T450 LPXR, Chroma, www.chroma.com) and 590 nm (FF593 BrightLine, Semrock, http://www.semrock.com) and then passed through band filters at 475 nm (475/28 nm,

BrightLine HC; Semrock, http://www.semrock.com) and 628 nm (628/40 nm, BrightLine; Semrock). The Ca^{2+} fluorescence signals were calculated from regions of interest in guard cells that included the nucleus. During Ca^{2+}-imaging, changes in stomatal aperture were monitored with far-red light, which was provided by a halogen bulb in the microscope lamp filtered through a far-red light bandpass filter (713/30 nm).

2.4.2 Calibration of R-GECO1-mTurquoise

The fluorescence of R-GECO1-mTurquoise (RG-mT) was calibrated with guard cells in isolated epidermal strips, which were bathed in 10 mM KCl, 1 mM $CaCl_2$, 10 mM MES-BTP, pH 6.0. The ratio signal of RG-mT was converted into cytosolic Ca^{2+} concentrations by using the ratio signal of FURA2. The Ca^{2+} dye FURA2 is widely used to study the cytosolic Ca^{2+} signals in guard cells (McAinsh *et al.*, 1990; Grabov & Blatt, 1998; Levchenko *et al.*, 2005) and the calibration of FURA2 is described below. Guard cells in epidermal strips, which were isolated from RG-mT expressing plants, were impaled with a double-barreled electrode, of which the tip of one barrel was filled with 10 mM FURA2 and the rest with 300 mM KCl, while the second barrel was filled solely with 300 mM KCl. FURA2 was slowly injected into the guard cells through the FURA2 containing barrel, by imposing a -300 pA current (approximately 100 s) to the cells. The emission ratio signal of RG-mT and excitation ratio values of FURA2 were simultaneous monitored by the charge multiplying CDD camera. The RG-mT ratio signals were plotted with those of FURA2 against the Ca^{2+} concentration calculated from FURA2 ratio signal (see below). A Hill function was fitted to the relation between the RG-mT ratio and Ca^{2+} concentration.

2.4.3 Calibration of FURA2

FURA2 was calibrated for guard cells in a similar manner as previously described (Levchenko *et al.*, 2008; Stange *et al.*, 2010; Voss *et al.*, 2016). To this propose, FURA2 was repetitively excited at 345, 360 and 390 nm with UV-flashlight pulses (VisiChrome high-speed polychromator system, Visitron Systems, http://www.visitron.de) for 200 ms, and a time interval of 5 s. The FURA2 emission signal was guided through a dichroic mirror (FT 410; Zeiss, Germany) and a 510 nm bandpass filter (D510/40M, Chroma Technology Corp), before the images were recorded with the CCD camera using the Visiview software package (Visitron). The FURA2 F345/F390 excitation ratio was

converted into the cytosolic free calcium according to the equation of Grynkiewicz *et al.,* (1985):

$$[\mathrm{Ca}^{2+}]_{\mathrm{free}} = K_d \frac{(R - R_{min})F_{min}}{(R_{max} - R)F_{max}}$$

where K_d is the dissociation constant of FURA2 for Ca^{2+} (270 nM), which was determined for *V. faba* guard cells by Levchenko *et al* (2005). R represents the FURA2 emission ratio of signals obtained at 345 and 390 nm, R_{min} and R_{max} correspond to minimal and maximal FURA2 ratio, respectively. F_{min}/F_{max} is the fluorescence ratio of unbound and bound form of FURA2, measured at 390 nm.

To determine the R_{min} in guard cells, epidermal strips were incubated in a bath solution containing 10 mM CsCl, 1 mM $LaCl_3$ and 10 mM MES-BTP, pH 6.0, which blocked K^+- and non-selective cation channels. Guard cells were impaled with double-barreled electrodes; the tip of one barrel was filled with 10 mM FURA2, while the other contained 250 mM BAPTA and the rest of both barrels were filled with 300 mM KCl. After loading of FURA2, BAPTA was injected into the cytosol with currents ranging from -150 to -300 pA. BAPTA-injection caused a decrease for the F345/F390 ratio to an average value of 0.23 (SE=0.002, n=6).

R_{max} was determined with guard cells that were loaded with FURA2 just as described above, but the second barrel of the electrode was filled with 300 mM KCl, instead of BAPTA. The epidermal strips were kept in a bath solution with 10 mM KCl, 1 mM $CaCl_2$ and 10 mM MES-BTP pH 6.0. Guard cells were clamped to -300 mV for 30 s, to get a massive increase of the cytosolic free Ca^{2+} concentration and a rise of the F345/F390 ratio to an average value of 5.34 (SE=0.16, n=6).

All images were analyzed offline with the Image-J/Fiji software package (Schindelin *et al.*, 2012). The statistical and mathematical analysis of the data was carried out with Graphpad Prism 6 (GraphPad Software, USA, https://www.graphpad.com) and Origin Pro 8 (Originlab Corporation, USA, https://www.originlab.com).

2.5 Estrogen-induced guard cell specific expression system

2.5.1 The inducible constructs

The original estrogen-induced construct of pLB12 was generated in the lab of M. D. Curtis and U. Grossniklaus (Department of Plant and Microbial Biology, University of Zürich, Switzerland). The vector map has been published by Brand *et al.,* (2006).

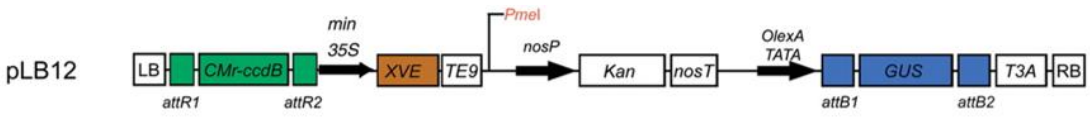

Fig. 2.4 The schematic illustration of the estrogen-induced pLB12 vector.

The main components of pLB12 are represented by boxes and include a bacterial toxin gene CMr-ccdB (for negative selection), an XVE activator, a kanamycin-resistance gene driven by a Nos promoter for plants, and an OlexA responder. LB, Left border; RB, Right border; TE9, TE9 terminator; T3A, terminator; attR1/2 and attB1/2, Gateway att recombination sites.

A USER cassette (Nour-Eldin *et al.*, 2006) and the guard cell specific promoter *pGC1* were inserted, to replace the *GUS* and *CMr-ccdB*, respectively. First, the *GUS* was deleted and replaced by a USER cassette with the following procedure. The sequences upstream (fragment A) and downstream (fragment B) of *GUS* were amplified using the primer pairs A and B. These primers contained *MauBI*/*AsiSI* and a *Swa* I restriction sites (See **Primers**). Fragment A and B were ligated to the pNB1 #16 construct with a USER reaction. A completed fragment AB containing the *Swa* I USER cassette was obtained after *MauBI/AsiSI* digestion and the recovery from pNB1 #16. The *GUS* in the original pLB12 was removed using the *MauBI/AsiSI* enzymes, which the restriction sites are located upstream and downstream of *GUS*. Fragment AB was linked to pLB12 to get the intermediate construct pLB12 without *GUS* (pLB12-M). Next, to replace the *CMr-ccdB* with a guard cell specific promoter *pGC1*, *pGC1* was first introduced to pDONR201 by gateway BP reaction. Subsequently a gateway LR reaction was carried out for pLB12-M and pDONR201-pGC1 to obtain pLB12-pGC1. The linear pLB12-pGC1 was obtained after digested with *Nt.BbvCI* and *Swa* I enzymes. The Gene Of Interests (GOIs), including *Venus*, *CIPK23:Venus, CIPK23^{T190D}:Venus, or CIPK23^{K60N}:Venus*, were amplified with primers that contain *Swa* I restriction site, and then cloned into pLB12-pGC1 with the USER cloning technique. The constructs were verified by sequencing. The modified construct is presented here:

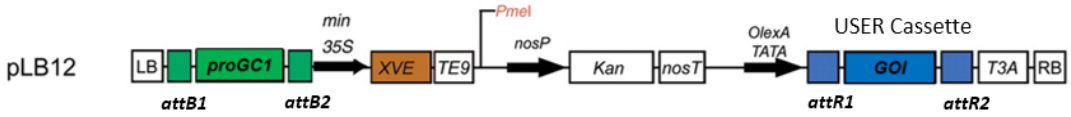

Fig. 2.5 The schematic illustration of modified pLB12.

The *GUS* and *CMr-ccdB* in the original pLB12 vector were replaced with a USER cassette and a guard cell specific promoter *pGC1*, respectively. The USER cassette was used to introduce a Gene of Interest to the construct with the USER cloning technique. The diagram was revised after Brand *et al.,* (2006).

2.5.2 *Arabidopsis* transformation and screening

Arabidopsis was transformed in the flowering stage using the floral dip method with the *Agrobacterium tumefaciens* strain GV3101 (Zhang *et al.*, 2006). The Agrobacterium cells were cultured in YEP liquid containing appropriate antibiotics at 28 °C for overnight. In the stationary growth phase (OD 1.5-2.0), the cells were collected by centrifugation and gently resuspended in 5% sucrose solution. Silwet L-77 was added to the cell suspension at a final concentration of 0.02% (v/v) before floral dipping. The flower stalk of *Arabidopsis* plants was inverted and dipped into the cell suspension for 10 s with gentle agitation. After dipping, the plants were covered with a plastic bag for 16 h, before placing them back into the greenhouse. In general, the transformation was conducted twice, with an interval of one week, to enhance the number of transformed seeds.

Screening of the transgenic seeds was performed on agar plates with kanamycin (for the estrogen-induced plants). Seeds were sterilized with 7% NaClO (1:1 v/v) for 2 min and rinsed with sterile water for at least 6 times to remove the bleach. Seeds were resuspended in water and pipetted onto the selective plates. After the vernalization at 4 °C for 2-3 d, the plates were transferred to the growth cabinet. After 2 weeks, the transformed seedlings had healthy green cotyledons, whereas the cotyledons of non-transformed seedlings displayed a white color and died. The selected plants were transferred to soil to continue growth and collect seeds. The screening was repeated with the new generation, until all the seedlings survived on the selection plates.

2.5.3 Induction of gene expression with estrogen

The expression of genes of interest that were introduced with the pLB12 vector was induced by immersion of whole rosettes in estrogen containing solutions. Before the

treatment, the pots were covered carefully with a plastic wrap to avoid the soil falling down, thereafter the shoots were put upside down into a solution with 10 µM 17-ß-estradiol or control solution (0.01% ethanol) for 50-60 min (**Fig. 2. 6**). For single leaf treatment, the plants were put horizontally and only a single leaf was immersed to the solution. After the treatment, the shoots/leaf were transferred to fresh water for 10 s (repeat 3 times) to wash the estradiol solution from the leaves. Plants were put back to the growth cabinet and experiments were performed in the period of 24-48 h after the estrogen treatment.

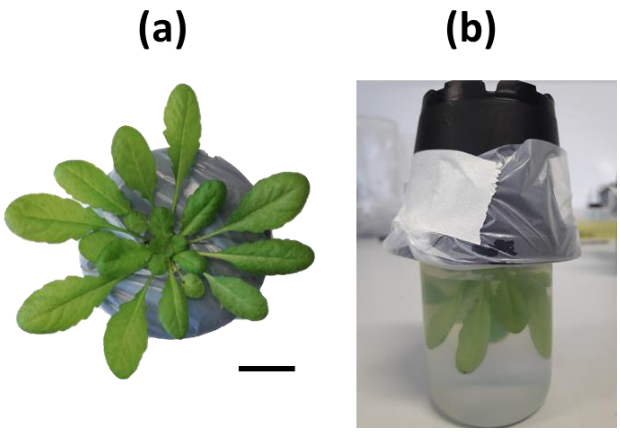

Fig. 2. 6 The estrogen-dependent induction of gene expression in guard cells.

(a) The pot was wrapped with plastic to avoid the soil falling into the solution.

(b) The shoot of the plant was immersed to 10 µM 17-ß-estradiol solution for 50-60 min.

2.5.4 Quantification of transcript levels in estrogen-treated guard cells

Quantitative real-time PCR assays were conducted with guard cell samples, which were collected from *Arabidopsis* leaves, according to the method described by Bauer *et al* (2013). Briefly, leaves from 2 plants were cut from the rosettes and the veins were removed with razor blades. The remaining of the leaves was blended in ice-water for 1 min at maximum speed (Braun, Germany. repeat 2 times). Intact stomata were collected by pouring the suspension on a nylon filter (⌀=210 µm). The isolated guard cells were frozen in liquid N_2 and then stored at -80 °C.

Total RNA of guard cell enriched samples was isolated using the NucleoSpin RNA Plant Kit (Macherey-Nagel, Germany) according to the manual of the manufacturer. The genomic DNA was removed from the RNA samples before the complementary DNA synthesis, by adding 2 µL 10 x DNase buffer, 1 µL DNase I, 0.5 µL Ribolock (RNase Inhibitor) to 2.5 µg

total RNA, and adjusted the volume to 20 µL with RNase free H_2O. The sample was incubated at 37 °C for 45 min. The residual RNA was precipitated with 10 µL NH_4Ac (5 M), 1 µL glycogen, 70 µL isopropanol and 80 µL RNase free H_2O. After overnight incubation at -20 °C, the RNA samples were centrifuged at maximum speed at 4 °C for 45 min. The RNA pellet was washed with ice-cold ethanol (70%) and eluted in 12 µL RNase free H_2O. The quality and concentration of RNA were checked, using a Nanodrop ND-1000 spectrophotometer (Thermo Fisher Scientific, USA).

Complementary DNA (cDNA) was synthesized in two step process. A mixture with 7 µL purified RNA, 2 µL 5x M-MLV buffer, 0.5 µL dNTPs and 0.4 µL Oligo dT primers was incubated at 70 °C for 2 min, and then rapidly transferred on ice. Subsequently, 0.4 µL M-MLV RT RNase was added to the mixture. Thereafter, the cDNA was generated by incubation of the samples at 42 °C for 1 h. The gene expression levels were quantified by using a total of 20 µL of the mixture, which contained 2 µL cDNA (1:20 diluted in HPLC water), 8 µL of each gene-specific primer (20 µM) (TIB MOLBIOL, Germany) and 2 µL fluorescent dye SYBR®Green. The reaction was carried out with a Realplex Mastercycler (Eppendorf, Germany). The gene expression levels were calculated based on standards, with a known concentration, and normalized to 10,000 transcripts of actin 2 and 8. The primer pairs used for qPCR are given in the **Primers** list.

2.5.5 Confocal microscopy

The estrogen-induced gene expression in guard cells transformed with the pLB12 vector was studied with a confocal laser scanning microscope, based on the expression of Venus/YFP. Images of the abaxial side epidermis were acquired with a microscope (Leica DMI6000), which is equipped with a Leica TCS SP5 II confocal laser scanning device (Leica Microsystems) and a 40×/1.2 water immersion objective (HCX PL APO lambda blue 40.0 × 1.2 Water UV). Venus was excited at 514 nm with an argon laser, and the emission signal from 525 to 555 nm was detected. The LAS X program was used to process the images.

2.6 Stomatal aperture assays and gas exchange measurements

Stomatal aperture assays were carried out to compare the average opening of stomata in intact plants at midday. Stomata on the abaxial side of leaves in intact plants were imaged before application of estrogen (0 h) and the same leaf was analyzed 24 h after

exposure to the human hormone. Apertures were monitored with a water immersion objective (W Plan-Apochromat, 63x/1.0, Zeiss) that was mounted on an upright microscope (Axioskop 2FS, Zeiss). Stomatal apertures were determined using Fiji/Image J (Schindelin *et al.*, 2012).

Gas exchange measurements were performed using intact plants, as previously described (Muller *et al.*, 2017). The transpiration rate of leaves was monitored in a custom-made gas exchange setup, equipped with two Infra-Red-Gas-Analyzers (IRGA) (HCM-1000, Walz, www.walz.com). The air stream through the cuvettes was regulated by the mass flow meters and set to 0.96 l/min, 50% relative humidity and 400 ppm CO_2. Photon flux density was 125 µmol m^{-2} s^{-1}. For experiments in which stomata were stimulated with ABA, detached leaves were incubated in distilled water, to which ABA was added at a final concentration of 10 µM with a syringe.

2.7 The heterologous expression system of *Xenopus laevis* oocyte

2.7.1 cRNA generation for expression studies with oocytes

Mature oocytes of the smooth African clawed frog *Xenopus laevis* were employed for the electrophysiological characterization of plant ion channels and proteins that regulate these channels. The cDNAs of AKT1, SLAC1, SLAH3, CIPK11, CIPK23, $CIPK23^{T190D}$, $CIPK23^{K60N}$, CBL1, CBL9, CPK6, CPK23 and OST1 (link the first 12 aa of CBL1 at its N-terminus to target to the plasma membrane) (Geiger *et al.*, 2009a; Maierhofer *et al.*, 2014a) were cloned into oocyte expression vectors of pGEM or pNB1#16. cRNAs were generated by using the mMessage mMachine T7 transcription kit (Ambion, Austin, USA) according to the manufacturer manual. Fresh oocytes were injected with cRNA, using a nano-injection machine (Nanoject, Drummond Scientific Company). Oocytes were injected with a quantity of 6 ng cRNA for each of the proteins studied, unless stated otherwise.

2.7.2 Oocyte voltage clamp recordings

Oocytes were transferred to a custom-made measuring chamber, which was connected to a perfusion system that enabled a rapid change of bath solutions during the measurement. The voltage clamp recordings were conducted with the two electrode

voltage clamp technique (See also **Fig. 2.1**). Both the current and voltage electrodes were backfilled with 3 M KCl, and inserted into AgCl/Ag half-cells that were plugged into headstages of a voltage clamp amplifier (Turbo TEC 10X, NPI electronics). Two micromanipulators (Marzhauser MM33, Drummond) were positioned on opposite sites of the chamber, to impale the oocytes. A reference electrode, filled with 3 M KCl, was placed in the measuring chamber and connected to the ground. The current signal was low pass filtered at 1 kHz and sampled with a 16 bit AD/DA interface at 0.2 kHz (ITC16 ST, Instrutech Corporation, New York, USA). Voltage pulse protocols were controlled with PatchMaster software (HEKA-Elektronik).

Oocytes that expressed AKT1 were first recorded in 100 mM LiCl solution (containing 1 mM $CaCl_2$, 1 mM $MgCl_2$, 1 mM $LaCl_3$, 10 mM MES/Tris, pH 5.6) to determine the leak conductance, and subsequently recorded in a bath solution with 30 mM KCl (containing 1 mM $CaCl_2$, 1 mM $MgCl_2$, 1 mM $LaCl_3$, 10 mM MES/Tris, pH 5.6), of which the ion strength was adjusted with LiCl to 100 mM. AKT1 was studied with stepwise voltage pulses of 2 s, from a holding potential of -20 mV, to test potentials ranging from 20 to -200 mV in 20 mV decrements (Geiger *et al.*, 2009a).

SLAC1 expressing oocytes were perfused with solutions that contained 10 mM MES/Tris (pH 5.6), 1 mM $Ca(gluconate)_2$, 1 mM $Mg(gluconate)_2$, 30 mM NaCl, and 1 mM $LaCl_3$, unless stated otherwise. In experiments with SLAH3, NaCl was replaced by 30 mM $NaNO_3$ (Maierhofer *et al.*, 2014a). Oocytes expressing SLAC1, or SLAH3, were clamped from a holding potential of 0 mV, stepwise to test potentials for 20 s, which were applied from +40 to −180 mV with 20 mV decrements. Instantaneous currents were acquired using 50 ms voltage pulses, ranging from +70 to −150 mV with 10 mV decrements.

3. Results

3.1 ABA-induced Ca^{2+} signals accelerate stomatal closure

The first part of the Results is dedicated to Ca^{2+} signals in guard cells that induced by ABA. This work has been published in the New Phytologist with the title:
"*Calcium signals in guard cells enhance the efficiency by which abscisic acid triggers stomatal closure*". All the movies mentioned in the thesis can be downloaded from New Phytologist, with the link: https://doi.org/10.1111/nph.15985.

3.1.1 Current-ejected ABA triggers single guard cell movement

The waxy cuticles on the leaf surface prevent external solutions reaching stomata. Nano-infusion can overcome this problem, by application of solutions through pressure-injection via open stomata into the apoplast of intact leaves (Hanstein & Felle, 2004; Koers *et al.*, 2011; Guzel Deger *et al.*, 2015). By using this approach, it was shown that 20 µM ABA stimulates stomatal closure within approximately 20 min (Guzel Deger *et al.*, 2015). However, optical properties of the leaf surface are changed after filling solution to the apoplast, which will cause problems if this technique is used in the experiments based on quantitative fluorescence microscopy. Thus, a non-invasive technique called "current-ejection" was established, in which ABA is applied to single guard cells in intact *Arabidopsis* leaves with microelectrodes (**Fig. 3.1a**). Guard cells in intact leaves were stimulated with ABA in single-barreled electrodes that were slowly moved toward a guard cell on the abaxial epidermis, using a micromanipulator. Unlike impalement, the tip of electrodes just touched the guard cell wall, instead of penetrating the plasma membrane (**Fig. 3.1a**). In this configuration, a negative current, provided by a microelectrode amplifier, forces the negatively charged molecules such as ABA^-, out of the glass microcapillary into the guard cell wall.

Application of ABA with a current of -0.8 nA for 20-30 s to the guard cell wall caused cell shrinking after a lag time of only 1.44 min (SE=0.29, n=9. **Fig. 3.1b** and **c**). Current-ejected ABA reduced the stomatal aperture rapidly (**Movie S1**) with a maximal velocity of 0.28 µm $min.^{-1}$ (SE = 0.05, n=9). Interestingly, stomata did not close completely, as ABA had a strong impact on the guard cell that was in contact with the current ejection electrode (asterisk in **Fig. 3.1b**, left panel), but less on the adjacent one (**Fig. 3.1b**). The asymmetric

response indicates that the current ejection caused a high ABA level only close to the tip of the electrode, while the ABA level remained too low to stimulate the neighboring cell. In contrast with ABA, application of benzoic acid (the control solution) to guard cell wall did not induce stomatal closure (**Fig. 3.1c**).

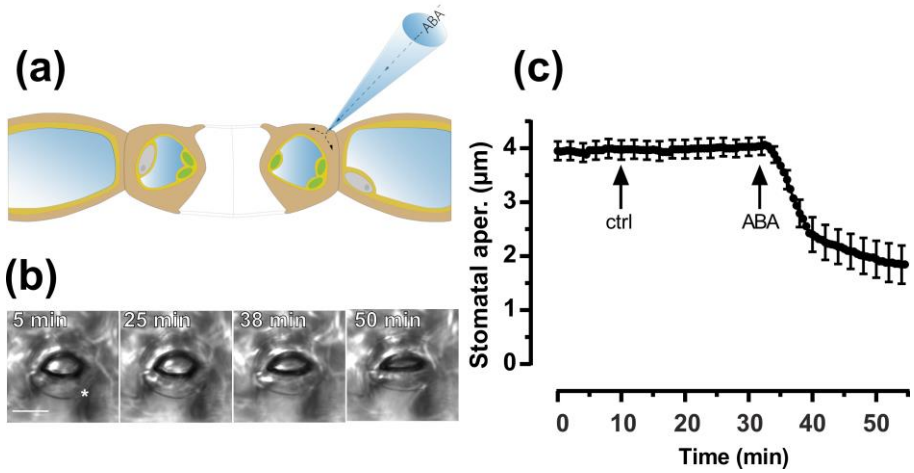

Fig. 3.1 Stimulation of a single guard cell in an intact leaf by current ejection of ABA.

(a) Cartoon of the current ejection technique. Either 50 µM ABA, or benzoic acid (control) was filled to the tip of a microelectrode, which was brought contact with the guard cell wall in an intact leaf. The negatively charged ABA^- was ejected into the cell wall by applying -0.8 nA current.

(b) Time series of images of a stoma in an intact leaf subsequently stimulated with benzoic acid and ABA. The time points marked in the images correspond to the time axis shown in (c). The place where guard cell wall was current ejected is indicated by the asterisk. Scale bar=10 µm.

(c) Graph with changes of the average stomatal aperture plotted against time, the stomata were subsequently stimulated with benzoic acid and ABA, as indicated by arrows. Average data are shown, ± SE, n=9.

3.1.2 Quantification of ABA concentrations evoked by current ejection.

The ABA concentration imposed on the surface of guard cell walls after the current ejection was estimated with the fluorescent dye Lucifer Yellow CH (LY) (Stewart, 1978). As a first step the fluorescence of LY was calculated to the concentration of the dye. To this purpose, a range of LY concentrations (0; 1; 2.5; 5 and 10 µM) were pressure injected into the standard bath solution with 1 s pulses (at 30 psi) using a Picospritzer II microinjection system (General Valve). The LY signals at the tip of the capillaries were plotted to the corresponding concentrations, and the relationship was fitted with a linear

equation with R^2=0.99 (**Fig. 3.2a**). The fluorescence intensities of LY thus can convert to the LY concentration based on this calibration graph (**Fig. 3.2a**).

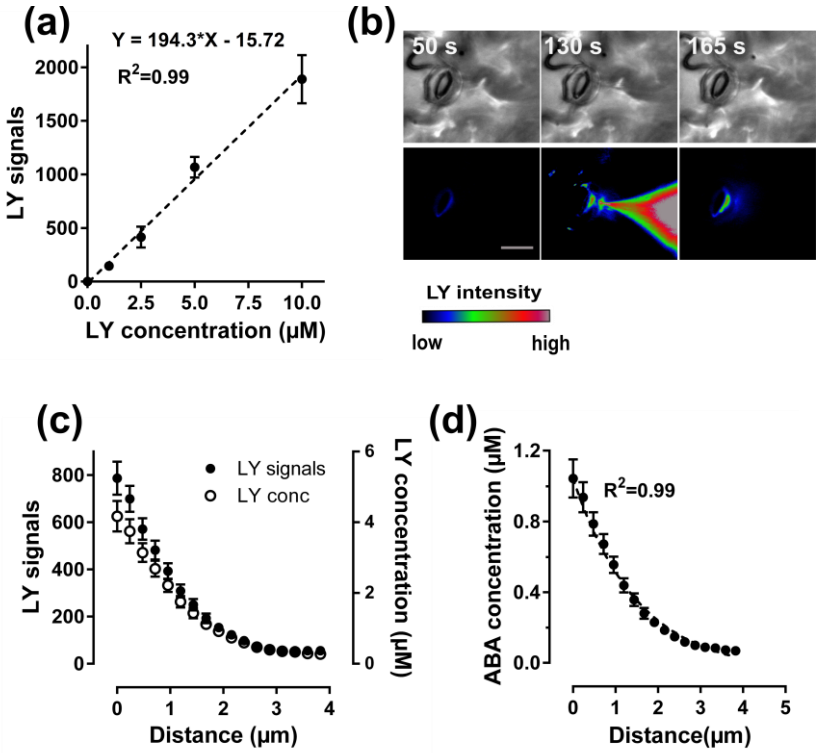

Fig. 3.2 Estimation of ABA concentration in the guard cell wall, imposed by current ejection.

(a) Calibration curve of Lucifer Yellow CH (LY). Capillaries with an opening of 0.5 µm were filled with a range of concentrations (0; 1; 2.5; 5 and 10 µM) of LY, and the dye was pressure ejected into a bath solution. The emission signal (520 nm) at the tip of the capillaries was captured by the CCD camera, and fitted to the LY concentration in the capillary with a linear equation. Average data are presented, ± SE, n=5 for each concentration measurements.

(b) Current injection of LY into a guard cell wall. The tip of the microelectrode was filled with 50 µM LY, and injected with a current of -0.8 nA for 30 s, starting at t=100 s. *Upper panels*, brightfield images of a stoma in an intact *Arabidopsis* leaf, acquired at 50, 130 and 165s, as indicated in the images. *Lower panels*, pseudocolor images of LY fluorescence signal in guard cell wall. LY injection caused a local transient increase in the fluorescence signal at the tip of the electrode. The signal decreased in time after termination of the current ejection.

(c) The LY concentration plotted against the distance from the tip of the electrode, determined at the time of t=130 s. Average data are presented, ± SE, n=12.

(d) The concentration of current ejected ABA in the guard cell wall plotted against the distance from the tip of the microelectrode. The ABA was concentration was calculated with use of the LY signals in (c), and a flux ratio of J_{ABA}/J_{LY} = 0.25.

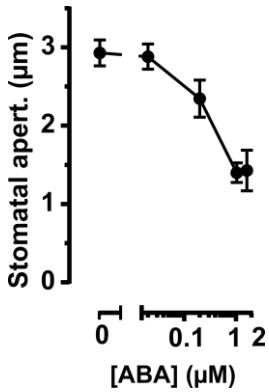

Fig. 3.3 Dose-response curve of ABA-induced stomatal closure.
Guard cells in intact leaves were current injected with different concentrations of ABA, with a current of -0.8 nA for 30 s. Average data are presented, ± SE, n=10.

To quantify the amount of ABA that was ejected into the guard cell wall, the fluorescent dye Lucifer Yellow CH (LY) was current ejected to guard cell wall, using the same conditions as described for ABA above (**Fig. 3.1a** and **b**). LY signals were mainly confined to the cell wall, close to the tip of the electrode (**Movie S2**; **Fig. 3.2b** and **c**). The fluorescence signal and concentration of LY decreased exponentially with distance from the tip (=4.2 µM) (**Fig. 3.2b** and **c**). The amount of ABA that was imposed to guard cells by current ejection was estimated based on these LY data. The ratio between the flux of ABA and LY, injected into the guard cell wall, is J_{ABA}/J_{LY} = 0.25 (see also **2.3.2**), it was thus estimated that approximately 1 µM (=4.2 x 0.25) of ABA was imposed onto the guard cell wall (**Fig. 3.2d**). A dose response relationship for ABA was obtained with a range of ABA concentration in the electrode tip, by using the current-ejection method. These experiments showed that stomatal closure response saturated at a local ABA concentration of 1 µM, whereas 0.02 µM ABA was too low to cause a change in stomatal aperture (**Fig. 3.3**).

3.1.3 Calibration of R-GECO1-mTurquoise in guard cells

The new ratiometric Ca^{2+} reporter R-GECO1-mTurquoise (RG-mT) was chosen to study Ca^{2+} signals, since it displays a strong Ca^{2+}-dependent fluorescence change, and has an internal reference, which enables ratiometric measurements (Zhao *et al.*, 2011b; Keinath *et al.*, 2015; Waadt *et al.*, 2017). The K_d of RG-mT has been calibrated in root cells (Waadt *et al.*, 2017), however, no calibration data were available for guard cells. To this end, the FURA2 dye was used to determine the cytosolic free Ca^{2+} concentration and calibrate RG-

mT. As shown in **Fig. 3.4a**, FURA2 was current injected into the upper guard cell of a stoma after impalement with a double-barreled electrode. It was observed that both the FURA2 and RG-mT ratio signals altered with a similar pattern in response to the change of cytosolic free Ca^{2+} concentration. As shown in **Fig. 3.4a** and **b**, FURA2 and RG-mT ratio signals rose gradually during the injection (**movie S3**), while they slowly decreased to steady levels after the termination of current injection. To obtain the parameters for the FURA2 calculation, the minimal cytosolic free Ca^{2+} concentrations in guard cells were acquired by injecting the Ca^{2+} chelator BAPTA (**Fig. 3.4c**), whereas the maximal cytosolic Ca^{2+} levels were obtained with voltage pulses to -300 mV (**Fig. 3.4d**). The FURA2 (F345/390) ratio was converted into the cytosolic free Ca^{2+} concentration in **Fig. 3e**, according to the equation that was described by Grynkiewicz *et al.*, (1985) (see also **2.4.3**).

$$[\mathrm{Ca}^{2+}]_{\mathrm{free}} = K_d \frac{(R - R_{min})F_{min}}{(R_{max} - R)F_{max}}$$

where K_d is the dissociation constant of FURA2 for Ca^{2+} (270 nM), which was determined for *V. faba* guard cells by Levchenko *et al* (2005). R represents the FURA2 emission ratio of signals obtained at 345 and 390 nm, R_{min} and R_{max} correspond to the minimal and maximal FURA2 ratio, respectively. F_{min}/F_{max} is the fluorescence ratio of unbound and bound form of FURA2, measured at 390 nm.

The simultaneously measured FURA2 and RG-mT ratio values (628/475 nm) were plotted in **Fig. 3.4e**. The relation between the RG-mT ratio and Ca^{2+} concentration was fitted with a Hill function:

$$R = R_{max} \frac{[Ca^{2+}]^h}{K_d + [Ca^{2+}]^h}$$

where R represents the RG-mT emission ratio of signals obtained at 628 and 475 nm, R_{max} corresponds to the maximal RG-mT ratio. K_d is the dissociation constant of RG-mT for Ca^{2+} and h is the Hill coefficient.

which reveals a K_d of 401 nM (SE=17) for RG-mT in guard cells, and a Hill coefficient of 0.81. The determined K_d value in this study is similar to those that have been previously reported for R-GECO1 by Zhao *et al.*, (2011c) and Akerboom *et al.*, (2013). The

relationship between the RG-mT ratio and the cytosolic free Ca^{2+} concentration was therefore used to determine the cytosolic Ca^{2+} level in the experiments described below.

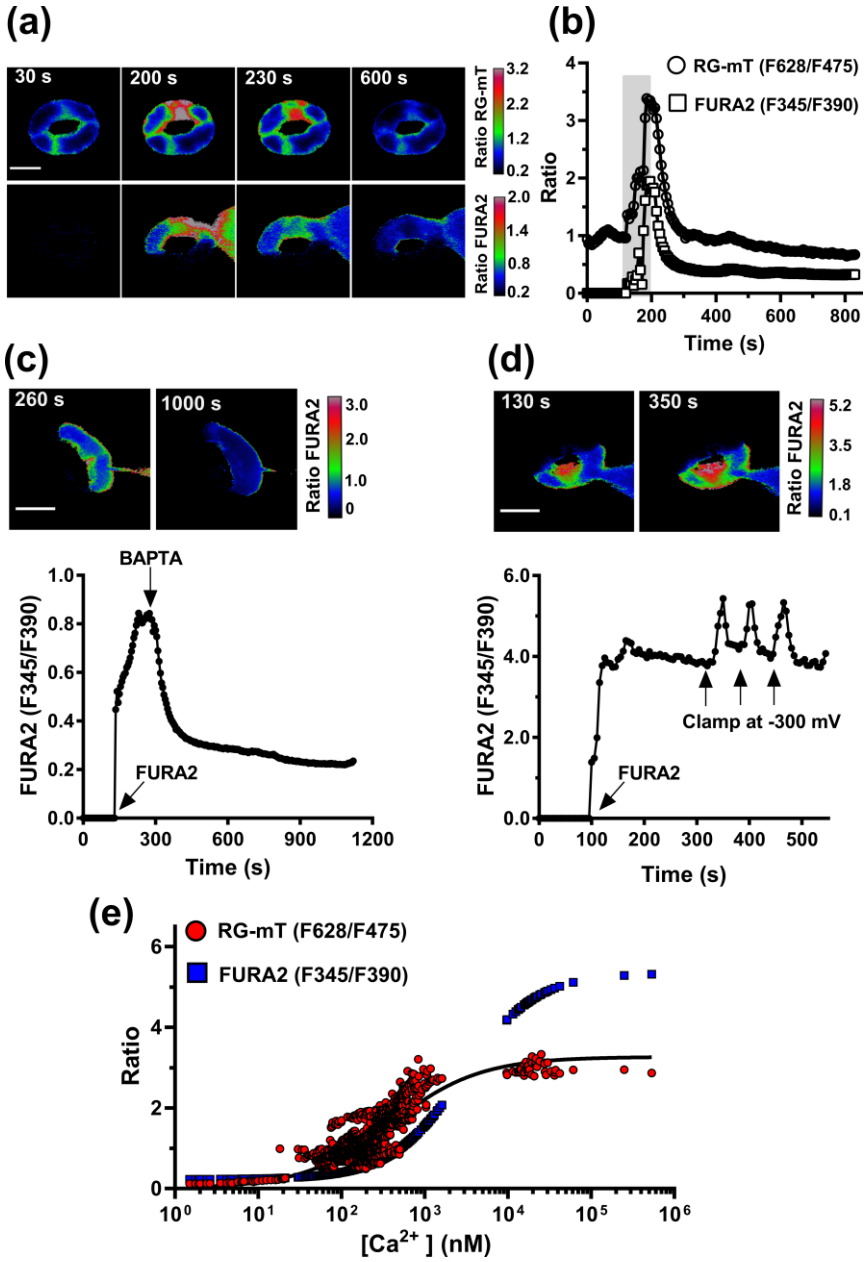

Fig. 3.4 Calibration of RG-mT with FURA2 in *Arabidopsis* guard cells.

(a) The fluorescence ratio images of RG-mT (628/475 nm, top panel) and FURA2 ratio (345/390 nm, bottom panel) in an *Arabidopsis* guard cell. FURA2 was current-injected into the RG-mT expressing guard cell (upper cell), from 120 to 180 s, as shown in (b). Representative images recorded at the indicated times show a similar change in the RG-mT and FURA2 signals. The scale bar represents 10 µm. See also Movie S3.

(b) The ratio signal changes of RG-mT and FURA2 over time in the upper guard cell in (a). The gray area indicates the period of FURA2 injection.

(c-d) Calibration of the FURA2 signal with minimal and maximal values of the fluorescence excitation (345/390 nm) ratio. *Upper panels*, false-colored images that indicate the FURA2 ratio in Arabidopsis guard cells. *Lower panels*, time-dependent changes in the FURA2 ratio of the same cells as in the upper panels. Arrows indicate the time points at which FURA2 or BAPTA were current injected, or at which the cell was clamped to -300 mV. Note, that the injection of BAPTA lowered the FURA2 ratio to a value of 0.23 (SE=0.002, n=6), whereas the hyperpolarizing pulses increased the FURA2 ratio to an average value of 5.34 (SE=0.16, n=6).

(e) Fluorescence ratio values of RG-mT and FURA2 plotted against the cytosolic free Ca^{2+} concentration (logarithmic scale) in guard cells, which were calculated from the FURA2 signal. The FURA2 and RG-mT signals were measured simultaneously in *Arabidopsis* guard cells (n= 2179 from 21 guard cells), as shown in (a) and (b). The RG-mT data were fitted with a Hill equation.

3.1.4 ABA-induced guard cell responses split up in three groups

Current ejection of ABA stimulated stomatal closure in all experiments (n=41) (**Fig. 3.5a-c**), however, the cytosolic Ca^{2+} response of guard cells varied and could be divided into three groups. In the first group (22 out of 44 guard cells), a transient rise in the cytosolic free Ca^{2+} concentration occurred during the period in which the stomata closed (**Fig. 3.5a**, **Movie S4**). In the second group (7 out of 41 of guard cells), ABA-triggered Ca^{2+} signals that arose before the stomata started to close (**Fig. 3.5b**, **Movie S5**). Finally, Ca^{2+} signals were not detected in the remaining 12 out of 41 cells (**Fig. 3.4c**, **Movie S6**). In contrast to the experiments with ABA, stomata did not close after the current ejection of benzoic acid in any of the 24 experiments (**Fig. 3.5d** and **e**). Transient changes of the cytosolic free Ca^{2+} concentration were observed in 2 out of 24 guard cells, but the amplitudes were smaller as those elicited by ABA (**Fig. 3.5d** and **e**).

The occurrence of two types of ABA-dependent Ca^{2+} responses was studied by plotting the time period between ABA stimulation and Ca^{2+} peak against time. The obtained frequency distribution was fitted with a single, double or triple Gaussian functions. According to the corrected Akaike's Information Criterion (AICc) (Burnham *et al.*, 2011), a relationship with two Gaussian functions (solid line in **Fig. 3.6a**, R^2= 0.99) was 55 times more likely than that of single Gaussian function (dotted line in **Fig. 3.6a**, R^2=0.75), while a triple (striped line in **Fig. 3.6a**, R^2=0.99) Gaussian function was 10^{37} less likely as the sum of two Gaussian functions. These data thus demonstrate that ABA can trigger an

early (before stomatal closure), or later (during stomatal closure) Ca^{2+} signal in guard cells.

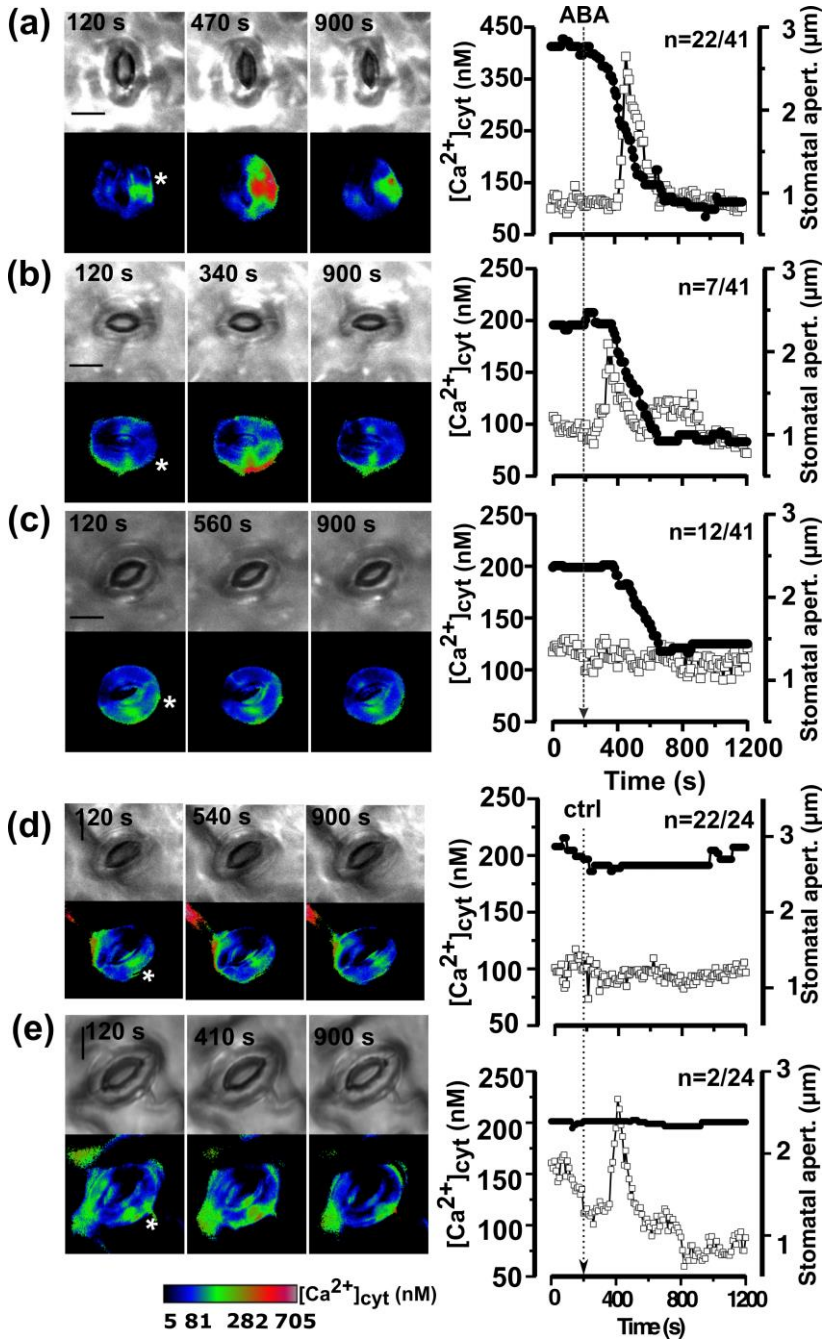

Fig. 3.5 ABA-induced Ca^{2+} signals occur either before or during the stomatal closing. Time-course of changes in stomatal aperture and the cytosolic free Ca^{2+} concentration in guard cells.

(a-e) *Left panels*, brightfield (top images) and pseudo-color images (lower images) were obtained at indicated time points, showing the stomatal aperture and the cytosolic Ca^{2+} concentration in guard cells, respectively. The asterisks in the pseudo-color images mark the position at which the guard cell wall was in contact with the current-ejection electrode. The calibration

bar below the images links the color-code to $[Ca^{2+}]_{cyt}$. Scale bar=10. See also Movie S4 to 6 for a, b and c.

(a-e) *Right panels*, time-course of changes in stomatal aperture and the cytosolic free Ca^{2+} concentration in the same guard cells, as in the *Left panels*. Current ejection of ABA (a-c) or benzoic acid (d-e), as indicated by the arrow. Data are shown for representative cells, which either shows the cytosolic free Ca^{2+} signals occurred during stomatal closure (a), before stomatal closure (b), or no change in the cytosolic Ca^{2+} level (c). Benzoic acid induced an increase in the cytosolic free Ca^{2+} level in only 2 out of 24 cells (d and e), but nevertheless, the stomata remained open.

3.1.5 ABA-induced Ca^{2+} signals speed up stomatal closure

Interestingly, the occurrence of Ca^{2+} signals could be linked to the speed of stomatal closure. As shown in **Fig. 3.6b,** the speed of stomatal closure was faster in stomata that displayed Ca^{2+} signals, as compared to those in which Ca^{2+} signals were absent (one-way ANOVA, P=0.002). On average, the time point of half-maximal closure was 289 s (SE= 19, n=22) in stomata with Ca^{2+} signals, whereas this value increased to 410 s (SE=27, n=12) in stomata without Ca^{2+}-signals.

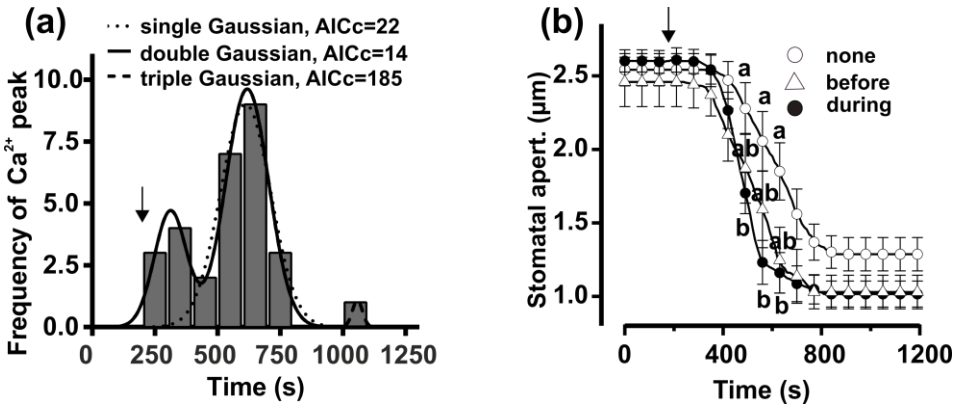

Fig. 3.6 ABA-induced Ca^{2+} signals in guard cells accelerate stomatal closure.

(a) Frequency distribution of the time period between stimulation with ABA and occurrence of a peak in the cytosolic Ca^{2+} level, which was calculated for the same cells as displayed in Fig. 3.5a-c. The time was binned in intervals of 100 s. The frequency distribution was fitted with a single (dotted line), double (solid line) or triple (striped line) Gaussian function. The corrected Akaike's Information Criterion (AICc) was used to calculate which function was most likely to describe the data correctly. The time point of current ejection of ABA is marked with the arrow.

(b) Time-dependent changes of stomatal aperture from the same experiments as shown in Fig. 3.5a-c. Date are averaged for stomata in which ABA-induced Ca^{2+} signal occurred before

stomatal closure (open triangles, n=7), during stomatal closure (closed circles, n=22), or without Ca^{2+} signals (open circles, n=12). The arrow indicates the time point of ABA application. Stomatal apertures that are significantly different between groups are marked with characters (one-way ANOVA, Tukey's test, $P < 0.05$).

3.1.6 Elevated cytosolic Ca^{2+} levels activate the S-type anion channels SLAC1 and SLAH3

Previous studies have shown that elevated cytosolic Ca^{2+} levels activate plasma membrane anion channels in guard cells of *Arabidopsis*, *V. faba* and tobacco (Schroeder & Hagiwara, 1989; Hedrich *et al.*, 1990; Allen *et al.*, 1999a; Chen *et al.*, 2010b; Stange *et al.*, 2010). However, the dynamics of this response has not been studied in *Arabidopsis*. In order to study the Ca^{2+}-dependent activation of anion channels, guard cells that expressed RG-mT were impaled with double-barreled electrodes. A hyperpolarizing pulse to -180 mV triggered a weak cytosolic Ca^{2+} signal (**Fig. 3.7a** and **b**), whereas a pronounced increase in cytosolic Ca^{2+} concentration was detected in the guard cells upon stronger stimulation with pulses to -200 and -220 mV (**Movie S7**). During the pulses, inward K^+ channels were activated and facilitated K^+ influx, and these channels deactivated again at -100 mV in approximately 0.5 s (Roelfsema & Prins, 1997). After termination of the hyperpolarizing pulses, a conductance remained active, as indicated by the arrows, which slowly increased and reached maximum conductance 13.8 s after the peak in the cytosolic Ca^{2+} level (SE=0.9, n=27). This inward conductance deactivated when the cytosolic Ca^{2+} concentration returned to the initial level (**Fig. 3.7a**). This slow activating and deactivating current is similar to the Ca^{2+}-dependent anion channel current that was previously described for *V. faba* and tobacco guard cells (Chen *et al.*, 2010b; Stange *et al.*, 2010), and this is probably carried by Ca^{2+}-activated S-type anion channels.

However, it is still unknown which genes are responsible for conducting Ca^{2+}-activated anion current. In *Arabidopsis*, SLAC1 and SLAH3 represent S-type anion channels of guard cells (Negi *et al.*, 2008; Vahisalu *et al.*, 2008), and we thus tested if hyperpolarizing pulses could activate inward current in loss-of-function mutants of SLAC1 and SLAH3. In wild type, plasma membrane currents were detected at -100 mV after hyperpolarizing pulses to -180, -200 and -220 mV (**Fig. 3.7c,** shown by dotted lines), just as in guard cells expressing RG-mT (**Fig. 3.7a**). A similar current magnitude was elicited in the *slah3-1* single mutant (SLAC1 is functional), but in *slac1-3* (SLAH3 is functional), these currents

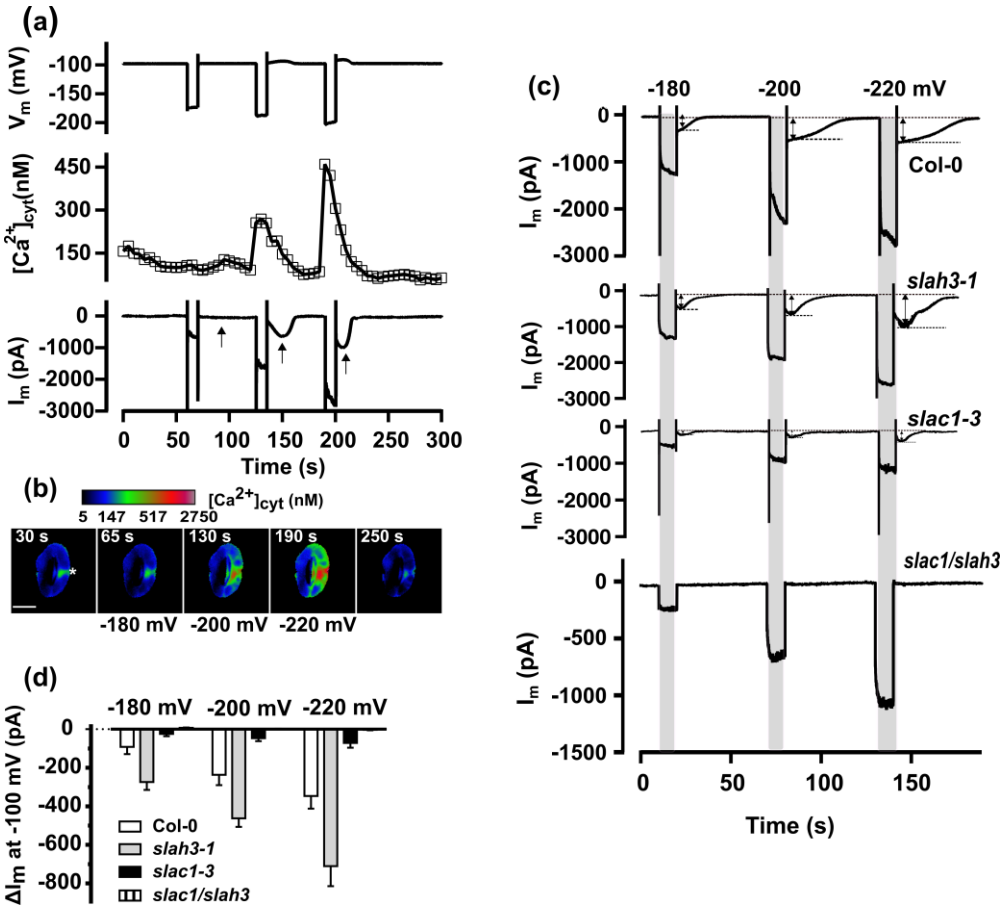

Fig. 3.7 The cytosolic Ca^{2+} signals activate S-type anion channels in guard cells. Guard cells in intact leaves were stimulated with hyperpolarizing voltage pulses, applied via double-barreled electrodes.

(a) Hyperpolarizing pulses of 10s to -180, -200 and -220 mV (upper trace), provoked a transient increase of the cytosolic free Ca^{2+} concentration (middle trace), and led to the activation of an inward conductance (lower trace, indicated by the arrows) that slowly activated and deactivated after returning to the holding potential of -100 mV.

(b) False-color images showing the cytosolic free Ca^{2+} concentration that were acquired before, during and after the hyperpolarizing pulses, in the same guard cell as in (a). The position impaled with the double-barreled electrode is marked with an asterisk. Scale bar=10 µm. The calibration bar of the RG-mT signal, above to the images, links the color-code to $[Ca^{2+}]_{cyt}$. See also Movie S7.

(c) Hyperpolarizing voltage pulses, indicated by the gray area, triggered inward currents (shown by the dotted lines), which slowly deactivated after termination of the voltage pulses in guard cells of Col-0, *slah3-1,* and *slac1-3*. Note that the slowly deactivating conductance was absent in the *slac1/slah3* mutant.

(d) The average S-type anion channel currents, measured as shown in (c), in Col-0 wild type, *slah3-1*, *slac1-3* and *slac1/slah3*. Errors bars represent SE (Col-0, n=9; *slah3-1*, n=6; *slac1-3*, n= 10; *slac1/slah3,* n=13).

were only detected in 6 out of 10 guard cells. On average the inward currents in *slac1-3* also had a reduced magnitude (**Fig. 3.7c** and **d**). No Ca^{2+}-activated currents were detected in *slac1/slah3* guard cells (**Fig. 3.7c** and **d**), which strongly suggests that the Ca^{2+}-activated conductance is carried by S-type anion channels, and both SLAC1 and that SLAH3 contribute to this conductance in *Arabidopsis* guard cells.

3.1.7 Loss of OST1 impairs ABA-induced stomatal closure and -Ca^{2+} signals

The ABA signal pathway in guard cells consists of a Ca^{2+}-dependent and -independent (OST1) branches. It has been showed that stomata of OST1 mutants fail to close in

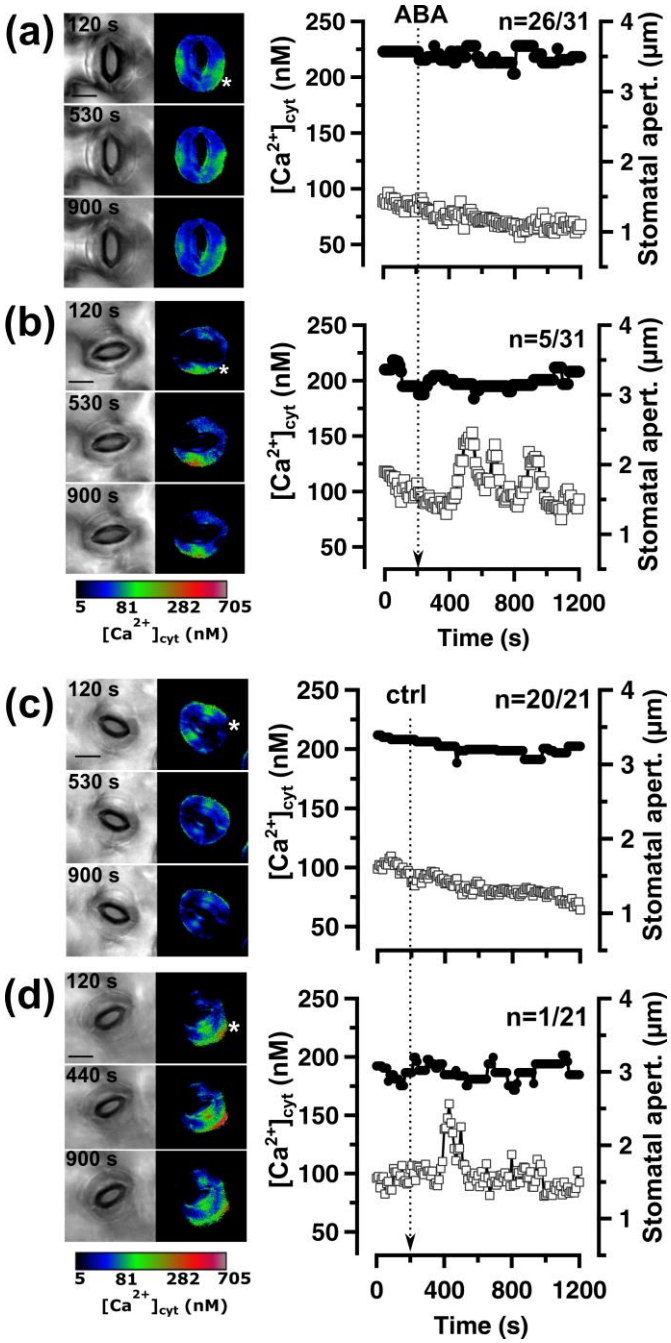

Fig. 3.8 ABA evoked Ca^{2+} signals are strongly impaired in *ost1-3* guard cells. Guard cells of *ost1-3*, transformed with RG-mT were stimulated with ABA (a, b) or benzoic acid (c, d).

(a-d) *left panels.* Brightfield and false-colored images, presenting the stomatal aperture and cytosolic free Ca^{2+} concentration in the same stoma, were obtained at three time points, as indicated in the brightfield images. The position at which current ejection electrode was in contact with the guard cell wall is marked with an asterisk. The calibration bar below the images links the color-code to $[Ca^{2+}]_{cyt}$. Scale bar=10 µm. See also Movie 8 and 9.

(a-d) *Right panels*. Time-dependent changes of stomatal aperture and the cytosolic free Ca^{2+} concentration of the same guard cells, as in the *panels* on the left. Guard cells of *ost1-3* transformed with RG-mT were stimulated with ABA (a and b), or benzoic acid (c and d), as indicated by the arrows.

response to ABA or low humidity (Merlot *et al.*, 2002; Mustilli *et al.*, 2002; Yoshida *et al.*, 2002; Geiger *et al.*, 2009b), but it is unclear why the Ca^{2+} dependent branch (CPKs and CIPKs) of ABA signaling does not compensate the loss of OST1. Scherzer *et al.,* (2012) proposed that OST1 may be essential for the function of CPKs and CIPKs. The impact of the loss of OST1 on ABA-induced Ca^{2+} signals therefore was studied with guard cells of *ost1-3* that express RG-mT. In contrast to wild type (**Fig. 3.5**), ABA failed to stimulate stomatal closure in *ost1-3*. In line with this phenotype, the cytosolic Ca^{2+} signals were strongly impaired in *ost1-3* guard cells (**Fig. 3.8a, Movie S8**). ABA-induced Ca^{2+} signals were only detected in 5 out of 31 guard cells (**Fig. 3.8b, Movie S9**), whereas Ca^{2+} signals were measured in 1 out of 21 *ost1-3* guard cells after current ejection of benzoic acid (**Fig. 3.8d**). Despite of the Ca^{2+} signals observed in *ost1-3* guard cells, all stoma remained open. ABA thus provoked Ca^{2+} signals in approximately 1 out of 6 *ost1-3* guard cells, whereas it triggered Ca^{2+} elevation in 29 out of 41 wild type guard cells (**Fig. 3.5**). These data suggest that OST1 is of key importance for ABA-triggered Ca^{2+} signals.

3.1.8 Cytosolic Ca^{2+} signals trigger rapid activation of anion channels in *ost1-3*

Our study showed that OST1 plays a role in ABA-induced Ca^{2+} signals (**Fig. 3.8**), but it remains unclear if OST1 also has an impact on Ca^{2+}-activation of anion channels. Hyperpolarizing voltage pulses were therefore used to stimulate *ost1-3* guard cells, which express RG-mT (**Fig. 3.9a** and **b**). As in wild type, a transient increase in the cytosolic free Ca^{2+} concentration was elicited by voltage pulses to -180, -200 and -220 mV (**Movie S10**). In response to the voltage pulses, S-type anion channels were activated (**Fig. 3.7c**). The

amplitude of cytosolic Ca^{2+} transients was plotted against the corresponding S-type anion channel currents at -100 mV in **Fig. 3.9d**. The data were fitted with a Hill equation, which revealed a half-maximal response at a change of the cytosolic Ca^{2+} concentration of 90 nM (SE=26), and a maximal anion channel current of -516 pA (SE=74) for wild type (**Fig. 3.9d**).

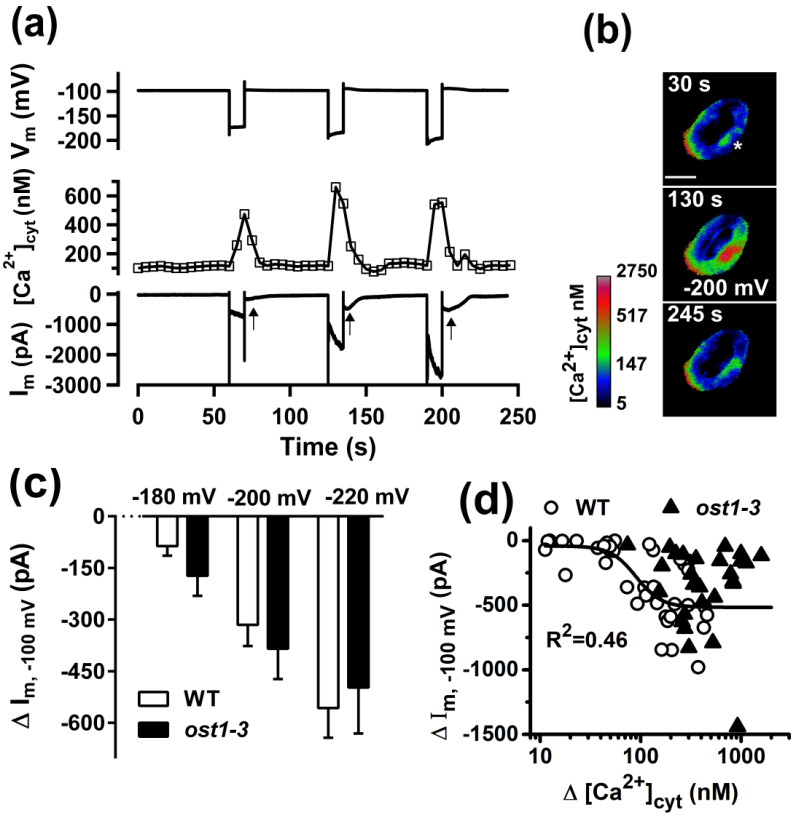

Fig. 3.9 Ca^{2+}-dependent activation of S-type anion channels in *ost1-3*. Guard cells of *ost1-3* in intact leaves were stimulated with hyperpolarizing voltage pulses via double-barreled electrodes.

(a) A guard cell of *ost1-3* was impaled with a double-barreled electrode and clamped at -100 mV. Hyperpolarizing voltage pulses of 10 s from the holding potential to -180, -200 or -220 mV (upper trace) elicited a transient increase of the cytosolic free Ca^{2+} concentration (middle traces). Currents carried by S-type anion channels (lower trace, indicated by the arrows) were observed after the voltages returned to -100 mV.

(b) False-color images, showing the cytosolic free Ca^{2+} concentration, were obtained before, during and after the application of the -200 mV voltage pulse to the same guard cell as in (a). The asterisk marks the position where the guard cell was impaled by the electrode. Scale bar=10 µm. The calibration bar links the color-code to $[Ca^{2+}]_{cyt}$. See also Movie 10.

(c) Average change in S-type anion channel currents in WT and *ost1*-3. The currents were induced by hyperpolarizing pulses of -180, -200 and -220 mV. Data are from experiments shown in Fig. 3.7a (n=13) and Fig. 3.9a (n=9). Error bars represent SE.

(d) The relationship between the S-type anion channel currents and the cytosolic Ca^{2+} concentration in wild type and *ost1-3*. Data are extracted from Fig. 3.7a (37 voltage pulses, n=13 guard cells) and Fig. 3.9a (27 voltage pulses, n=9). The data points of WT were fitted with a Hill function, which revealed a half-maximal response at a change of the cytosolic Ca^{2+} concentration of 90 nM (SE=26), and a maximal anion channel current of -516 pA (SE=74). The Hill function did not converge with the data of *ost1-3*.

However, the Hill equation failed to fit the data of *ost1-3*. It was noticed that the mutant had more cells with large cytosolic Ca^{2+} signals changes (**Fig. 3.9d**), while they had similar S-type anion channel currents (**Fig. 3.9c**). This indicates that the Ca^{2+} responsiveness was slightly lower in *ost1-3* guard cells, compared to the wild type.

3.2 CIPK23 inhibits stomatal closure

The first part of the Results provides evidence for a role of Ca^{2+} signals in enhancing ABA-induced stomatal closure, while the second part is dedicated to protein kinases that transduce these signals (Zhu, 2016; Hedrich & Geiger, 2017; Kudla *et al.*, 2018). Our studies focus on the mechanism by which CIPK23 regulates stomatal movements.

3.2.1 Expression of CIPK23 variants in guard cells

Previous studies with CIPK23 were carried out with the loss-of-function mutants, which revealed that these mutants have an improved drought stress resistance, and enhanced stomatal closure in response to ABA (Cheong *et al.*, 2007; Nieves-Cordones *et al.*, 2012; Sadhukhan *et al.*, 2019). However, these phenotypes counteract the findings in oocytes that CIPK23 activates SLAC1 and SLAH3 (Maierhofer *et al.*, 2014a). To test if CIPK23 direct regulates stomatal movements, our studies focused on plants with CIPK23 gain-of-function in guard cells, instead of analyzing the phenotype of loss-of-function mutants. To this purpose, a phosphomimic $CIPK23^{T190D}$ (constitutively active) was generated, by substitution of Thr-190 in the activation loop with Asp. Previous studies showed that a similar substitution mimics phosphorylation and enhances kinase activity in CIPK24/SOS2 (Gong *et al.*, 2002b), as well as CIPK3, 8, 9, 17, and 26 (Gong *et al.*, 2002a; Pandey *et al.*, 2008; Gao *et al.*, 2012; Lyzenga *et al.*, 2013; Song *et al.*, 2018; Yadav *et al.*, 2018). A kinase-dead $CIPK23^{K60N}$ variant was also created by a replacement of Lys-60 with Asn (Li *et al.*, 2006).

The wild type CIPK23, $CIPK23^{T190D}$, and $CIPK23^{K60N}$ variants were tagged with a Venus subunit at the C terminus. Alternatively, a sole Venus unit was introduced into guard cells of Col-0. The expression of all four constructs was controlled spatially and temporally, by using an estrogen-induced system (Brand *et al.*, 2006). CIPK23-Venus fusion proteins and Venus were under control of the *OlexA* promoter, which is controlled by the transcription factor *XVE* (derived from the human estrogen receptor) (Brand *et al.*, 2006). Guard cell-specific expression was accomplished by using the pGC1 promoter (Yang *et al.*, 2008), which drove the expression of XVE. In the presence of estrogen, XVE moves into the nucleus and binds to its responder *OlexA,* which then specifically stimulates the expression of the CIPK23-Venus constructs in guard cells.

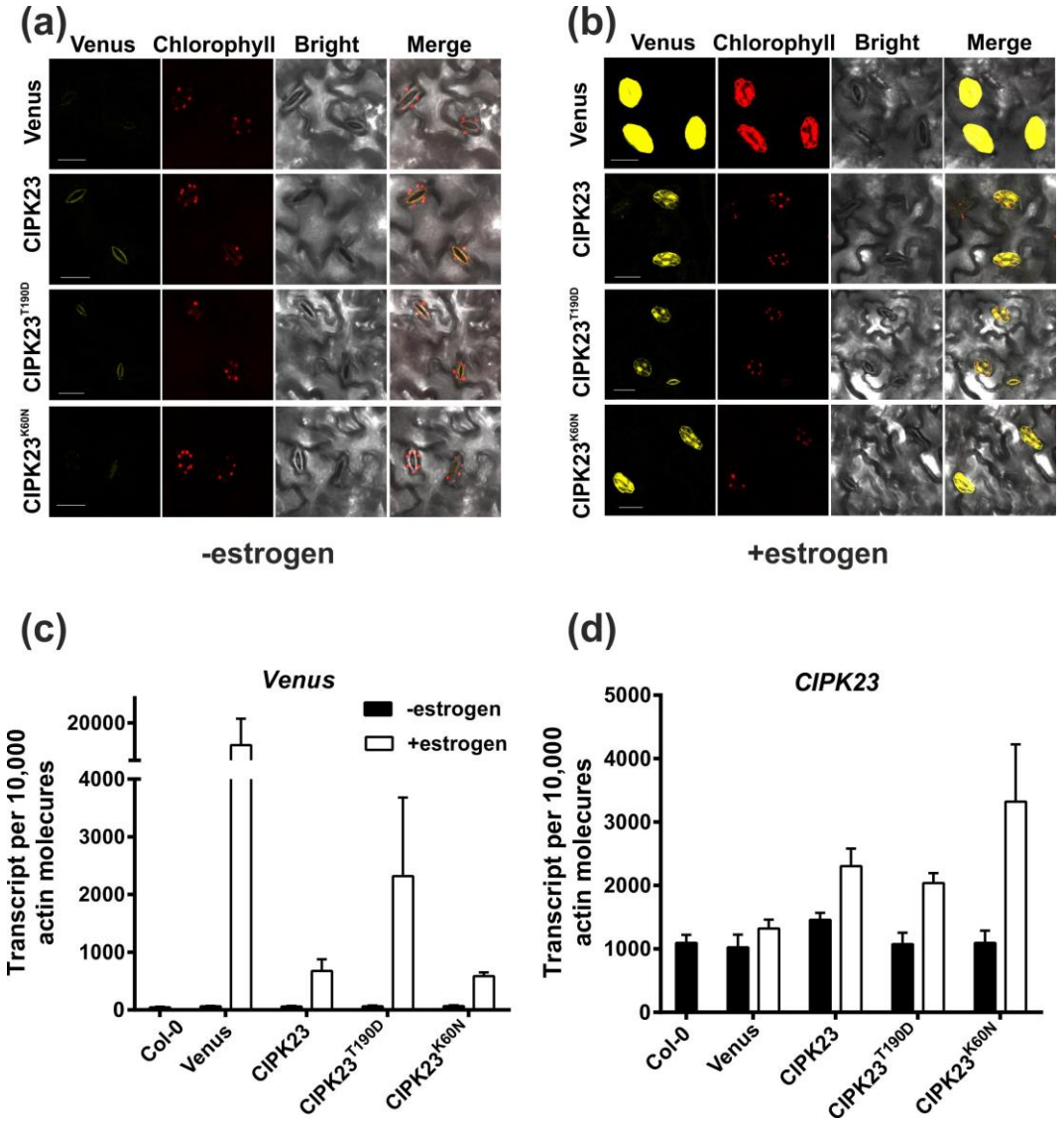

Fig. 3.10 Fluorescence of Venus, and expression of CIPK23 variants in guard cells with or without estrogen treatment.

(a,b) Representative images of Venus and chlorophyll fluorescence obtained 24 h after control (a), or estrogen induction (b), from guard cells in intact leaves. Images from the top to bottom are sole Venus, CIPK23-Venus, CIPK23^{T190D}-Venus and CIPK23^{K60N}-Venus. Scale bar=20 µm.

(c,d) Expression levels of *Venus* and *CIPK23* in guard cells of Venus, and CIPK23, CIPK23^{T190D} and CIPK23^{K60N} plants treated with or without 10 µM ß-17-estradiol. Transcript numbers of *Venus* (c) and *CIPK23* (d) were quantified in guard cell samples isolated from the leaves 3 h after the treatments, and normalized to 10,000 actin molecules. Data show mean ± SE, n=4-6.

To test if the inducible system worked properly in guard cells, we tested if the transgenic plants were sensitive to estrogen application, by monitoring the Venus fluorescence in

intact leaves with the Laser Scanning Microscope. Venus fluorescence was detected specifically in guard cells (**Fig. 3.10b),** for the period from 16 to 72 h after the estrogen (10 µM 17-ß-estradiol, +estrogen) treatment. In contrast, plants treated with control solution (0.01% ethanol, -estrogen) had only a weak autofluorescence on the stomatal pores (**Fig. 3.10a**). RT-qPCR analysis was also carried out with guard cell samples isolated from the homozygous plants, either treated with estrogen or control solution. The transcript number of *Venus* is shown in **Fig. 3.10c** and was dramatically increased upon estrogen treatment. Likewise, estrogen treatment enhanced the number of *CIPK23* transcripts, in plants that were transformed with the CIPK23 variants, but not in those that only had the Venus unit (**Fig. 3.10d**), suggesting the estrogen itself does not affect CIPK23 expression. In the absence of estrogen, similar levels of *CIPK23* transcripts were measured in guard cells of the transformed plants and wild type (**Fig. 3.10d**). These data thus show that the inducible system is tightly controlled by estrogen.

3.2.2 CIPK23 alters stomatal movements in response to light/darkness and ABA

The impact of expression of the CIPK23 variants on stomatal movements was studied with intact plants. For this purpose, stomatal aperture assays were carried out with the same leaves before and after estrogen, or control treatment. For all lines, a similar stomatal aperture was found before and after the control treatment (**Fig. 3.11a)**. However, stomata of CIPK23^{T190D} line were opened to a further extent after estrogen treatment (**Fig. 3.11a** and **b**). In line with stomatal aperture assays, transpiration measurements showed that a higher stomatal conductance of CIPK23^{T190D} plants compared to Venus, CIPK23, CIPK23^{T190D} and CIPK23^{K60N}, after estrogen treatment (**Fig. 3.11d**). Stimulation with light enhanced the transpiration in all lines, but the transpiration of CIPK23^{T190D} remained higher than that of others (**Fig. 3.11d**). The difference in transpiration was not observed if plants were not treated with estrogen (**Fig. 3.11c**). These data indicate that the phosphomimic CIPK23^{T190D} stimulates stomata opening.

In addition to the plants that specifically express CIPK23 in guard cells, experiments were also conducted with plants that either constitutively express CIPK23, or have lost CIPK23 function. Consistent with estrogen-induced plants, transpiration was higher in LKS,OE

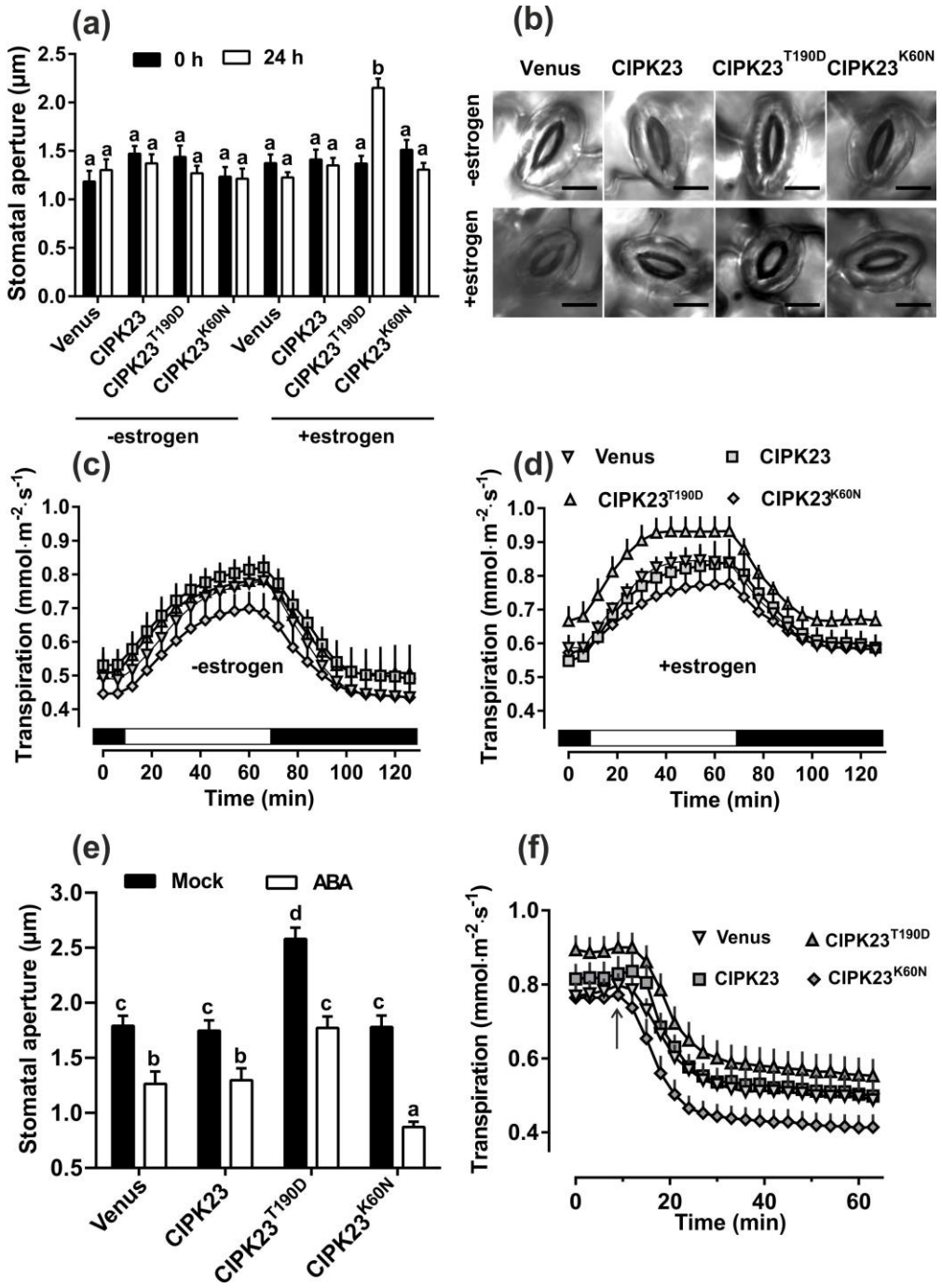

Fig. 3.11 Phosphomimic CIPK23^{T190D} stimulates stomatal opening, while CIPK23^{K60N} enhances stomatal closure.

(a) Stomatal apertures were determined before estrogen treatment (dark bar) and with the same leaves 24 h after control, or estrogen treatment (white bar), in intact plants. Data are mean ± SE, n > 40. Note that only CIPK23^{T190D} has stomata with a larger aperture after estrogen treatment.

(b) Representative images of the stomatal aperture in intact plants obtained 24 h after the application of control (upper panel) or estrogen (lower panel) solution. Scale bar=10 µm.

(c,d) Transpiration of whole plants 24-48 h after the treatment with control (c) or estrogen (d) solution, plotted against time. The plants were exposed to light (100 µmol·m^{-2}·s^{-1}) as indicated by the white bar below the graph. Data represent mean ± SE, n=4-6.

(e) Aperture of stomata in intact leaves that were excised 24 h after estrogen treatment. The leaves were immersed in bath solution for 2 h and illuminated with light (100 µmol·m^{-2}·s^{-1}). Stomatal apertures were examined 30 min after mock (closed bar), or 5 µM ABA (open bar) treatment (n > 40).

(f) Transpiration of leaves plotted against time. The leaves were stimulated with ABA. Experiments were conducted with estrogen-induced leaves, which were detached 24 h after the treatment. A final concentration of 10 µM ABA was applied to the leaf petiole as indicated by the arrow, n=5-7.

than wild type Col-0 and *lks1-3* (Xu *et al.*, 2006), either in darkness or light (**Fig. 3.12b**). We also noticed that the wide opened stomata in LKS,OE were detected but not estrogen-induced wild type CIPK23 plants, the difference may be caused by the difference in transcript level, since *CIPK23* expression in LKS,OE was approximately 3 times higher than that of in estrogen-induced plant (**Fig. 3.12a**). In sum, our data demonstrate that CIPK23 expression stimulates stomatal opening.

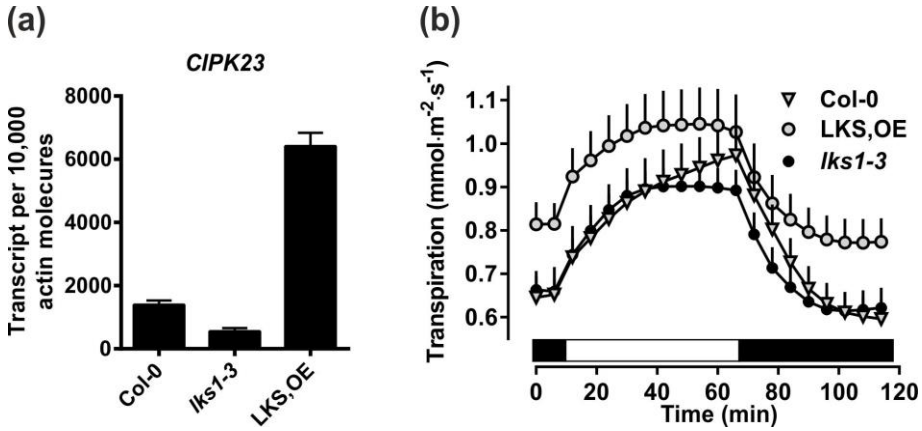

Fig. 3.12 CIPK23 stimulates stomatal opening.

(a) Expression levels of *CIPK23* in guard cells of Col-0, *lks1-3* and LKS,OE. Transcript numbers were quantified from guard cells that isolated from leaves. Data shown as mean ± SE, n=6.

(b) The transpiration of intact plants in response to light and darkness, as indicated by the white and black bar. Data shown as mean ± SE, n=5-8.

In addition to their impact on stomatal opening, the effect of the gain-of-function (estrogen-induced) CIPK23 variants on ABA-induced stomatal closure was also studied. Stomata in detached leaves were opened in bath solution, by exposure to white light (100

µmol·m^{-2}·s^{-1}). In line with the results described above, stomata were further open in estrogen-induced CIPK23^{T190D} leaves as in other lines before ABA treatment. Upon application of 5 µM ABA for 30 min, stomatal pores closed in all lines, however, the reduction in aperture was more pronounced in CIPK23^{K60N} as in other lines (**Fig. 3.11e**) Transpiration measurements with intact leaves also showed that CIPK23^{K60N} enhanced the response of stomata to ABA (**Fig. 3.11f**).

3.2.3 CIPK23 enhances guard cell inward K^+ channel activity

Previous studies suggested that CIPK23 affects stomatal movement by regulating inward K^+ channel activity (Cheong *et al.*, 2007; Nieves-Cordones *et al.*, 2012; Mao *et al.*, 2016; Sadhukhan *et al.*, 2019). It was shown that CIPK23 is able to phosphorylate and activate AKT1 in *Arabidopsis* roots (Li *et al.*, 2006; Xu *et al.*, 2006; Geiger *et al.*, 2009a), but it is not yet clear if CIPK23 modulates inward K^+ channels in guard cells. The activity of K^+ channels in guard cells of intact leaves was therefore recorded with double-barreled intercellular electrodes. As shown in **Fig. 3.13a** and **c**, outward and inward K^+ channels were activated with voltage pulses ranging from 20 to -200 mV. The inward K^+ channel currents in estrogen-stimulated guard cells of CIPK23, CIPK23^{T190D} and CIPK23^{K60N} plants were approximately 2 times larger (compared at -180 mV), as those in Venus. However, no impact of estrogen treatment was found for the outward K^+ channel activity (**Fig. 3.13a** and **b**). In the absence of estrogen, the K^+ channel activity was not different between the CIPK23 lines and the Venus transformed control (**Fig. 3.13c** and **d**). In line with the impalement data, we also observed that AKT1 transcript levels were increased in estrogen-induced guard cells that expressed the CIPK23 variants (**Fig. 3.14**). The inward K^+ channel activity was also measured in guard cells of CIPK23 overexpression plant, just as with the estrogen-induced plants, constitutively expression of CIPK23 enhanced the activity of inward K^+ channels, whereas it was impaired in *lks1-3* mutant (**Fig. 3.15a** and **b**).

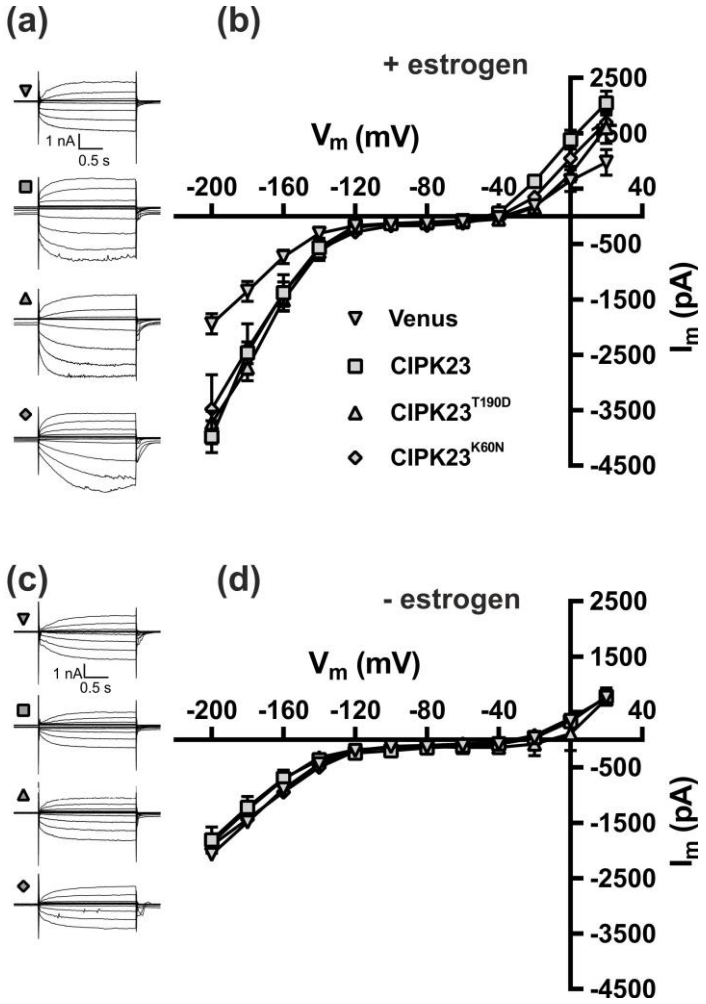

Fig. 3.13 CIPK23 variants increase inward K^+ channel conductance in guard cells. K^+ channels were recorded in guard cells treated with estrogen (a, b), or without estrogen (c, d), with double-barreled microelectrodes.

(a,c) Current traces of K^+ channels in guard cells. Guard cells, 24-48 h after the estrogen (a) or control (c) treatments, were impaled with double-barreled electrodes. Current traces were recorded with voltage pulses from the holding potential of -100 mV stepwise for 2 s to values ranging from 20 to -200 mV with 20 mV decrements.

(b,d) Steady-state K^+ channel currents plotted against the membrane voltages. Data, from measurements as shown in a and c, given as means ± SE, n=9-12.

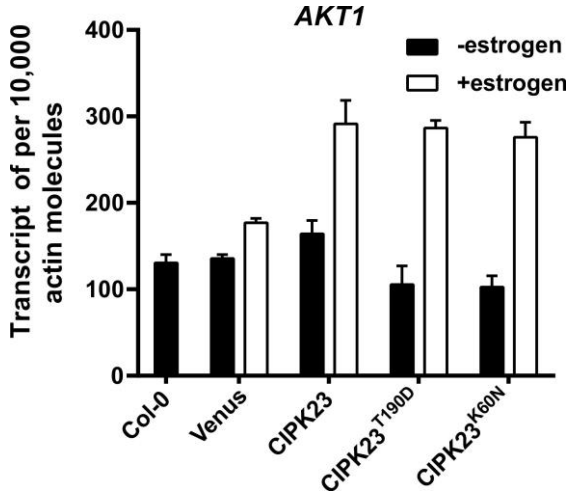

Fig. 3.14 CIPK23 enhances the expression of *AKT1* in guard cells.

Transcript numbers of *AKT1* were quantified in guard cells that were isolated from the leaves 3 h after control (closed bar), or estrogen (open bar) treatment. Data are mean ± SE, n=6-8.

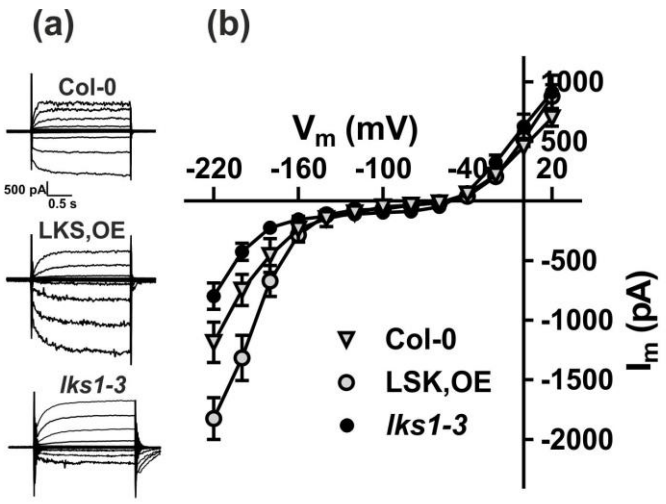

Fig. 3.15 CIPK23 stimulates guard cell inward K^+ channels. Guard cell K^+ channels were recorded with double-barreled electrodes.

(a) Representative K^+ channel currents in guard cells of Col-0, *lks1-3* and LKS,OE. Guard cells in intact leaves were impaled with double-barrel electrodes and clamped at -100 mV. Currents traces were obtained by application of bipolar voltage pulses ranging from 20 to -200 mV with double-barreled electrodes.

(b) Steady-state currents of Col-0, *lks1-3* and LKS,OE plotted against the membrane potential. Data are given as mean values ± SE, n=10-14.

3.2.4 Activation of AKT1 by CIPK23 does not depend on its protein kinase activity

CIPK23 was shown to activate the inward K^+ channel AKT1 in *Xenopus* oocytes (Li *et al.*, 2006; Xu *et al.*, 2006; Geiger *et al.*, 2009a). In addition, it was reported that $CIPK23^{K60N}$, which loses CIPK23 kinase activity after replacement of Lys-60 (located at ATP binding pocket) with Asn, prohibits activation of AKT1 by the protein kinase in oocytes (Li *et al.*, 2006). However, our in planta data show that the inward K^+ channel activity is enhanced in the estrogen-induced guard cells that expressed $CIPK23^{K60N}$ (**Fig. 3.13a** and **b**), just as CIPK23 and $CIPK23^{T190D}$. These contrasting findings prompted us to investigate if the activation of AKT1 by CIPK23 is dependent on its protein kinase activity, by using the oocyte expression system. Oocyte whole-cell currents were recorded with the two-electrode voltage clamp technique in a bath solution containing 30 mM KCl. Inward K^+ currents were recorded with oocytes in which AKT1 was coexpressed with wild type CIPK23/CBL9, but not if only AKT1 was expressed (**Fig. 3.16a** and **c**). This result is in line with the previous studies (Li *et al.*, 2006; Xu *et al.*, 2006; Geiger *et al.*, 2009a). Just as for wild type CIPK23, $CIPK23^{K60N}$/CBL9 and $CIPK23^{T190D}$/CBL9 were also capable of stimulating AKT1 (**Fig. 3.16a** and **c**). Similar results were obtained if CIPK23 and its variants were expressed with CBL1, although the current amplitude with $CIPK23^{K60N}$ and $CIPK23^{T190D}$ was slightly reduced compared to wild type CIPK23 (**Fig. 3.16b** and **d**). Apparently, these results with $CIPK23^{K60N}$ are unexpectedly in line with the impact of $CIPK23^{K60N}$ on inward K^+ channels in guard cells, although they counteract a previous study (Li *et al.*, 2006). Collectively, these data show that $CIPK23^{K60N}$, just like wild type CIPK23, and $CIPK23^{T190D}$, can activate AKT1 not only in guard cells but also in oocytes.

The activation of AKT1 by the kinase-dead $CIPK23^{K60N}$ implies that this activation relies on the interaction between both proteins, rather than the kinase activity. It was therefore tested if CIPK23 can stimulate AKT1 in the absence of CBL proteins. As shown in **Fig. 3.16d**, neither $CIPK23^{K60N}$ nor $CIPK23^{T190D}$ were able to elicit AKT1-derived K^+ currents without CBL1. However, wild type CIPK23 could activate AKT1 without CBL1, albeit the activity was weaker as in the presence of CBL1 (**Fig. 3.16d**). These results are in line with those that were reported previously by Li *et al.,* (2006). Our data indicate that the interaction between CBL1/9 and CIPK23 is important for stimulating AKT1, whereas the kinase activity of CIPK23 is not required.

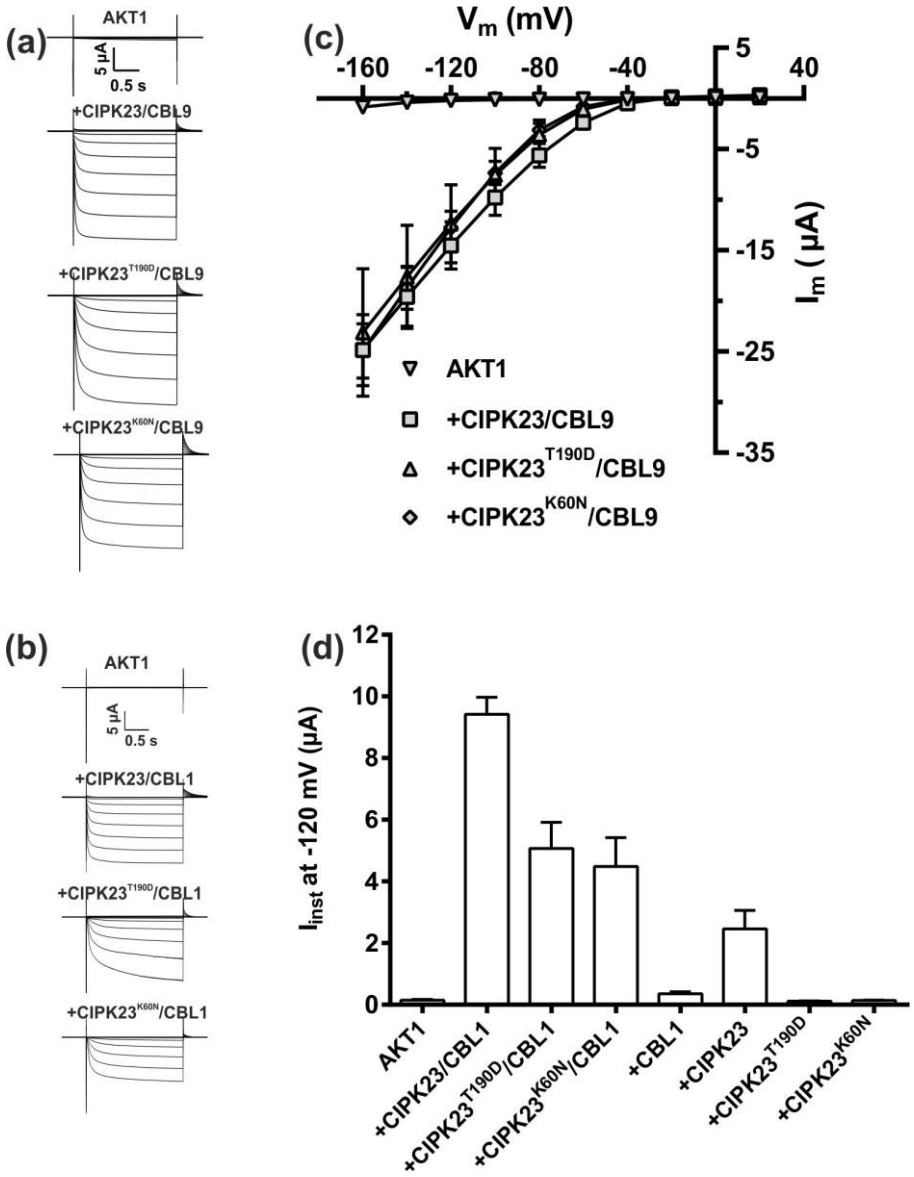

Fig. 3.16 CIPK23-activation of AKT1 does not require the kinase activity of CIPK23.

(a,b) Whole-cell currents recorded in *Xenopus* oocytes that expressed AKT1 only, or with variants of CIPK23 and CBL9 (a), or CBL1 (b). The oocytes were stimulated with voltage pulses from a holding potential of -20 mV to test values ranging from 20 to -160 mV in 20 mV decrements, using a bath solution with 30 mM KCl. Note that CIPK23^{K60N} can activate AKT1 either with CBL9 (a), or CBL1 (b).

(c) Average values of steady-state currents in oocytes coexpressing AKT1 with CIPK23/CBL9, CIPK23^{T190D}/CBL9, or CIPK23^{K60N}/CBL9, plotted against the applied voltages. Data from measurements as shown in (a) given as the mean of 4-5 experiments ± SE.

(d) Average values of steady-state currents at -120 mV in oocytes coexpressed AKT1 with CIPK23 variants in the presence or absence of CBL1. Data are shown as mean ± SE (n=4-5).

The autoinhibitory FISL/NAF motif in C terminus of CIPK23 serves as the CBL1/9 binding site, and it is important for forming the CIPK23-CBL1 (or CBL9) complex and targeting CIPK23 to the plasma membrane (Xu *et al.*, 2006; Hashimoto *et al.*, 2012; Bender *et al.*, 2018). We therefore further studied the impact of the C terminus of CIPK23 on ATK1 activation, by introducing a constitutively active CIPK23, CIPK23$^{T190D+V182K}$ΔC to the measurements. CIPK23$^{T190D+V182K}$ΔC cannot interact with CBL1/9, as the FISL/NAF motif is lacking, nevertheless, this variant has a high protein kinase activity (Chaves-Sanjuan *et al.*, 2014). Like CIPK23^{T190D}, CIPK23$^{T190D+V182K}$ΔC failed to provoke AKT1 currents in the absence of CBL1 (**Fig. 3.17a** and **b**). These results indicate that C terminus, which interacts with CBL1/9, is essential for the activation of AKT1 by CIPK23.

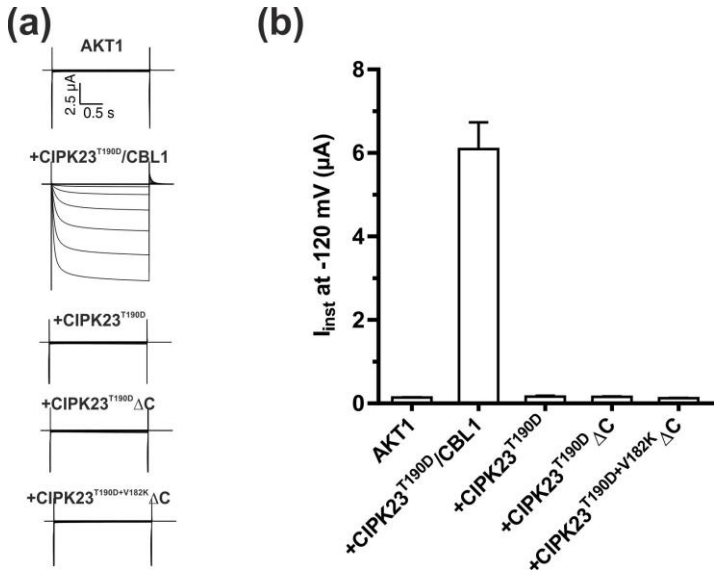

Fig. 3.17 The C terminus of CIPK23 is important for the activation of AKT1

(a) Current traces of oocytes expressing only AKT1, or AKT1 with CIPK23^{T190D}/CBL9, CIPK23^{T190D}, CIPK23^{T190D}ΔC, or CIPK23$^{T190D+V182K}$ΔC.

(b) Average values of whole-oocyte currents at −120 mV from oocytes expressing AKT1, with the indicated proteins. Data are shown as mean ± SE, n=6-8.

3.2.5 CIPK23 inhibits guard cell S-type anion channel activity

The gain-of-function CIPK23 and CIPK23^{T190D} stimulated stomata to open, whereas CIPK23^{K60N} enhanced stomatal closure in response to ABA (**Fig. 3.11** and **Fig. 3.12**). In contrast, all CIPK23 variants had the same impact on the activity of inward K^+ channels (**Fig. 3.13**). Apparently, the stomatal phenotypes caused by CIPK23 constructs do not match with the influence of CIPK23 on the inward K^+ channel AKT1.

CIPK23 not only can regulate AKT1 (Li *et al.*, 2006; Xu *et al.*, 2006; Geiger *et al.*, 2009a), but also SLAC1 and SLAH3, based on experiments with *Xenopus* oocytes (Maierhofer *et al.*, 2014a). Thus, it is possible that CIPK23-regulates stomatal movements by modulating S-type anion activity in guard cells. We therefore examined the activity of anion channels in guard cells, by using double-barreled electrodes, filled with 300 mM CsCl. As shown in **Fig. 3.18a** and **b**, S-type anion channel currents were provoked with the voltage pulses from holding the potential of 0 mV stepwise for 2 s to test values ranging from 20 to -120 mV.

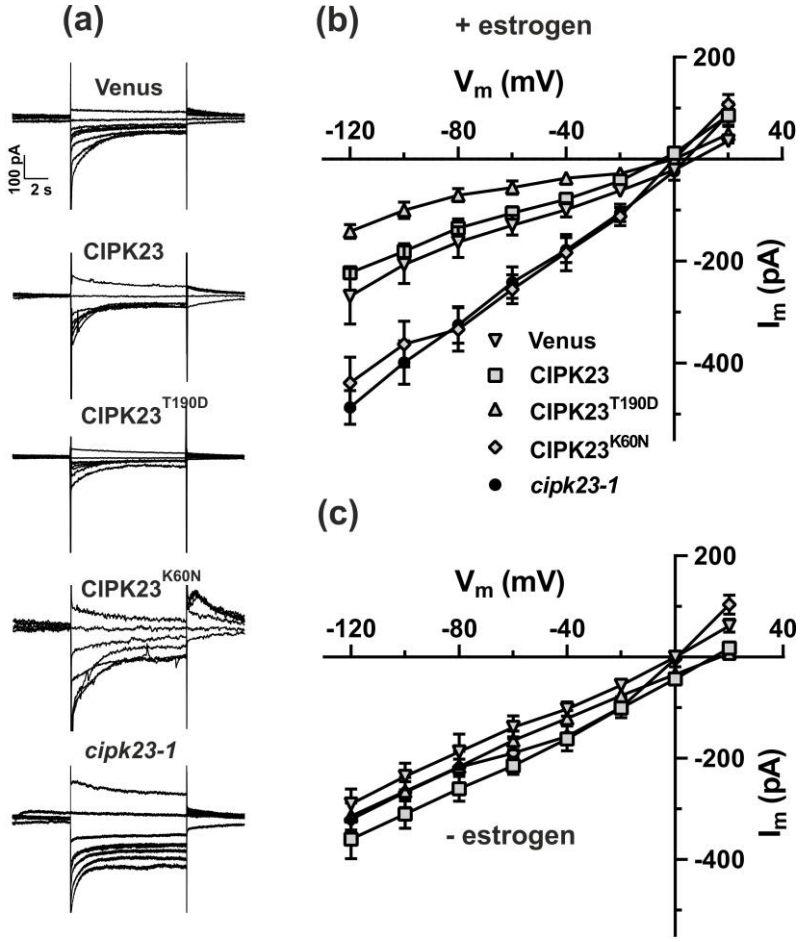

Fig. 3.18 CIPK23 suppresses the S-type anion channel conductance of guard cells.

(a) Currents of S-type anion channels from estrogen-treated guard cells. Guard cells in intact leaves were impaled 24 h after estrogen treatment, with double-barreled electrodes filled with 300 mM CsCl, and clamped to a holding potential of 0 mV. Current traces were obtained by applying voltage pulses ranging from 20 to -120 mV with 20 mV decrements.

(b,c) Average values of instantaneous currents of S-type anion channels in estrogen- (b) or control-treated (c) guard cells, plotted against the test potential. Data presented as mean values ± SE, n=9-13.

These experiments revealed that the estrogen-induced expression of CIPK23 (wild type) did not alter the currents carried by S-type anion channels, relative to the guard cells that only expressed Venus. However, the expression of CIPK23^{T190D} reduced the activity of S-type anion channels, while CIPK23^{K60N}, or the loss of function *cipk23-1* mutant showed an enhanced conductance of these channels (**Fig. 3.18a** and **b**). Moreover, no difference in S-type anion channel currents was found in the guard cells in the absence of estrogen treatment (**Fig. 3.18c**). These data indicate that CIPK23 inhibits the activity of S-type anion channels in guard cells.

In line with the results with the estrogen-induced lines, constitutive expression of CIPK23 in guard cells (LKS,OE) reduced the activity of S-type anion channels, whereas the channel activity was enhanced in the *lks1-3* mutant (**Fig. 3.19)**.

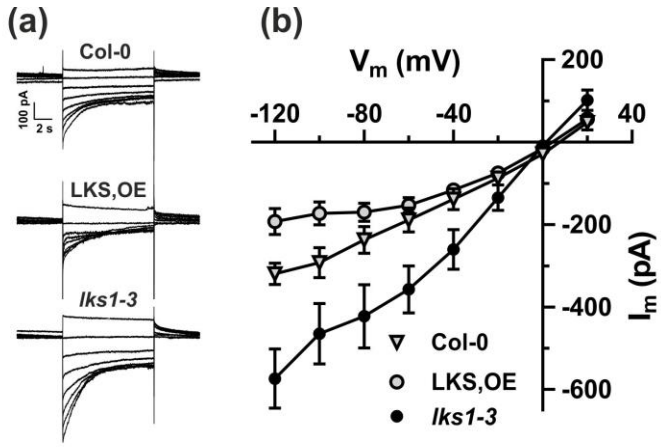

Fig. 3.19 CIPK23 attenuates S-type anion conductance in guard cells.

(a) S-type anion channel currents were measured with double-barrel electrodes filled with 300 mM CsCl. Current traces were obtained by applying voltage pulses from a holding potential of 0 mV to the test values ranging from 20 to -120 mV with 20 mV decrements.

(b) Average values of instantaneous currents plotted against the test voltages, for guard cells of Col-0, *lks1-3* and LKS,OE. Data are given as mean values ± SE, n= 11-18.

In contrast to the impact of CIPK23 on inward K^+ channels, changes in S-type anion channel activity are in line with the stomatal phenotypes. In line with the function of anion channels, a decline in S-type anion channel activity promotes stomatal opening in CIPK23^{T190D}, whereas the enhancement of anion channel activity makes CIPK23^{K60N} guard cells more sensitive to ABA. We also found that the expression level of anion channels SLAC1 and SLAH3 were altered in estrogen-induced CIPK23^{T190D} plants, but not in

CIPK23^{K60N} (**Fig. 3.20**), which suggests that the inhibition of S-type anion channels by CIPK23^{T190D} is partly compensated by upregulating the transcript abundance of SLAC1. Altogether, these data suggest that CIPK23 affects stomatal movements by inhibition of S-type anion channels.

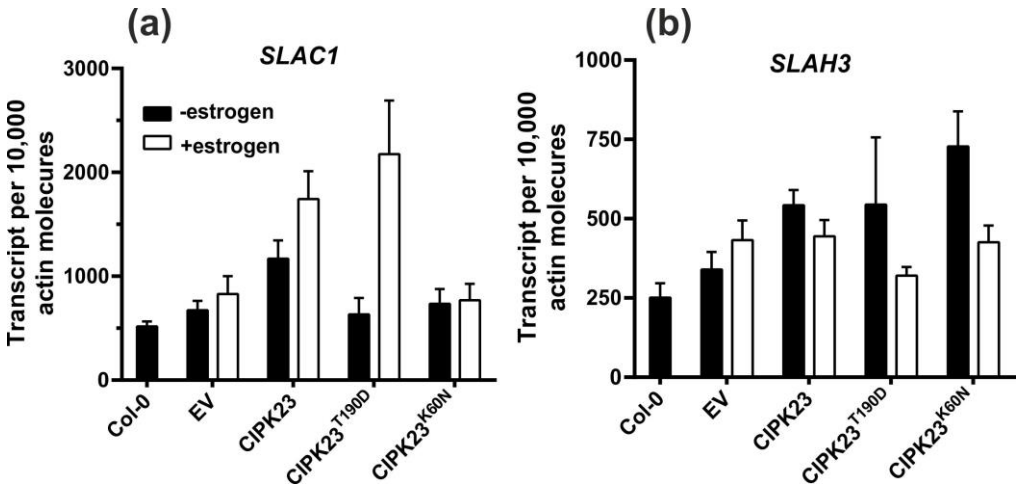

Fig. 3.20 Transcript levels of S-type anion channels in guard cells.

The expression level of *SLAC1* (a) or *SLAH3* (b) was quantified for guard cells that were isolated from leaves, 3 h after estrogen or control treatment. Data are mean values ± SE, n=5-8.

3.2.6 CIPK23^{T190D} fails to activate SLAC1 and SLAH3 in oocytes

In contrast to its inhibitory effect on S-type anion channels in guard cells, CIPK23 was shown to activate SLAC1 and SLAH3 in *Xenopus* oocytes (Maierhofer *et al.*, 2014a). These contrasting results prompted us to investigate in more detail how CIPK23 affects S-type anion channels in oocytes, which express SLAC1 only, or together with CIPK23/CBL1, CIPK23^{T190D}/CBL1 and CIPK23^{K60N}/CBL1. As shown in **Fig. 3.21a** and **c**, SLAC1-derived currents were detected in the oocytes that expressed SLAC1 with the wild type CIPK23/CBL1 complex, which is consistent with the previous study (Maierhofer *et al.*, 2014a). However, neither the kinase dead CIPK23^{K60N}/CBL1 nor the phosphomimic CIPK23^{T190D}/CBL1 could stimulate the SLAC1 channel (**Fig. 3.21a** and **c**).

In addition to SLAC1, *Arabidopsis* guard cells express SLAH3, (Negi *et al.*, 2008; Vahisalu *et al.*, 2008; Geiger *et al.*, 2011; Guzel Deger *et al.*, 2015). In contrast to SLAC1, SLAH3 has a stronger voltage dependency and is not stimulated by OST1 (Geiger *et al.*, 2011). To address if CIPK23 has a similar impact on SLAH3, oocytes that expressed SLAH3 solely, or

with CIPK23 variants were studied. Just as with SLAC1, in presence of 30 mM $NaNO_3$, SLAH3-derived currents were acquired in the oocytes coexpressed SLAH3 with wild type CIPK23/CBL1, but not in the ones with $CIPK23^{T190D}$- or $CIPK23^{K60N}$/CBL1 (**Fig. 3.21b** and **d**). These data show that both $CIPK23^{T190D}$ and $CIPK23^{K60N}$ fails to stimulate SLAC1 and SLAH3 in oocytes.

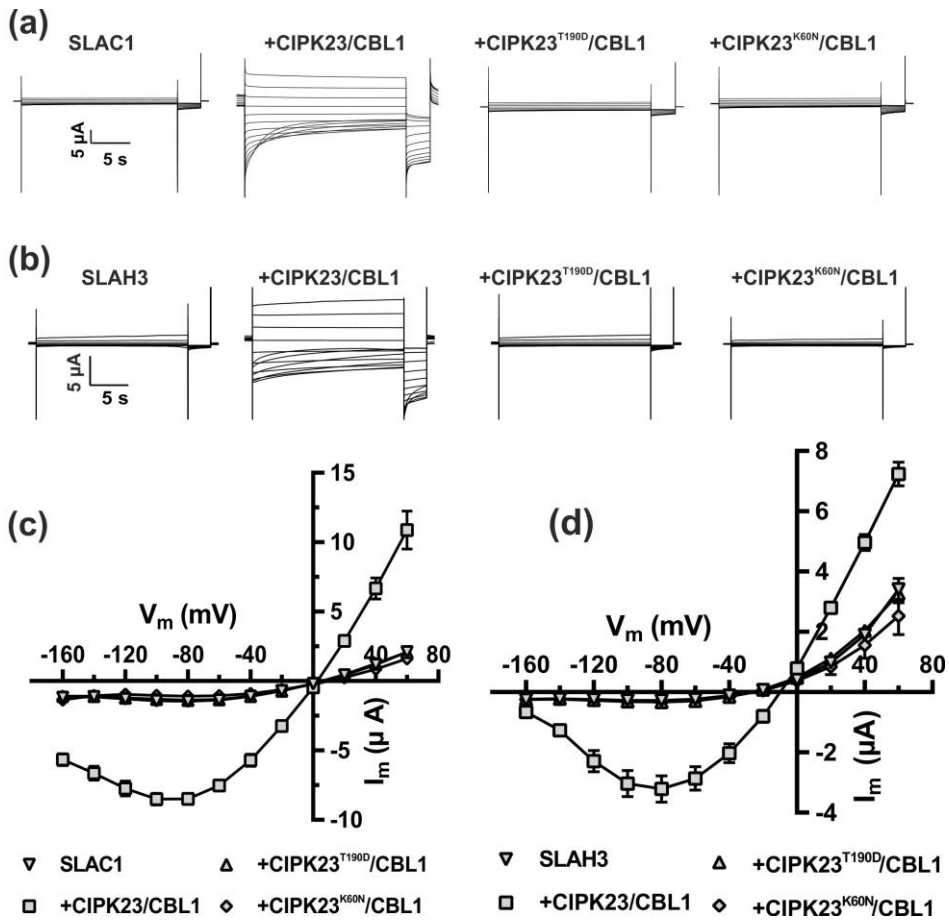

Fig. 3.21 $CIPK23^{T190D}$ and $CIPK23^{K60N}$ fail to activate SLAC1 and SLAH3 in oocytes.

(a,b) Currents recorded in *Xenopus* oocytes expressing SLAC1 (a), or SLAH3 (b). Oocytes were expressing only the S-type anion channel (left panel), or with CIPK23 variants and CBL1, as indicated. Oocytes were stimulated with 20 s voltage pulses from a holding potential of 0 mV to test values ranging from 60 to -180 mV with 20 mV decrements, followed by a 2.5 s voltage pulse to -120 mV. Oocytes were perfused with 30 mM NaCl (a) or $NaNO_3$ (b) during the measurements.

(c,d) Steady-state SLAC1 (c) or SLAH3 (d) currents, measured in *Xenopus* oocytes as shown in (a) and (b), were plotted against the membrane potential. Data presented as mean values ± SE, n=5.

The T190D mutation of CIPK23 was expected to lead to a constitutively active form of CIPK23, based on results with CIPK24/SOS2 (Gong *et al.*, 2002b), as well as CIPK3, 8, 9, 17 and 26 (Gong *et al.*, 2002a; Pandey *et al.*, 2008; Gao *et al.*, 2012; Lyzenga *et al.*, 2013; Song *et al.*, 2018; Yadav *et al.*, 2018). However, CIPK23^{T190D} was unable to activate SLAC1 and SLAH3, contrasting to wild type CIPK23. We therefore tested if other variants of CIPK23 can stimulate SLAC1 in oocytes. To this purpose, SLAC1 was coexpressed with constitutively active CIPK23$^{T190D+V182K}$ΔC in oocytes. Just as with CIPK23^{T190D}, the constitutively active CIPK23$^{T190D+V182K}$ΔC could not activate SLAC1 (**Fig. 3.22a**), whereas a neutral mutation CIPK23^{V182K}, which V182K is used to stabilize the CIPK23 activation loop at the active site (Chaves-Sanjuan *et al.*, 2014), was able to activate SLAC1. Collectively, these data show that CIPK23 variants, denoted as constitutively active forms, are unable to activate SLAC1 in oocytes.

In the plants with estrogen-induced CIPK23 expression, CIPK23 variants were tagged with a Venus, and for this reason, CIPK23^{T190D} was also tested in *Xenopus* oocytes with a Venus attached to its C terminus. Just as with CIPK23^{T190D}, CIPK23^{T190D}-Venus could not activate SLAC1 (**Fig. 3.22b**).

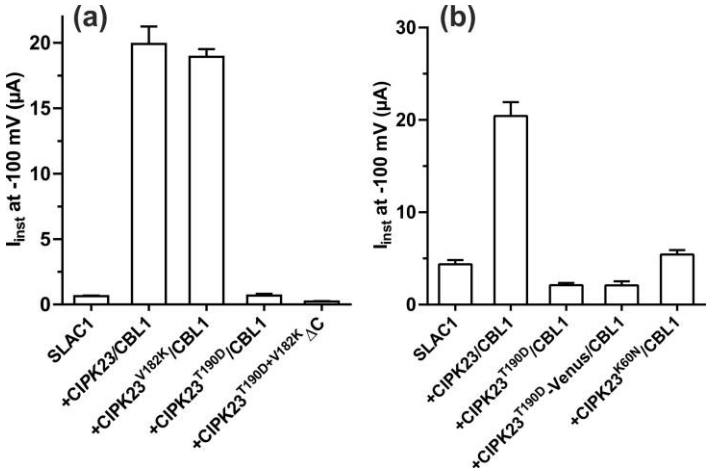

Fig. 3.22 CIPK23 variants, denoted as constitutively active forms, cannot activate SLAC1 in oocytes.

(a) Instantaneous currents recorded at -100 mV from oocytes expressing SLAC1 solely, or with the CIPK23 variants and CBL1. Measurements were carried out in the bath solution containing 50 mM NaCl. Data are shown as mean ± SE, n=4-6.

(b) Oocytes expressing SLAC1, with or without the indicated CIPK23 variants, were recorded in a 50 mM chloride-based bath solution. Instantaneous whole-cell currents at -100 mV are shown. Data are mean ± SE, n=4-6.

3.2.7 CIPK23^{T190D} suppresses CPK23- and CIPK11-activated SLAC1

The simple activation modules of OST1-SLAC1, CPKs-SLAC1 and CBL/CIPKs-SLAC1 have been proved in the heterologous system of *Xenopus* oocytes (Geiger *et al.*, 2010; Brandt *et al.*, 2012; Scherzer *et al.*, 2012; Brandt *et al.*, 2015). However, signaling pathways in guard cells frequently have the crosstalk, and influence each other. Thus, we decided to test whether the activation of SLAC1 by these kinases is influenced by the CIPK23^{T190D}. As shown in **Fig. 3.23,** CIPK23^{T190D} did not influence OST1-, CPK6-, CPK21-induced SLAC1 currents. However, CIPK23^{T190D}/CBL1 dramatically inhibited CPK23-stimulated anion channel currents, whereas this inhibition did not occur with CIPK23^{K60N}/CBL1 (**Fig. 3.23d**). These data thus show that CIPK23^{T190D} is able to inhibit CPK23-mediated SLAC1 and this inhibition is dependent on CIPK23 kinase activity.

In addition to the protein kinases OST1, CPK6, CPK21, and CPK23, CIPK11/CBL5 complex was shown to activate SLAC1 in oocytes, which was dependent on the N-myristoylation and S-acylation of CBL5 (Saito *et al.*, 2018). As CIPK23 has a similar structure with CIPK11, we tested if CIPK23 can compete for SLAC1 with CIPK11. Instead of CBL5, CBL1 was coexpressed with CIPK11 and SLAC1. Note that CBL1 also can be modified by N-myristoylation and S-acylation (Batistic *et al.*, 2008). Large anion currents were recorded from the oocytes expressing SLAC1 and CIPK11/CBL1 complex (**Fig. 3.23e**), just as shown in the previous study of Saito *et al.*, (2018) with CIPK11/CBL5. When the SLAC1, CIPK11 and CBL1, together with CIPK23, CIPK23^{T190D} or CIPK23^{K60N}, were expressed in oocytes, we found that both CIPK23^{T190D} and CIPK23^{K60N} strongly suppressed the CIPK11-mediated SLAC1 currents (**Fig. 3.23e**). This suggests that these CIPK23 variants can disrupt the activation of SLAC1 by CIPK11, by a mechanism that does not rely on the CIPK23 kinase activity. Together, these inhibitions that are mediated by CIPK23 may cause a reduction in S-type anion channel currents in guard cells (**Fig. 3.18**), albeit CIPK23 can activate SLAC1 in oocytes.

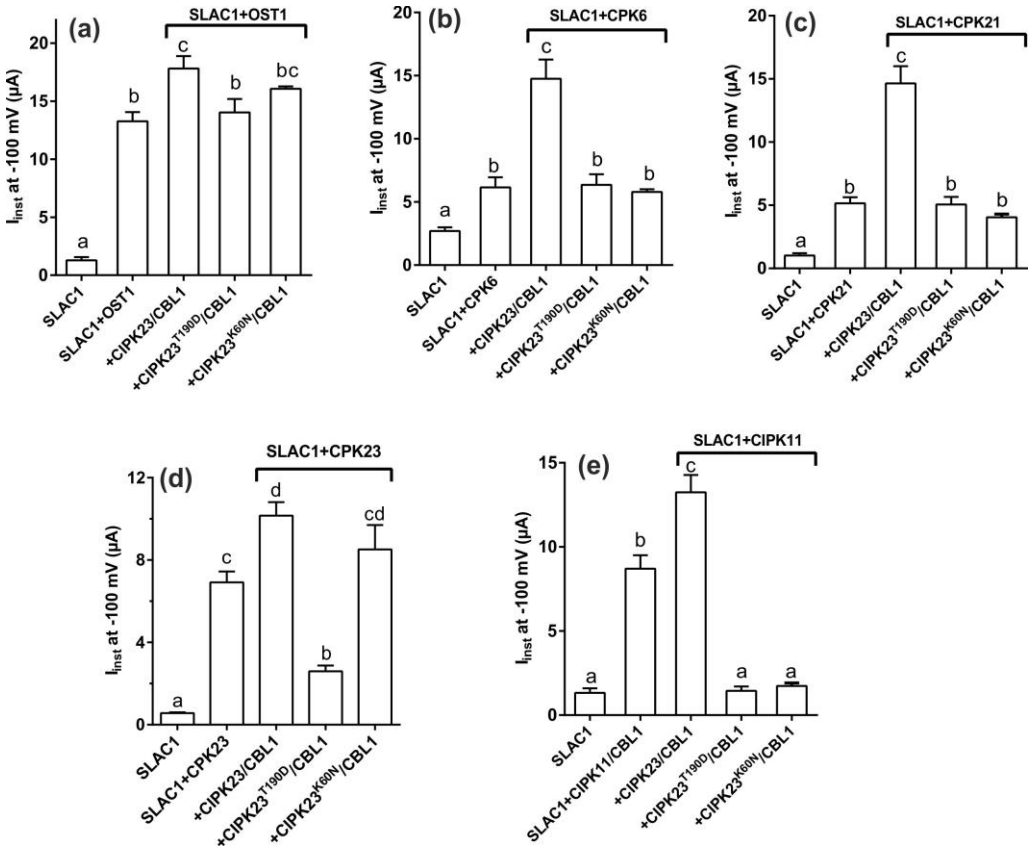

Fig. 3.23 CIPK23^{T190D} disrupts the activation of SLAC1 by CPK23 and CIPK11.

Instantaneous currents recorded at -100 mV from oocytes expressing SLAC1, with or without the indicated protein kinases. Whole cell currents were measured in 50 mM NaCl based bath solution. Following amounts of cRNA were injected into oocytes: SLAC1: 6 ng; CIPK11, CPK23, CPK21, CPK6, or OST1: 0.6 ng; CIPK23 variants and CBL1: 3 ng. Data are shown as mean ± SE, n=6-9. Statistical analysis was carried out with One-way ANOVA ($p<0.05$, Tukey test). Note that CIPK23^{T190D} interferes CPK23- (d) and CIPK11-activated (e) SLAC1, but it had little effect on OST1- (a), CPK6- (b), or CPK21-stimulated (c) SLAC1.

4. Discussion

The phytohormone ABA functions as a general stress signal in vascular plants (Milborrow, 2001), and can be synthesized in various cell types (Finkelstein, 2013). ABA is involved in regulation of many physiological and developmental processes, such as seed maturation and dormancy, root and shoot growth, and leaf senescence (Finkelstein, 2013). In addition to these relatively slow responses, ABA also can rapidly trigger stomatal closure upon drought stress, which prevents water loss from leaves (Cutler *et al.*, 2010; Roelfsema *et al.*, 2012; Munemasa *et al.*, 2015; Jezek & Blatt, 2017). ABA is thus important for plant growth and stress responses. Though ABA emerges as early as algae, still little is known about how and when ABA evolved as a stress hormone during the evolution (Cheng *et al.*, 2019; Sun *et al.*, 2019).

Studies have revealed that ABA-mediated stomatal closure is regulated by an ABA signaling chain, which consists of ABA receptors, PP2Cs, and two branches of protein kinases (Roelfsema *et al.*, 2012; Kollist *et al.*, 2014; Hedrich & Geiger, 2017). The Ca^{2+}-independent branch, mainly OST1, is essential for stomatal closure, since loss of OST1 function strongly disrupts the stomatal response to ABA (Mustilli *et al.*, 2002; Yoshida *et al.*, 2002; Acharya *et al.*, 2013). Though a Ca^{2+}-dependent branch also exists in guard cells, however, this branch cannot compensate for the loss of OST1. Many studies showed that Ca^{2+} signals are associated with ABA-induced stomatal closure (McAinsh *et al.*, 1990; Gilroy *et al.*, 1991; Allen *et al.*, 1999a; Allen *et al.*, 1999b; Marten *et al.*, 2007b), but it is still unclear if these Ca^{2+} signals are important for stomatal closure, how ABA triggers these signals, and which Ca^{2+} channels are involved. These questions will be discussed below.

4.1 ABA-induced Ca^{2+} signals and stomatal closure

4.1.1 ABA-evoked Ca^{2+} signals are mainly caused by fast changes in osmotic content of guard cells

In this study, application of ABA to wild type guard cells triggered two types of cytosolic Ca^{2+} signals (**Fig. 3.5a** and **b**). In most experiments, the Ca^{2+} signals were provoked during stomatal closure, instead of an earlier time point, as has been proposed by various papers (McAinsh *et al.*, 1990; Allen *et al.*, 2000; Allen *et al.*, 2001). It is likely that the

transient increase in the cytosolic Ca^{2+} concentration is caused by the fast changes in the osmotic content of guard cells, which arise at the start of stomatal closure (**Fig. 4.1**). Studies on guard cells of tobacco provide strong evidence in support of such a mechanism (Voss *et al.*, 2016). It was shown that fast changes in the osmotic content in guard cells could be imposed with hyperpolarizing pulses. During these pulses the cytosolic volume expanded rapidly, which leads to a sudden contraction in the vacuole. As a result, intercellular Ca^{2+} channels are activated, and cause a Ca^{2+} release from vacuole (Voss *et al.*, 2016). The occurrence of a similar sequence of events during ABA responses is supported by the results of *ost1-3* mutant. As guard cells with the *ost1-3* are insensitive to ABA, fast osmotic content changes will not occur, and as a result, the late ABA-induced Ca^{2+} signals do not occur in the *ost1-3* mutant (**Fig. 3.8a**).

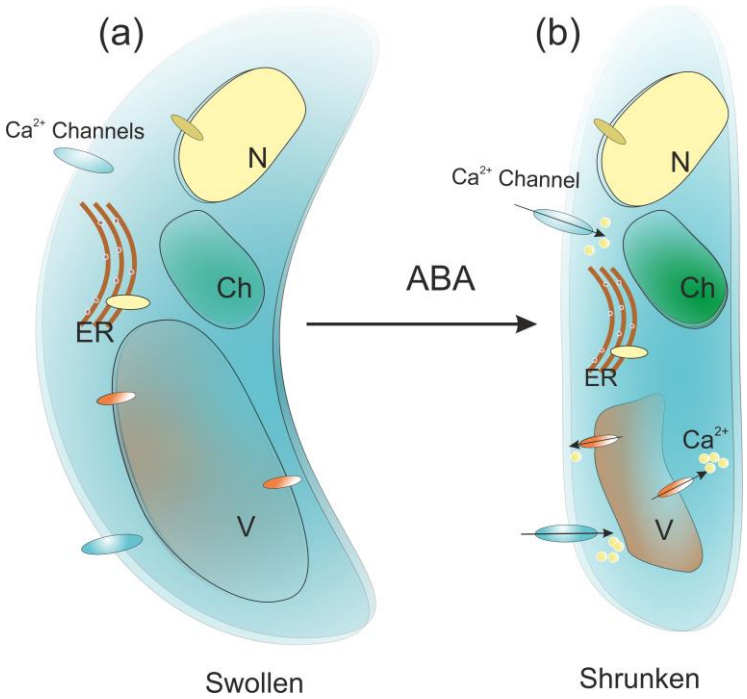

Fig. 4.1 Fast changes in the osmotic content of guard cells elicit Ca^{2+} signals.

(a) In the absence of ABA, guard cells are in a swollen state, and the vacuole is osmotically equilibrated with the cytosol. Ca^{2+} channels located at various membranes are maintained in a low activity state.

(b) ABA application causes fast changes in the osmotic content of guard cells, which leads to cell shrinking and compression of the vacuole. As a result, a large number of Ca^{2+} channels will become active and subsequently release Ca^{2+} into the cytosol, which induces a transient increase in the cytosolic Ca^{2+} concentration. Abbreviation, V: vacuole; ER: endoplasmic reticulum; Ch: chloroplasts.

Our experiments also showed that ABA can induce Ca^{2+} signals that proceed to stomatal closure (**Fig. 3.5c**). Apparently, ABA also can activate Ca^{2+} channels by a mechanism that parallels the change in osmotic pressure. This second mechanism may also explain why a small group of ABA-induced Ca^{2+} signals still occur in the guard cells of *ost1-3* (**Fig. 3.8b**), *abi1* and *abi2* (Allen *et al.*, 1999a), though their stomata do not close after application of ABA. The Ca^{2+} oscillations in guard cells that are induced by ABA in isolated epidermal tissue thus may depend on this second mechanism (Allen *et al.*, 1999a; Allen *et al.*, 2001; Klusener *et al.*, 2002; Islam *et al.*, 2010b). In contrast to osmotically induced Ca^{2+} signals, this second mechanism causes much weaker changes in the cytosolic Ca^{2+} level, which did not exceed 100 nM (**Fig. 3.8b**). In line with this hypothesis, osmotically induced Ca^{2+} signals are less likely to occur in isolated epidermal tissues, since the ABA-induced stomatal closure response is less pronounced, as in intact leaves (Islam *et al.*, 2010a). This suggests that ABA evokes the early Ca^{2+} signals through a mechanism that does not depend on OST1, but instead through an alternative pathway that stimulates non-selective cation channels in the guard cell plasma membrane (Hamilton *et al.*, 2000b; Pei *et al.*, 2000; Siegel *et al.*, 2009). However, it seems that both the early and osmotic pressure induced Ca^{2+} signals depend on the PYR/PYLs/RCARs ABA receptors, since studies indicate that ABA-evoked Ca^{2+} signals are strongly impaired in the quadruple mutant *pyr1/pyl1/pyl2/pyl4* (Wang *et al.*, 2013a).

4.1.2 Ca^{2+} signals accelerate ABA-induced stomatal closure

Studies with a variety of plant species revealed that guard cells utilize conserved mechanisms to control the Ca^{2+} homeostasis (Grabov & Blatt, 1998; Levchenko *et al.*, 2005; Marten *et al.*, 2007b; Levchenko *et al.*, 2008; Stange *et al.*, 2010; Voss *et al.*, 2018). In general, the free cytosolic Ca^{2+} concentration in guard cells is maintained at range from 100 to 250 nM, at the resting membrane potential. However, a transient increase in the Ca^{2+} level is elicited by a hyperpolarizing pulse of the plasma membrane to -180 mV, or more negative potentials. Guard cells of *Arabidopsis* do not differ in this respect from their relatives in other species (**Fig. 3.7**).

In this study, ABA induced a transient rise in the Ca^{2+} level in 3 out of 4 experiments, whereas 1 out of 4 stomata closed in the absence of Ca^{2+} signals (**Fig. 3.5c**). Earlier

studies showed that ABA-dependent Ca^{2+} signals were detected either in 8 out of 10 stomata (McAinsh et al., 1990), or in 14 out of 38 stomata of *C. communis* (Gilroy et al., 1991). In line with these Ca^{2+} imaging studies, the electrophysiological recording showed that ABA is able to stimulate S-type anion channels with, or without Ca^{2+} signals (Levchenko *et al.*, 2005; Marten *et al.*, 2007b). These data suggest that ABA-induced Ca^{2+} signals are common in guard cells, but not absolutely required for stomatal closure.

As discussed above, Ca^{2+} signals are not essential for ABA-induced stomatal closure, but nevertheless common in ABA-treated guard cells, implying that they have a specific function on stomatal closure. Our studies suggest that ABA-evoked Ca^{2+} signals enhance the velocity of stomatal closure (**Fig. 3.6b**), especially when these Ca^{2+} signals occurred during the stomatal closure. In this case, the osmotic imbalance caused by guard cells shrinking prompts Ca^{2+} release from intracellular stores (**Fig. 4.1**), which activates S-type anion channels. The Ca^{2+} signals would thus act in a feed-forward loop that boosts stomatal closure, which will help plants to shut the stomatal pores rapidly and limit water loss.

4.1.3 Ca^{2+}-dependent activation of SLAC1 and SLAH3 anion channels

Guard cell S-type anion channels comprise SLAC1 and SLAH3 (Negi *et al.*, 2008; Vahisalu *et al.*, 2008; Geiger *et al.*, 2011; Guzel Deger *et al.*, 2015), which are critical for ABA-induced stomatal closure. ABA-induced Ca^{2+} signals probably activate these anion channels, and thus enhance stomatal closure (**Fig. 4.2**). This speculation was verified by the observation that Ca^{2+} signals could activate S-type anion channels in wild type guard cells, but not in the *slac1/slah3* double knock-out mutant (**Fig. 3.7c** and **d**). The activation of SLAC1 and SLAH3 by the elevated cytosolic Ca^{2+} levels probably requires CPKs, or CBLs/CIPKs, which are capable of stimulating SLAC1 and SLAH3 in oocytes (Hedrich & Geiger, 2017; Kudla *et al.*, 2018).

The cytosolic Ca^{2+} signals not only regulate the plasma membrane ion channels but also the vacuolar TPKs (Two Pore K^+ channels) (**Fig. 4.2**). Stomatal conductance assay showed that stomatal closure kinetics were slower in TPK1 knock-out mutants and faster in TPK1 overexpression line (Gobert *et al.*, 2007; Latz *et al.*, 2013; Wang *et al.*, 2015). Ca^{2+} signals thus may serve as a unifying signal that can coordinate transport processes between the

plasma membrane and intracellular membranes (Wheeler & Brownlee, 2008). Such a coordinated response is likely to be important for rapid stomatal closure, in which osmolytes are first released from the vacuole into the cytosol and finally extruded across the plasma membrane into the apoplast (**Fig. 4.2**) (Wheeler & Brownlee, 2008; Kollist *et al.*, 2014).

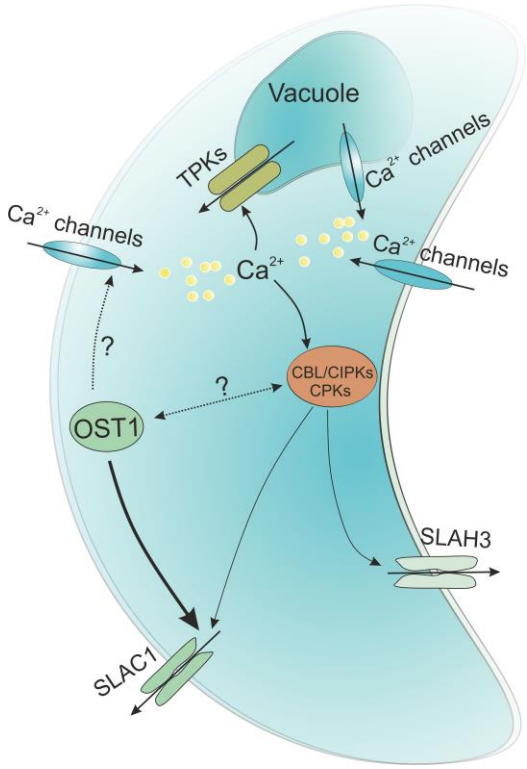

Fig. 4.2 Ca^{2+}-dependent signaling stimulates anion channels in guard cells. ABA initiates stomatal closure by activating the core component of OST1 protein kinase. OST1 phosphorylates and stimulates SLAC1, and causes rapid osmotic changes in guard cells, which in turn activate Ca^{2+} channels in membranes of the cell plasma, or organelles. As a result, it causes a transient increase in the cytosolic Ca^{2+} signals. These Ca^{2+} signals not only target the anion channels SLAC1 and SLAH3 via the Ca^{2+}-activated protein kinases (CBL/CIPKs complex and CPKs) but also TPKs in the tonoplast. Activation of these channels accelerates ion efflux from the cells, and thus enhances the speed of stomatal closure. OST1 and Ca^{2+} signals coordinately provoke ABA-induced stomatal closure, while OST1 also may have a direct impact on Ca^{2+} channels and the activity of CPKs.

4.1.4 Outlook of Ca^{2+} signals in stomatal movements

Receptors for various biotic and abiotic stimuli have been found in guard cells. These receptors can perceive the drought hormone ABA, as well as a variety of other signals such as CO_2, Microbe Associated Molecular patterns (MAMPs), and blue light. Just as

with ABA, Ca^{2+} oscillations have been recorded in isolated guard cells when they were challenged with CO_2 or flg22 (Young *et al.*, 2006; Thor & Peiter, 2014). However, it is still unclear to which extent CO_2 and flg22-induced Ca^{2+} signals are related to stomatal movements. The new generation of genetically encoded Ca^{2+} sensors and the current-ejection technique, now enables us to conduct experiments in intact leaves, and monitor Ca^{2+} signals and stomata movements simultaneously. It will be interesting to investigate if Ca^{2+} signals evoked by flg22 are similar to those triggered by ABA. The initial steps in flg22 and ABA signaling are different, but their pathways converge at the level of OST1 (Guzel Deger *et al.*, 2015), and OST1 is of major importance for triggering Ca^{2+} signals in the guard cell response to ABA (**Fig. 3.8**).

The newly developed R-GECO1-mTurquoise will also be of great advantage to study the nature of Ca^{2+} channels that give rise to Ca^{2+} signals in guard cells. ABA-induced activation of Ca^{2+}-permeable plasma membrane channels in guard cells was reported almost 20 years ago (Hamilton *et al.*, 2000; Pei *et al.*, 2000), but the genes encoding these channels still need to be uncovered. The OSCA channels, which are expressed in guard cells, have been associated with osmotically induced Ca^{2+} signals (Hou *et al.*, 2014; Yuan *et al.*, 2014). These channels are thus good candidates for those that generate Ca^{2+} signals during the acceleration phase of ABA-induced stomatal closure.

4.2 The role of CIPK23 in stomatal movements

Stomatal opening and closure are controlled by diverse ion channels in the plasma membrane of guard cells. The S-type anion channels SLAC1 and SLAH3 are main switches that adjust stomatal movements. We have shown that ABA-induced Ca^{2+} signals can activate S-type anion channels and thus enhance stomatal closure. However, S-type anion channels do not directly sense Ca^{2+} ions, and thus CPKs and/or CIPKs encoded protein kinases are required to provoke these responses. Here, we have uncovered that CIPK23, a downstream component of Ca^{2+} signals, affects stomatal movements by modulating the activity of SLAC1 and SLAH3, rather than the inward K^+ channel AKT1 activity.

4.2.1 CIPK23 regulation of AKT1 does not affect stomatal movements

Our data show that the overexpression of CIPK23 and CIPK23^{T190D} promoted stomatal opening, while CIPK23^{K60N} enhanced ABA-induced stomatal closure (**Fig. 3.11** and **Fig. 3.12**), which is in line with the previous studies (Cheong *et al.*, 2007; Nieves-Cordones *et al.*, 2012; Sadhukhan *et al.*, 2019). It was proposed that CIPK23-mediated stomatal movements are dependent on the interaction between CIPK23 and AKT1 (Nieves-Cordones *et al.*, 2012; Mao *et al.*, 2016; Sadhukhan *et al.*, 2019; Saito & Uozumi, 2019), based on the observation that both *cipk23* and *akt1* mutants exhibited similar stomatal response to drought stress and ABA (Nieves-Cordones *et al.*, 2012; Sadhukhan *et al.*, 2019). However, our data revealed that inward K^+ channel currents had a similar amplitude in the guard cells that expressed wild type CIPK23, CIPK23^{T190D}, and CIPK23^{K60N} (**Fig. 3.13a** and **b**), demonstrating that the impact of CIPK23 on AKT1 activity does not match with the influence of CIPK23 on stomatal movements. It is not surprising that the CIPK23-mediated AKT1 has little effect on stomatal movements, since AKT1 is a voltage-gated channel, of which the gating is strictly regulated by the plasma membrane potential (Geiger *et al.*, 2009a). In other words, CIPK23 only increases the maximal open probability of AKT1, but not the voltage-dependency. Activation of CIPK23 will only lead to a small depolarization of guard cells in the hyperpolarized state (Roelfsema & Prins, 1997). Thus, CIPK23-activated AKT1 probably will have little influence on stomatal movements. In line with this hypothesis, loss of KAT1 activity, or overexpression of KAT1,

also does not alter the stomatal movements in response to light, CO_2, and ABA (Szyroki *et al.*, 2001; Wang *et al.*, 2014).

But why does loss of AKT1 lead to a similar phenotype as *cipk23* mutants (Nieves-Cordones *et al.*, 2012)? One explanation could be that deficiency in AKT1 affects the K^+ homeostasis in the whole plant (Li *et al.*, 2006; Xu *et al.*, 2006), since the main pathway for K^+ uptake by roots is disrupted. Lower K^+ uptake, due to loss of AKT1, may change the ability of stomata to respond to drought stress.

4.2.2 The activation of AKT1 by CIPK23 is independent of its kinase activity

Previous studies showed that the activation of AKT1 by CIPK23 depends on the protein kinase activity of CIPK23. The kinase dead $CIPK23^{K60N}$ was unable to activate AKT1 in oocytes (Li *et al.*, 2006; Xu *et al.*, 2006). However, in our hands $CIPK23^{K60N}$ could enhance inward K^+ channel currents in guard cells (**Fig. 3.13a** and **b**) and could also activate AKT1 in oocytes (**Fig. 3.16**). These contrasting results may be explained by the cRNA expression time, as we observed that the activation of AKT1 by $CIPK23^{K60N}$ was not pronounced if the cRNA expression was shorter than 48 h. Li *et al.*, (2006) probably performed the associated measurements with oocytes that only had a short expression time of the cRNA. The guard cell and oocyte data in this thesis strongly suggest that the activation of AKT1 by CIPK23 does not rely on the protein kinase activity of CIPK23. This conclusion is supported by the finding that the constitutively active $CIPK23^{T190D+V182K}\Delta C$ failed to stimulate AKT1 (**Fig. 3.17**). Apparently, the C-terminus of CIPK23 is essential for the activation of AKT1. It is likely that the C-terminal domain of CIPK23 mediates the interaction with CBL1 or CBL9, and is required for AKT1 activation (Hashimoto *et al.*, 2012). Our findings explain why the constitutively active form of CIPK23 ($CIPK23^{T190D}$ ΔC) can neither restore the *cbl1/9* phenotype, nor activate AKT1 in oocytes (Xu *et al.*, 2006). A similar activation mechanism has been reported for CIPK6 and AKT2. The enhancement of AKT2 currents by CIPK6 is abolished if its C-terminal domain is removed. Moreover, the C-terminus of CIPK6 was important to translocate CBL4 and AKT2 from the ER (endoplasmic reticulum) membrane to the plasma membrane (Held *et al.*, 2011).

4.2.3 CIPK23 inhibits the activity of S-type anion channels and stimulates stomatal opening

CIPK23 has been shown to interact with and activate the S-type anion channels SLAC1 and SLAH3 in *Xenopus* oocytes (Maierhofer *et al.*, 2014a). Based on these results, stomata of *cipk23* mutants were expected to be more open, whereas closed stomata were speculated to occur in the CIPK23 gain-of-function plants. However, in contrast to these speculations, strong overexpression of wild type CIPK23 (LKS,OE) and the phosphomimic CIPK23^{T190D} led to more open stomata and an inhibition of S-type anion channels, when compared to control plants (**Fig. 3.11a-d**, **Fig. 3.12b**, **Fig. 3.18** and **Fig. 3.19**). Stomata of the kinase dead CIPK23^{K60N} and *cipk23* were hypersensitive to ABA, and displayed a higher activity of S-type anion channels (**Fig. 3.11e-f, Fig. 3.18** and **Fig. 3.19**) (Cheong *et al.*, 2007; Nieves-Cordones *et al.*, 2012; Sadhukhan *et al.*, 2019). These data suggest that CIPK23 is a negative regulator of stomatal closure, instead of a positive one, which was concluded, based on the oocyte data (Maierhofer *et al.*, 2014a).

Why does CIPK23 activate SLAC1 and SLAH3 in oocytes, but inhibit these channels in guard cells? One possibility could be that the expression of CIPK23 has a strong impact on the transcripts of other protein kinases that can activate S-type anion channels. Studies revealed that plants lacking CIPK23 increase the transcript abundance of CPK3, CPK6, CPK21 and OST1 (Maierhofer *et al.*, 2014a), which are components of ABA signaling and thus able to stimulate SLAC1 and SLAH3 (Geiger *et al.*, 2010; Geiger *et al.*, 2011; Brandt *et al.*, 2012; Scherzer *et al.*, 2012; Brandt *et al.*, 2015). This feedback regulation on CPK3, CPK6, CPK21, and OST1 may overcompensate the impact of loss of CIPK23, and lead to enhance S-type anion channel activity in *cipk23* guard cells (**Fig. 3.18** and **Fig. 3.19**), though a reduction in anion conductance is expected in *cipk23* guard cells, based on the oocyte data (**Fig. 3.21** and **Fig. 3.22**) (Maierhofer *et al.*, 2014a; Saito *et al.*, 2018). A similar regulatory mechanism was also reported for CPK23. Disruption of CPK23 increases the transcript levels of both ABI1 and CPK21, which alters the equilibrium between activating and deactivating signaling components (Geiger *et al.*, 2010) and results in an enhanced tolerance to drought stress in *cpk23* knock-out mutants (Ma & Wu, 2007).

In addition to a feedback mechanism of the transcript levels, CIPK23 may regulate other protein kinases that in turn control S-type anion channel activity. As shown in our results,

the activation of SLAC1 by CPK23 was inhibited by the phosphomimic CIPK23^{T190D} (**Fig. 3.23d**), and this inhibition may be accomplished by a phosphorylation event, because only the phosphomimic CIPK23^{T190D}, but not the kinase dead CIPK23^{K60N} could suppress the activation of SLAC1 by CPK23 (**Fig. 3.23d**). In contrast, the suppression of CIPK11-dependent SLAC1 activation occurred with CIPK23^{T190D} as well as CIPK23^{K60N} (**Fig. 3.23e**), suggesting that CIPK23 may compete for the interaction site of SLAC1 with CIPK11. This competition may block channel activation, since the similarity of protein sequences between CIPK23 and CIPK11 is as high as 66% (blastp, NCBI). These results suggest that CIPK23 employs at least two regulation mechanisms to inhibit the activity of SLAC1 (**Fig. 4.3**). CIPK23 may phosphorylate CPKs, while it competes with other CIPKs for the binding site of SLAC1.

4.2.4 Inhibition of S-type anion channel activity in guard cells

It has been shown that a set of protein kinases, including OST1, GHR1, CPK3, CPK6, CPK21, CPK23, and CIPK11, are able to activate the S-type anion channels SLAC1 and/or SLAH3 (Geiger *et al.*, 2010; Geiger *et al.*, 2011; Brandt *et al.*, 2012; Hua *et al.*, 2012; Scherzer *et al.*, 2012; Brandt *et al.*, 2015; Saito *et al.*, 2018; Sierla *et al.*, 2018). Moreover, stomata of *cpk4, cpk3/6*, *cpk8*, *cpk10,* and *cpk11* mutants did not close in response to ABA (Mori *et al.*, 2006; Zhu *et al.*, 2007; Zou *et al.*, 2010; Zou *et al.*, 2015). These protein kinases may over-activate anion channels during the drought stress/ABA responses, which would cause complete closure of stomata, and in turn lead to CO_2 starvation. To avoid this problem, guard cells require feedback mechanisms to finely and accurately control S-type anion channel activity. PP2Cs that functions as the ABA co-receptors seem to serve as a brake to control S-type anion channels in absence of ABA (**Fig. 4.3**), because these protein phosphatases can suppress the kinase activity of OST1 (Umezawa *et al.*, 2009; Vlad *et al.*, 2009), which is a critical activator of SLAC1 (Geiger *et al.*, 2009b). In addition, PP2Cs are able to directly interact with and dephosphorylate the N-terminus of SLAC1, which probably also prevents CPK6- and CPK23-dependent SLAC1 activation (Brandt *et al.*, 2015). However, PP2Cs are recruited and inhibited by the ABA receptors PYR/PYLs/RCARs in the presence of ABA (**Fig. 4.3**) (Ma *et al.*, 2009; Park *et al.*, 2009). Guard cells thus must trigger other regulatory proteins to continue controlling S-type anion channel activity

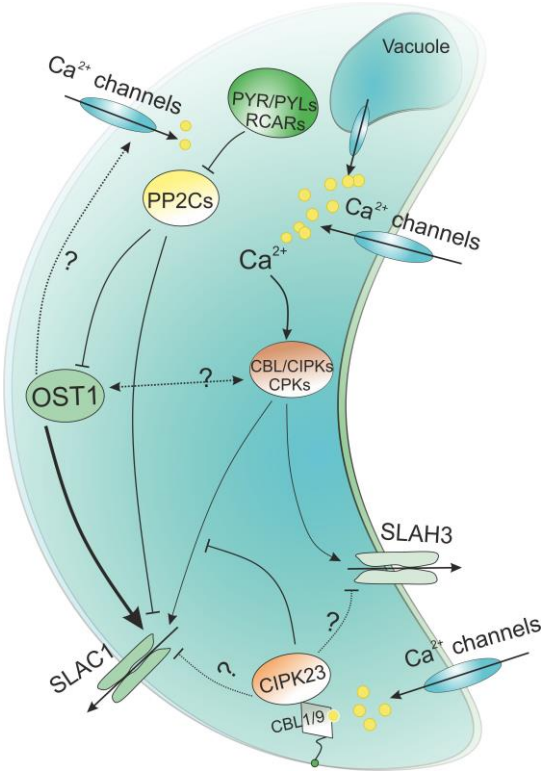

Fig. 4.3 Regulation of S-type anion channel activity in guard cells. In the absence of ABA, PP2Cs inhibit OST1 and thereby prevent activation of SLAC1. In addition, PP2Cs directly interact with and dephosphorylate SLAC1, which probably also prevents the activation of SLAC1 by CPK6 and CPK23. S-type anion channels are thus maintained in a low active state. In the presence of ABA, PP2Cs are recruited and inhibited by the ABA receptors PYR/PYLs/RCARs, which leads to OST1 activation. OST1 phosphorylates and stimulates the main anion channel SLAC1 to initiate stomatal closure. The fast osmotic content changes in guard cells caused by the OST1-SLAC1 module activate Ca^{2+}-permeable channels in the plasma membrane and the tonoplast, and thus lead to an increase in the cytosolic Ca^{2+} concentration. The cytosolic Ca^{2+} signals can activate the Ca^{2+} dependent protein kinases CPKs and CBL/CIPKs that positively regulate SLAC1 and SLAH3. Likewise, Ca^{2+} can also bind to CBL1 and 9, which anchors to the plasma membrane via N-myristoylation, the active complex CBL1/9-CIPK23 inhibits SLAC1 and SLAH3, via a so far uncovered mechanism.

when ABA is present. This speculation is supported by earlier studies, which showed that ABA can rapidly activate S-type anion channels in guard cells, but after approximately 5 min, the currents start to recover, even though ABA remains present (Roelfsema *et al.*, 2004; Levchenko *et al.*, 2005; Marten *et al.*, 2007b). A group of Ca^{2+}-dependent protein kinases, which negatively regulate ABA-induced stomatal closure, could function as negative feedback regulatory proteins. Studies show that loss of CPK9, CPK23, CPK33,

CIPK9, CIPK15(PKS3), CIPK17, CIPK23, CBL1/9, or CBL2/3, enhanced stomatal closure in response to ABA, and improved plant drought tolerance (Guo *et al.*, 2002; Cheong *et al.*, 2007; Ma & Wu, 2007; Nieves-Cordones *et al.*, 2012; Li *et al.*, 2016; Song *et al.*, 2018; Chen *et al.*, 2019; Sadhukhan *et al.*, 2019). Moreover, both CIPK23 and CPK9 are capable of inhibiting S-type anion channel activity in guard cells (**Fig. 3.18** and **Fig. 3.19**) (Chen *et al.*, 2019). It suggests that this second group of protein kinases represses the activity of S-type anion channels.

As discussed above, different Ca^{2+}-dependent protein kinases may display a counteractive role in ABA-mediated S-type anion channels and stomatal closure. Apparently, these Ca^{2+}-dependent protein kinases can be divided into two groups (I and II), one group (I) stimulates S-type anion channels and promotes stomatal closure, whereas the other (II) inhibits this response. Given that the activation of SLAC1 depends on the phosphorylation events (Geiger *et al.*, 2010; Brandt *et al.*, 2012; Maierhofer *et al.*, 2014a), the inhibition of the anion channel activity could be accomplished by dephosphorylation, which is mediated by protein phosphatases. Though the activity of PP2Cs has been reported to be inhibited by ABA-bound receptors *in vitro* (Ma *et al.*, 2009; Park *et al.*, 2009), this inhibition only partly takes place *in vivo* (Wang *et al.*, 2018). Enhancement of PP2C activity by a positive regulator can disrupt ABA-induced stomatal closure (Wang *et al.*, 2018). The group II Ca^{2+}-dependent protein kinases probably adopt a similar mechanism to control the S-type anion channel activity during ABA responses. Studies with CPK12 provide evidence to support this hypothesis. Biochemical assays showed that CPK12 interacts with and stimulates ABI2 phosphatase activity *in vitro* by phosphorylating Thr-16, Ser-101 and Thr-261 of ABI2 (Zhao *et al.*, 2011a). Moreover, loss of CPK12 expression leads to ABA hypersensitive phenotypes in *cpk12* RNAi lines (Zhao *et al.*, 2011a). It suggests that the activation of ABI2 by CPK12 can counteract the ABA signaling. In addition to CPKs, CIPKs may also have an important impact on PP2C activity. Studies show that stomatal closure is hypersensitive to ABA in the *cipk15 (pks3)* mutant, which may be linked to the protein phosphatases ABI1 and ABI2, since CIPK15 strongly interacts with ABI2, and to a lesser extent with ABI1 (Guo *et al.*, 2002). The CIPK15-ABI1/2 complex may thus control the phosphorylation of SLAC1 and SLAH3. In a preliminary phosphoproteomics, the phosphopeptide abundance of 3 protein

phosphatases, F2KP (Fructose-2,6-bisphosphatase), PAPP2C (Phytochrome-Associated Protein Phosphatase type 2C), PUX5 (serine/threonine protein phosphatase 2A 55, or Plant UBX-type ubiquitin-regulatory protein), are pronouncedly increased in CIPK23 overexpression guard cells, whereas they are decreased in *cipk23* knock-out mutant after ABA treatment. These protein phosphatases thus may be activated by the CIPK23-mediated phosphorylation, and may function as novel regulators to control S-type anion channel activity in guard cells. Collectively, group II Ca^{2+}-dependent protein kinases may stimulate protein phosphatase activity to balance the activation and suppression of anion channels, which allows guard cells to optimize the stomatal pore opening. This may enable plants to retain as much as possible water, while they also ensure the uptake of an adequate quantity of CO_2 for photosynthesis.

4.2.5 Outlook of Ca^{2+}-dependent protein kinases and stomatal movements

It was thought that Ca^{2+} signals are positively associated with ABA-induced stomatal closure (McAinsh *et al.*, 1990; Allen *et al.*, 2000; Schroeder *et al.*, 2001). The Ca^{2+}-dependent proteins that interpret these signals were thus expected to positively modulate this process. However, Ca^{2+}-dependent protein kinases do not display consistent results as the expectation, since a group of these protein kinases inhibits ABA-induced stomatal closure. These suggest that ABA-induced Ca^{2+} signals have dual roles in stomatal closure, which is apparently against the conventional hypothesis that Ca^{2+} signals are only positively associated with ABA-induced stomatal closure (McAinsh *et al.*, 1990; Allen *et al.*, 2000; Schroeder *et al.*, 2001).

Given that two groups of Ca^{2+}-dependent protein kinases display antagonistic effect on ABA-induced stomatal closure, these protein kinases thus need to be selectively activated at a specific time or response, so that they do not occur simultaneously. This specific activation is probably determined by the different concentrations, spatial and temporal information of Ca^{2+} signals (Dolmetsch *et al.*, 1998; Li *et al.*, 1998; Allen *et al.*, 2000; Geiger *et al.*, 2010; Scherzer *et al.*, 2012). However, the biochemical mechanism by which Ca^{2+} signals activate these protein kinases is awaiting to investigate.

Although much remains to be addressed concerning the Ca^{2+} sensitivity and activation of Ca^{2+}-dependent protein kinases, they display potential advantages in agriculture

application. Theoretically, modification of critical components of ABA signaling can dynamically improve plant drought tolerance. For example, overexpression of ABA receptor PYL5 in rice enhances drought tolerance (Kim *et al.*, 2014). However, it has a severe impact on total grain yield under paddy field conditions (Kim *et al.*, 2014), which suggests that alteration of key components of ABA signaling pose a negative impact on plant yield, despite of increase in plant drought tolerance. In contrast, Ca^{2+}-dependent protein kinases have a relatively weak role in ABA signaling. Gain or loss of these protein kinases does not affect plant growth and production, while enhance plant response to drought stress (Cheong *et al.*, 2007; Ma & Wu, 2007; Nieves-Cordones *et al.*, 2012; Sadhukhan *et al.*, 2019). Thus, Ca^{2+}-dependent protein kinases would be good candidate genes to apply in agriculture for improving crop drought tolerance. In our study, we also found that plants transformed with CIPK23 constructs did not show growth and yield difference compared to control plants, where the $CIPK23^{K60N}$ transgenic plants improved the efficiency of ABA-induced stomatal closure (**Fig. 3.11**), and enhanced inward K^+ channel activity (**Fig. 3.13**), which these results may provide useful information for breeders to modify ABA signaling in crop plants.

Overall, studies with ABA signaling will help us to understand the complex signaling network in stomatal guard cells, and put forward novel strategies to improve agricultural productivity, which will be an important means to guarantee global food security.

5. References

Acharya BR, Jeon BW, Zhang W, et al. 2013. Open Stomata 1 (OST1) is limiting in abscisic acid responses of Arabidopsis guard cells. *New Phytol.* **200**(4): 1049-1063.

Ache P, Becker D, Ivashikina N, et al. 2000. GORK, a delayed outward rectifier expressed in guard cells of Arabidopsis thaliana, is a K^+-selective, K^+-sensing ion channel. *FEBS Lett.* **486**(2): 93-98.

Akerboom J, Carreras Calderon N, Tian L, et al. 2013. Genetically encoded calcium indicators for multi-color neural activity imaging and combination with optogenetics. *Front. Mol. Neurosci.* **6**: 2.

Allen GJ, Chu SP, Harrington CL, et al. 2001. A defined range of guard cell calcium oscillation parameters encodes stomatal movements. *Nature* **411**(6841): 1053-1057.

Allen GJ, Chu SP, Schumacher K, et al. 2000. Alteration of stimulus-specific guard cell calcium oscillations and stomatal closing in Arabidopsis det3 mutant. *Science* **289**(5488): 2338-2342.

Allen GJ, Kuchitsu K, Chu SP, et al. 1999a. Arabidopsis *abi1-1* and *abi2-1* phosphatase mutations reduce abscisic acid-induced cytoplasmic calcium rises in guard cells. *Plant Cell* **11**(9): 1785-1798.

Allen GJ, Kwak JM, Chu SP, et al. 1999b. Cameleon calcium indicator reports cytoplasmic calcium dynamics in Arabidopsis guard cells. *Plant J.* **19**(6): 735-747.

Anderson JA, Huprikar SS, Kochian LV, et al. 1992. Functional expression of a probable Arabidopsis thaliana potassium channel in *Saccharomyces cerevisiae*. *Proc. Natl. Acad. Sci. U. S. A.* **89**(9): 3736-3740.

Assmann SM, Simoncini L, Schroeder J. 1985. Blue light activates electrogenic ion pumping in guard cell protoplasts of Vicia faba. *Nature* **318**(6043): 285.

Barbosa EGG, Leite JP, Marin SRR, et al. 2013. Overexpression of the ABA-dependent AREB1 transcription factor from Arabidopsis thaliana improves soybean tolerance to water deficit. *Plant Mol. Biol. Rep.* **31**(3): 719-730.

Batistic O, Sorek N, Schultke S, et al. 2008. Dual fatty acyl modification determines the localization and plasma membrane targeting of CBL/CIPK Ca^{2+} signaling complexes in Arabidopsis. *Plant Cell* **20**(5): 1346-1362.

Bauer H, Ache P, Lautner S, et al. 2013. The stomatal response to reduced relative humidity requires guard cell-autonomous ABA synthesis. *Curr. Biol.* **23**(1): 53-57.

Baunsgaard L, Venema K, Axelsen KB, et al. 1996. Modified plant plasma membrane H^+-ATPase with improved transport coupling efficiency identified by mutant selection in yeast. *Plant J.* **10**(3): 451-458.

Becker D, Hoth S, Ache P, et al. 2003. Regulation of the ABA-sensitive Arabidopsis potassium channel gene GORK in response to water stress. *FEBS Lett.* **554**(1-2): 119-126.

Ben-Ari G. 2012. The ABA signal transduction mechanism in commercial crops: learning from Arabidopsis. *Plant Cell Rep* **31**(8): 1357-1369.

Bender KW, Zielinski RE, Huber SC. 2018. Revisiting paradigms of Ca^{2+} signaling protein kinase regulation in plants. *Biochem. J.* **475**(1): 207-223.

Blatt MR. 1990. Potassium channel currents in intact stomatal guard cells: rapid enhancement by abscisic acid. *Planta* **180**(3): 445-455.

Blatt MR, Gradmann D. 1997. K^+-sensitive gating of the K^+ outward rectifier in Vicia guard cells. *J. Membr. Biol.* **158**(3): 241-256.

Bose J, Pottosin, II, Shabala SS, et al. 2011. Calcium efflux systems in stress signaling and adaptation in plants. *Front Plant Sci* **2**: 85.

Boudsocq M, Sheen J. 2013. CDPKs in immune and stress signaling. *Trends Plant Sci* **18**(1): 30-40.

Brand L, Horler M, Nuesch E, et al. 2006. A versatile and reliable two-component system for tissue-specific gene induction in Arabidopsis. *Plant Physiol.* **141**(4): 1194-1204.

Brandt B, Brodsky DE, Xue S, et al. 2012. Reconstitution of abscisic acid activation of SLAC1 anion channel by CPK6 and OST1 kinases and branched ABI1 PP2C phosphatase action. *Proc. Natl. Acad. Sci. U. S. A.* **109**(26): 10593-10598.

Brandt B, Munemasa S, Wang C, et al. 2015. Calcium specificity signaling mechanisms in abscisic acid signal transduction in Arabidopsis guard cells. *eLife* **4**, e03599.

Burnham KP, Anderson DR, Huyvaert KP. 2011. AIC model selection and multimodel inference in behavioral ecology: some background, observations, and comparisons. *Behav. Ecol. Sociobiol.* **65**(1): 23-35.

Cao M, Liu X, Zhang Y, et al. 2013. An ABA-mimicking ligand that reduces water loss and promotes drought resistance in plants. *Cell Res.* **23**(8): 1043-1054.

Cao Y, Ward JM, Kelly WB, et al. 1995. Multiple genes, tissue specificity, and expression-dependent modulationcontribute to the functional diversity of potassium channels in Arabidopsis thaliana. *Plant Physiol.* **109**(3): 1093-1106.

Castiglioni P, Warner D, Bensen RJ, et al. 2008. Bacterial RNA chaperones confer abiotic stress tolerance in plants and improved grain yield in maize under water-limited conditions. *Plant Physiol.* **147**(2): 446-455.

Chaves-Sanjuan A, Sanchez-Barrena MJ, Gonzalez-Rubio JM, et al. 2014. Structural basis of the regulatory mechanism of the plant CIPK family of protein kinases controlling ion homeostasis and abiotic stress. *Proc. Natl. Acad. Sci. U. S. A.* **111**(42): E4532-4541.

Chen DH, Liu HP, Li CL. 2019. Calcium-dependent protein kinase CPK9 negatively functions in stomatal abscisic acid signaling by regulating ion channel activity in Arabidopsis. *Plant Mol. Biol.* **99**(1-2): 113-122.

Chen YH, Hu L, Punta M, et al. 2010a. Homologue structure of the SLAC1 anion channel for closing stomata in leaves. *Nature* **467**(7319): 1074-1080.

Chen ZH, Hills A, Lim CK, et al. 2010b. Dynamic regulation of guard cell anion channels by cytosolic free Ca^{2+} concentration and protein phosphorylation. *Plant J.* **61**(5): 816-825.

Cheng S, Xian W, Fu Y, et al. 2019. Genomes of subaerial Zygnematophyceae provide insights into land plant evolution. *Cell* **179**(5): 1057-1067. e1014.

Cheong YH, Pandey GK, Grant JJ, et al. 2007. Two calcineurin B-like calcium sensors, interacting with protein kinase CIPK23, regulate leaf transpiration and root potassium uptake in Arabidopsis. *Plant J.* **52**(2): 223-239.

Clint GM, Blatt MR. 1989. Mechanisms of fusicoccin action: evidence for concerted modulations of secondary K^+ transport in a higher plant cell. *Planta* **178**(4): 495-508.

Corratge-Faillie C, Ronzier E, Sanchez F, et al. 2017. The Arabidopsis guard cell outward potassium channel GORK is regulated by CPK33. *FEBS Lett.* **591**(13): 1982-1992.

Cosgrove DJ, Hedrich R. 1991. Stretch-activated chloride, potassium, and calcium channels coexisting in plasma membranes of guard cells of *Vicia faba L*. *Planta* **186**(1): 143-153.

Cubero-Font P, Maierhofer T, Jaslan J, et al. 2016. Silent S-Type anion channel subunit SLAH1 gates SLAH3 open for chloride root-to-shoot translocation. *Curr. Biol.* **26**(16): 2213-2220.

Curran A, Chang IF, Chang CL, et al. 2011. Calcium-dependent protein kinases from Arabidopsis show substrate specificity differences in an analysis of 103 substrates. *Front Plant Sci* **2**: 36.

Cutler SR, Rodriguez PL, Finkelstein RR, et al. 2010. Abscisic Acid: emergence of a core signaling network. *Annu. Rev. Plant Biol.* **61**: 651-679.

Danquah A, de Zelicourt A, Boudsocq M, et al. 2015. Identification and characterization of an ABA-activated MAP kinase cascade in Arabidopsis thaliana. *Plant J.* **82**(2): 232-244.

Dayanandan P, Kaufman PB. 1975. Stomatal movements associated with potassium fluxes. *Am. J. Bot.* **62**(3): 221-231.

De Angeli A, Zhang J, Meyer S, et al. 2013. AtALMT9 is a malate-activated vacuolar chloride channel required for stomatal opening in Arabidopsis. *Nat Commun* **4**: 1804.

de Zelicourt A, Colcombet J, Hirt H. 2016. The role of MAPK modules and ABA during abiotic stress signaling. *Trends Plant Sci* **21**(8): 677-685.

Dempster J. 1997. A new version of the Strathclyde Electrophysiology software package running within the Microsoft Windows environment. *J. Physiol. (Lond.)* **504p**(Suppl.): P57-P57.

Diatloff E, Roberts M, Sanders D, et al. 2004. Characterization of anion channels in the plasma membrane of Arabidopsis epidermal root cells and the identification of a citrate-permeable channel induced by phosphate starvation. *Plant Physiol.* **136**(4): 4136-4149.

Dietrich P, Hedrich R. 1998. Anions permeate and gate GCAC1, a voltage-dependent guard cell anion channel. *Plant J.* **15**(4): 479-487.

Dolmetsch RE, Xu K, Lewis RS. 1998. Calcium oscillations increase the efficiency and specificity of gene expression. *Nature* **392**(6679): 933-936.

Dreyer I, Gomez-Porras JL, Riano-Pachon DM, et al. 2012. Molecular evolution of Slow and Quick Anion Channels (SLACs and QUACs/ALMTs). *Front Plant Sci* **3**: 263.

Duby G, Poreba W, Piotrowiak D, et al. 2009. Activation of plant plasma membrane H^+-ATPase by 14-3-3 proteins is negatively controlled by two phosphorylation sites within the H^+-ATPase C-terminal region. *J. Biol. Chem.* **284**(7): 4213-4221.

Edel KH, Kudla J. 2015. Increasing complexity and versatility: how the calcium signaling toolkit was shaped during plant land colonization. *Cell Calcium* **57**(3): 231-246.

Eisenach C, Baetz U, Huck NV, et al. 2017. ABA-induced stomatal closure involves ALMT4, a phosphorylation-dependent vacuolar anion channel of Arabidopsis. *Plant Cell* **29**(10): 2552-2569.

Eisenach C, Papanatsiou M, Hillert EK, et al. 2014. Clustering of the K^+ channel GORK of Arabidopsis parallels its gating by extracellular K^+. *Plant J.* **78**(2): 203-214.

Falhof J, Pedersen JT, Fuglsang AT, et al. 2016. Plasma membrane H^+-ATPase regulation in the center of plant physiology. *Mol Plant* **9**(3): 323-337.

Finkelstein R. 2013. Abscisic acid synthesis and response. *Arabidopsis Book* **11**: e0166.

Fischer RA. 1968. Stomatal opening: role of potassium uptake by guard cells. *Science* **160**(3829): 784-785.

Forster S, Schmidt LK, Kopic E, et al. 2019. Wounding-induced stomatal closure requires jasmonate-mediated activation of GORK K^+ channels by a Ca^{2+} sensor-kinase CBL1-CIPK5 complex. *Dev. Cell* **48**(1): 87-99 e86.

Frachisse JM, Thomine S, Colcombet J, et al. 1999. Sulfate is both a substrate and an activator of the voltage-dependent anion channel of Arabidopsis hypocotyl cells. *Plant Physiol.* **121**(1): 253-261.

Fuchs S, Grill E, Meskiene I, et al. 2013. Type 2C protein phosphatases in plants. *FEBS J.* **280**(2): 681-693.

Fuglsang AT, Guo Y, Cuin TA, et al. 2007. Arabidopsis protein kinase PKS5 inhibits the plasma membrane H^+-ATPase by preventing interaction with 14-3-3 protein. *Plant Cell* **19**(5): 1617-1634.

Fuglsang AT, Kristensen A, Cuin TA, et al. 2014. Receptor kinase-mediated control of primary active proton pumping at the plasma membrane. *Plant J.* **80**(6): 951-964.

Fujii H, Chinnusamy V, Rodrigues A, et al. 2009. In vitro reconstitution of an abscisic acid signalling pathway. *Nature* **462**(7273): 660-664.

Fujii H, Zhu JK. 2009. Arabidopsis mutant deficient in 3 abscisic acid-activated protein kinases reveals critical roles in growth, reproduction, and stress. *Proc. Natl. Acad. Sci. U. S. A.* **106**(20): 8380-8385.

Fujino M. 1967. Role of adenosinetriphosphate and adenosinetriphosphatase in stomatal movement. *Sci Bull Fac Educ Nagasaki Univ* **18**: 1-47.

Fujita Y, Nakashima K, Yoshida T, et al. 2009. Three SnRK2 protein kinases are the main positive regulators of abscisic acid signaling in response to water stress in Arabidopsis. *Plant Cell Physiol.* **50**(12): 2123-2132.

Gao P, Kolenovsky A, Cui Y, et al. 2012. Expression, purification and analysis of an Arabidopsis recombinant CBL-interacting protein kinase3 (CIPK3) and its constitutively active form. *Protein Expr. Purif.* **86**(1): 45-52.

Gaymard F, Pilot G, Lacombe B, et al. 1998. Identification and disruption of a plant shaker-like outward channel involved in K^+ release into the xylem sap. *Cell* **94**(5): 647-655.

Geiger D, Becker D, Vosloh D, et al. 2009a. Heteromeric AtKC1·AKT1 channels in Arabidopsis roots facilitate growth under K^+-limiting conditions. *J. Biol. Chem.* **284**(32): 21288-21295.

Geiger D, Maierhofer T, Al-Rasheid KA, et al. 2011. Stomatal closure by fast abscisic acid signaling is mediated by the guard cell anion channel SLAH3 and the receptor RCAR1. *Sci Signal* **4**(173): ra32.

Geiger D, Scherzer S, Mumm P, et al. 2010. Guard cell anion channel SLAC1 is regulated by CDPK protein kinases with distinct Ca^{2+} affinities. *Proc. Natl. Acad. Sci. U. S. A.* **107**(17): 8023-8028.

Geiger D, Scherzer S, Mumm P, et al. 2009b. Activity of guard cell anion channel SLAC1 is controlled by drought-stress signaling kinase-phosphatase pair. *Proc. Natl. Acad. Sci. U. S. A.* **106**(50): 21425-21430.

Gepstein S, Jacobs M, Taiz L. 1982. Inhibition of stomatal opening in Vicia faba epidermal tissue by vanadate and abscisic acid. *Plant Sci.* **28**(1): 63-72.

Gilroy S, Fricker MD, Read ND, et al. 1991. Role of calcium in signal transduction of *Commelina* guard cells. *Plant Cell* **3**(4): 333-344.

Gobert A, Isayenkov S, Voelker C, et al. 2007. The two-pore channel TPK1 gene encodes the vacuolar K^+ conductance and plays a role in K^+ homeostasis. *Proc. Natl. Acad. Sci. U. S. A.* **104**(25): 10726-10731.

Goh CH, Kinoshita T, Oku T, et al. 1996. Inhibition of blue light-dependent H^+ pumping by abscisic acid in Vicia guard-cell protoplasts. *Plant Physiol.* **111**(2): 433-440.

Gong D, Gong Z, Guo Y, et al. 2002a. Biochemical and functional characterization of PKS11, a novel Arabidopsis protein kinase. *J. Biol. Chem.* **277**(31): 28340-28350.

Gong D, Gong Z, Guo Y, et al. 2002b. Expression, activation, and biochemical properties of a novel Arabidopsis protein kinase. *Plant Physiol.* **129**(1): 225-234.

Gosti F, Beaudoin N, Serizet C, et al. 1999. ABI1 protein phosphatase 2C is a negative regulator of abscisic acid signaling. *Plant Cell* **11**(10): 1897-1909.

Grabov A, Blatt MR. 1998. Membrane voltage initiates Ca^{2+} waves and potentiates Ca^{2+} increases with abscisic acid in stomatal guard cells. *Proc. Natl. Acad. Sci. U. S. A.* **95**(8): 4778-4783.

Grynkiewicz G, Poenie M, Tsien RY. 1985. A new generation of Ca^{2+} indicators with greatly improved fluorescence properties. *J. Biol. Chem.* **260**(6): 3440-3450.

Guo Y, Xiong L, Song CP, et al. 2002. A calcium sensor and its interacting protein kinase are global regulators of abscisic acid signaling in Arabidopsis. *Dev. Cell* **3**(2): 233-244.

Guzel Deger A, Scherzer S, Nuhkat M, et al. 2015. Guard cell SLAC1-type anion channels mediate flagellin-induced stomatal closure. *New Phytol* **208**(1): 162-173.

Hamilton DW, Hills A, Kohler B, et al. 2000. Ca^{2+} channels at the plasma membrane of stomatal guard cells are activated by hyperpolarization and abscisic acid. *Proc. Natl. Acad. Sci. U. S. A.* **97**(9): 4967-4972.

Hanstein SM, Felle HH. 2004. Nanoinfusion: an integrating tool to study elicitor perception and signal transduction in intact leaves. *New Phytol* **161**(2): 595-606.

Harper JF, Breton G, Harmon A. 2004. Decoding Ca^{2+} signals through plant protein kinases. *Annu. Rev. Plant Biol.* **55**: 263-288.

Hashimoto K, Eckert C, Anschutz U, et al. 2012. Phosphorylation of calcineurin B-like (CBL) calcium sensor proteins by their CBL-interacting protein kinases (CIPKs) is required for full

activity of CBL-CIPK complexes toward their target proteins. *J. Biol. Chem.* **287**(11): 7956-7968.

Hayashi M, Inoue S, Takahashi K, et al. 2011. Immunohistochemical detection of blue light-induced phosphorylation of the plasma membrane H^+-ATPase in stomatal guard cells. *Plant Cell Physiol.* **52**(7): 1238-1248.

He ZH, Zhong JW, Sun XP, et al. 2018. The maize ABA receptors ZmPYL8, 9, and 12 facilitate plant drought resistance. *Front. Plant Sci.* **9**.

Hedrich R. 2012. Ion channels in plants. *Physiol. Rev.* **92**(4): 1777-1811.

Hedrich R, Busch H, Raschke K. 1990. Ca^{2+} and nucleotide dependent regulation of voltage dependent anion channels in the plasma-membrane of guard-cells. *EMBO J.* **9**(12): 3889-3892.

Hedrich R, Geiger D. 2017. Biology of SLAC1-type anion channels - from nutrient uptake to stomatal closure. *New Phytol* **216**(1): 46-61.

Hedrich R, Marten I. 1993. Malate-induced feedback regulation of plasma membrane anion channels could provide a CO_2 sensor to guard cells. *EMBO J.* **12**(3): 897-901.

Hedrich R, Marten I, Lohse G, et al. 1994. Malate-sensitive anion channels enable guard-cells to sense changes in the ambient CO_2 concentration. *Plant J.* **6**(5): 741-748.

Hedrich R, Moran O, Conti F, et al. 1995. Inward rectifier potassium channels in plants differ from their animal counterparts in response to voltage and channel modulators. *Eur. Biophys. J.* **24**(2): 107-115.

Held K, Pascaud F, Eckert C, et al. 2011. Calcium-dependent modulation and plasma membrane targeting of the AKT2 potassium channel by the CBL4/CIPK6 calcium sensor/protein kinase complex. *Cell Res.* **21**(7): 1116-1130.

Hetherington AM, Brownlee C. 2004. The generation of Ca^{2+} signals in plants. *Annu. Rev. Plant Biol.* **55**: 401-427.

Horak H, Sierla M, Toldsepp K, et al. 2016. A dominant mutation in the HT1 kinase uncovers roles of MAP kinases and GHR1 in CO_2-induced stomatal closure. *Plant Cell* **28**(10): 2493-2509.

Hosy E, Vavasseur A, Mouline K, et al. 2003. The Arabidopsis outward K^+ channel GORK is involved in regulation of stomatal movements and plant transpiration. *Proc. Natl. Acad. Sci. U. S. A.* **100**(9): 5549-5554.

Hou C, Tian W, Kleist T, et al. 2014. DUF221 proteins are a family of osmosensitive calcium-permeable cation channels conserved across eukaryotes. *Cell Res.* **24**(5): 632-635.

Hsu PK, Takahashi Y, Munemasa S, et al. 2018. Abscisic acid-independent stomatal CO_2 signal transduction pathway and convergence of CO_2 and ABA signaling downstream of OST1 kinase. *Proc. Natl. Acad. Sci. U. S. A.* ***115****(42), E9971-E9980.*

Hu HH, Boisson-Dernier A, Israelsson-Nordstrom M, et al. 2010. Carbonic anhydrases are upstream regulators of CO_2-controlled stomatal movements in guard cells. *Nat. Cell Biol.* **12**(1): 87-U234.

Hua D, Wang C, He J, et al. 2012. A plasma membrane receptor kinase, GHR1, mediates abscisic acid- and hydrogen peroxide-regulated stomatal movement in Arabidopsis. *Plant Cell* **24**(6): 2546-2561.

Imes D, Mumm P, Bohm J, et al. 2013. Open stomata 1 (OST1) kinase controls R-type anion channel QUAC1 in Arabidopsis guard cells. *Plant J.* **74**(3): 372-382.

Islam MM, Hossain MA, Jannat R, et al. 2010a. Cytosolic alkalization and cytosolic calcium oscillation in Arabidopsis guard cells response to ABA and MeJA. *Plant Cell Physiol.* **51**(10): 1721-1730.

Islam MM, Munemasa S, Hossain MA, et al. 2010b. Roles of *At*TPC1, vacuolar Two Pore Channel 1, in *Arabidopsis* stomatal closure. *Plant Cell Physiol.* **51**(2): 302-311.

Ivashikina N, Deeken R, Fischer S, et al. 2005. AKT2/3 subunits render guard cell K^+ channels Ca^{2+} sensitive. *J. Gen. Physiol.* **125**(5): 483-492.

Jammes F, Song C, Shin D, et al. 2009. MAP kinases MPK9 and MPK12 are preferentially expressed in guard cells and positively regulate ROS-mediated ABA signaling. *Proc. Natl. Acad. Sci. U. S. A.* **106**(48): 20520-20525.

Jezek M, Blatt MR. 2017. The membrane transport system of the guard cell and its integration for stomatal dynamics. *Plant Physiol.* **174**(2): 487-519.

Jojoa-Cruz S, Saotome K, Murthy SE, et al. 2018. Cryo-EM structure of the mechanically activated ion channel OSCA1.2. *eLife* **7**.

Joshi-Saha A, Valon C, Leung J. 2011. A brand new START: abscisic acid perception and transduction in the guard cell. *Sci Signal* **4**(201): re4.

Keinath NF, Waadt R, Brugman R, et al. 2015. Live cell imaging with R-GECO1 sheds light on flg22- and chitin-induced transient $[Ca^{2+}]_{cyt}$ patterns in Arabidopsis. *Mol Plant* **8**(8): 1188-1200.

Keller BU, Hedrich R, Raschke K. 1989. Voltage-dependent anion channels in the plasma-membrane of guard-cells. *Nature* **341**(6241): 450-453.

Kim H, Lee K, Hwang H, et al. 2014. Overexpression of PYL5 in rice enhances drought tolerance, inhibits growth, and modulates gene expression. *J Exp Bot* **65**(2): 453-464.

Kim TH, Bohmer M, Hu HH, et al. 2010. Guard cell signal transduction network: advances in understanding abscisic acid CO_2, and Ca^{2+} signaling. *Annu. Rev. Plant Biol.* **61**: 561-591.

Kim TH, Hauser F, Ha T, et al. 2011. Chemical genetics reveals negative regulation of abscisic acid signaling by a plant immune response pathway. *Curr. Biol.* **21**(11): 990-997.

Kinoshita T, Doi M, Suetsugu N, et al. 2001. Phot1 and phot2 mediate blue light regulation of stomatal opening. *Nature* **414**(6864): 656-660.

Kinoshita T, Shimazaki K. 1999. Blue light activates the plasma membrane H^+-ATPase by phosphorylation of the C-terminus in stomatal guard cells. *EMBO J.* **18**(20): 5548-5558.

Klusener B, Young JJ, Murata Y, et al. 2002. Convergence of calcium signaling pathways of pathogenic elicitors and abscisic acid in *Arabidopsis* guard cells. *Plant Physiol.* **130**(4): 2152-2163.

Koers S, Guzel-Deger A, Marten I, et al. 2011. Barley mildew and its elicitor chitosan promote closed stomata by stimulating guard-cell S-type anion channels. *Plant J.* **68**(4): 670-680.

Kollist H, Nuhkat M, Roelfsema MR. 2014. Closing gaps: linking elements that control stomatal movement. *New Phytol* **203**(1): 44-62.

Kong D, Hu HC, Okuma E, et al. 2016. L-Met activates Arabidopsis GLR Ca^{2+} channels upstream of ROS production and regulates stomatal movement. *Cell Rep.* **17**(10): 2553-2561.

Koornneef M, Reuling G, Karssen CM. 1984. The isolation and characterization of abscisic-acid insensitive mutants of Arabidopsis thaliana. *Physiol. Plant.* **61**(3): 377-383.

Kudla J, Becker D, Grill E, et al. 2018. Advances and current challenges in calcium signaling. *New Phytol* **218**(2): 414-431.

Kuhn JM, Boisson-Dernier A, Dizon MB, et al. 2006. The protein phosphatase *AtPP2CA* negatively regulates abscisic acid signal transduction in Arabidopsis, and effects of *abh1* on *AtPP2CA* mRNA. *Plant Physiol.* **140**(1): 127-139.

Laanemets K, Wang YF, Lindgren O, et al. 2013. Mutations in the SLAC1 anion channel slow stomatal opening and severely reduce K^+ uptake channel activity via enhanced cytosolic $[Ca^{2+}]$ and increased Ca^{2+} sensitivity of K^+ uptake channels. *New Phytol* **197**(1): 88-98.

Latz A, Mehlmer N, Zapf S, et al. 2013. Salt stress triggers phosphorylation of the Arabidopsis vacuolar K^+ channel TPK1 by calcium-dependent protein kinases (CDPKs). *Mol Plant* **6**(4): 1274-1289.

Lawson T. 2009. Guard cell photosynthesis and stomatal function. *New Phytol.* **181**(1): 13-34.

Lebaudy A, Vavasseur A, Hosy E, et al. 2008. Plant adaptation to fluctuating environment and biomass production are strongly dependent on guard cell potassium channels. *Proc. Natl. Acad. Sci. U. S. A.* **105**(13): 5271-5276.

Lefoulon C, Boeglin M, Moreau B, et al. 2016. The Arabidopsis AtPP2CA protein phosphatase inhibits the GORK K^+ efflux channel and exerts a dominant suppressive effect on phosphomimetic-activating mutations. *J. Biol. Chem.* **291**(12): 6521-6533.

Lesk C, Rowhani P, Ramankutty N. 2016. Influence of extreme weather disasters on global crop production. *Nature* **529**(7584): 84-87.

Levchenko V, Guinot DR, Klein M, et al. 2008. Stringent control of cytoplasmic Ca^{2+} in guard cells of intact plants compared to their counterparts in epidermal strips or guard cell protoplasts. *Protoplasma* **233**(1-2): 61-72.

Levchenko V, Konrad KR, Dietrich P, et al. 2005. Cytosolic abscisic acid activates guard cell anion channels without preceding Ca^{2+} signals. *Proc. Natl. Acad. Sci. U. S. A.* **102**(11): 4203-4208.

Li CL, Wang M, Wu XM, et al. 2016. THI1, a thiamine thiazole synthase, interacts with Ca^{2+}-dependent protein kinase CPK33 and modulates the S-type anion channels and stomatal closure in Arabidopsis. *Plant Physiol.* **170**(2): 1090-1104.

Li J, Assmann SM. 1996. An abscisic acid-activated and calcium-independent protein kinase from guard cells of fava bean. *Plant Cell* **8**(12): 2359-2368.

Li J, Wang XQ, Watson MB, et al. 2000. Regulation of abscisic acid-induced stomatal closure and anion channels by guard cell AAPK kinase. *Science* **287**(5451): 300-303.

Li L, Kim BG, Cheong YH, et al. 2006. A Ca^{2+} signaling pathway regulates a K^+ channel for low-K response in Arabidopsis. *Proc. Natl. Acad. Sci. U. S. A.* **103**(33): 12625-12630.

Li WH, Llopis J, Whitney M, et al. 1998. Cell-permeant caged $InsP_3$ ester shows that Ca^{2+} spike frequency can optimize gene expression. *Nature* **392**(6679): 936-941.

Liang S, Lu K, Wu Z, et al. 2015. A link between magnesium-chelatase H subunit and sucrose nonfermenting 1 (SNF1)-related protein kinase SnRK2.6/OST1 in Arabidopsis guard cell signalling in response to abscisic acid. *J Exp Bot* **66**(20): 6355-6369.

Liese A, Romeis T. 2013. Biochemical regulation of in vivo function of plant calcium-dependent protein kinases (CDPK). *BBA-Mol. Cell Res.* **1833**(7): 1582-1589.

Linder B, Raschke K. 1992. A slow anion channel in guard-cells, activating at large hyperpolarization, may be principal for stomatal closing. *FEBS Lett.* **313**(1): 27-30.

Lloyd FE. 1908. *The physiology of stomata*: Carnegie Institution of Washington.

Loftfield J. 1921. The behaviour of stomata. *Publ. Carnegie Inst.* **314**: 1-104.

Long SB, Campbell EB, Mackinnon R. 2005. Crystal structure of a mammalian voltage-dependent Shaker family K^+ channel. *Science* **309**(5736): 897-903.

Lyzenga WJ, Liu H, Schofield A, et al. 2013. Arabidopsis CIPK26 interacts with KEG, components of the ABA signalling network and is degraded by the ubiquitin-proteasome system. *J Exp Bot* **64**(10): 2779-2791.

Ma SY, Wu WH. 2007. AtCPK23 functions in Arabidopsis responses to drought and salt stresses. *Plant Mol. Biol.* **65**(4): 511-518.

Ma Y, Szostkiewicz I, Korte A, et al. 2009. Regulators of PP2C phosphatase activity function as abscisic acid sensors. *Science* **324**(5930): 1064-1068.

MacRobbie E, Lettau J. 1980. Ion content and aperture in “isolated” guard cells of Commelina communis L. *J. Membr. Biol.* **53**(3): 199-205.

Macrobbie EAC. 1992. Calcium and ABA-induced stomatal closure. *Philos. Trans. R. Soc. Lond., B, Biol. Sci.* **338**(1283): 5-18.

Maierhofer T, Diekmann M, Offenborn JN, et al. 2014a. Site- and kinase-specific phosphorylation-mediated activation of SLAC1, a guard cell anion channel stimulated by abscisic acid. *Sci Signal* **7**(342): ra86.

Maierhofer T, Lind C, Huttl S, et al. 2014b. A single-pore residue renders the Arabidopsis root anion channel SLAH2 highly nitrate selective. *Plant Cell* **26**(6): 2554-2567.

Malcheska F, Ahmad A, Batool S, et al. 2017. Drought-enhanced xylem sap sulfate closes stomata by affecting ALMT12 and guard cell ABA synthesis. *Plant Physiol.* **174**(2): 798-814.

Manohar M, Shigaki T, Hirschi KD. 2011. Plant cation/H^+ exchangers (CAXs): biological functions and genetic manipulations. *Plant Biol.* **13**(4): 561-569.

Mao J, Manik SM, Shi S, et al. 2016. Mechanisms and physiological roles of the CBL-CIPK networking system in Arabidopsis thaliana. *Genes* **7**(9).

Marten H, Hedrich R, Roelfsema MR. 2007a. Blue light inhibits guard cell plasma membrane anion channels in a phototropin-dependent manner. *Plant J.* **50**(1): 29-39.

Marten H, Konrad KR, Dietrich P, et al. 2007b. Ca^{2+}-dependent and -independent abscisic acid activation of plasma membrane anion channels in guard cells of *Nicotiana tabacum*. *Plant Physiol.* **143**(1): 28-37.

Marten I, Hoth S, Deeken R, et al. 1999. AKT3, a phloem-localized K^+ channel, is blocked by protons. *Proc. Natl. Acad. Sci. U. S. A.* **96**(13): 7581-7586.

Matsuoka D, Yasufuku T, Furuya T, et al. 2015. An abscisic acid inducible Arabidopsis MAPKKK, MAPKKK18 regulates leaf senescence via its kinase activity. *Plant Mol. Biol.* **87**(6): 565-575.

McAinsh MR, Brownlee C, Hetherington AM. 1990. Abscisic acid-induced elevation of guard cell cytosolic Ca^{2+} precedes stomatal closure. *Nature* **343**(6254): 186.

Melcher K, Ng LM, Zhou XE, et al. 2009. A gate-latch-lock mechanism for hormone signalling by abscisic acid receptors. *Nature* **462**(7273): 602-608.

Melotto M, Underwood W, Koczan J, et al. 2006. Plant stomata function in innate immunity against bacterial invasion. *Cell* **126**(5): 969-980.

Merilo E, Laanemets K, Hu H, et al. 2013. PYR/RCAR receptors contribute to ozone-, reduced air humidity-, darkness-, and CO_2-induced stomatal regulation. *Plant Physiol.* **162**(3): 1652-1668.

Merlot S, Leonhardt N, Fenzi F, et al. 2007. Constitutive activation of a plasma membrane H^+-ATPase prevents abscisic acid-mediated stomatal closure. *EMBO J.* **26**(13): 3216-3226.

Merlot S, Mustilli AC, Genty B, et al. 2002. Use of infrared thermal imaging to isolate Arabidopsis mutants defective in stomatal regulation. *Plant J.* **30**(5): 601-609.

Meyer S, Mumm P, Imes D, et al. 2010. AtALMT12 represents an R-type anion channel required for stomatal movement in Arabidopsis guard cells. *Plant J.* **63**(6): 1054-1062.

Miao C, Xiao L, Hua K, et al. 2018. Mutations in a subfamily of abscisic acid receptor genes promote rice growth and productivity. *Proc. Natl. Acad. Sci. U. S. A.* **115**(23): 6058-6063.

Michard E, Dreyer I, Lacombe B, et al. 2005. Inward rectification of the AKT2 channel abolished by voltage-dependent phosphorylation. *Plant J.* **44**(5): 783-797.

Milborrow BV. 2001. The pathway of biosynthesis of abscisic acid in vascular plants: a review of the present state of knowledge of ABA biosynthesis. *J Exp Bot* **52**(359): 1145-1164.

Mitula F, Tajdel M, Cieśla A, et al. 2015. Arabidopsis ABA-activated kinase MAPKKK18 is regulated by protein phosphatase 2C ABI1 and the ubiquitin–proteasome pathway. *Plant Cell Physiol.* **56**(12): 2351-2367.

Miyazono K, Miyakawa T, Sawano Y, et al. 2009. Structural basis of abscisic acid signalling. *Nature* **462**(7273): 609-614.

Mori IC, Murata Y, Yang Y, et al. 2006. CDPKs CPK6 and CPK3 function in ABA regulation of guard cell S-type anion- and Ca^{2+}-permeable channels and stomatal closure. *PLoS Biol.* **4**(10): e327.

Morison TLaJIL. 2010. Guard cell photosynthesis. *Plant Physiology and Development, Sixth Edition*.

Motoda H, Sasaki T, Kano Y, et al. 2007. The membrane topology of ALMT1, an aluminum-activated malate transport protein in wheat (*Triticum aestivum*). *Plant Signal Behav* **2**(6): 467-472.

Mouline K, Very AA, Gaymard F, et al. 2002. Pollen tube development and competitive ability are impaired by disruption of a Shaker K^+ channel in Arabidopsis. *Genes Dev.* **16**(3): 339-350.

Muller HM, Schafer N, Bauer H, et al. 2017. The desert plant Phoenix dactylifera closes stomata via nitrate-regulated SLAC1 anion channel. *New Phytol* **216**(1): 150-162.

Mumm P, Imes D, Martinoia E, et al. 2013. C-terminus-mediated voltage gating of Arabidopsis guard cell anion channel QUAC1. *Mol Plant* **6**(5): 1550-1563.

Munemasa S, Hauser F, Park J, et al. 2015. Mechanisms of abscisic acid-mediated control of stomata! aperture. *Curr. Opin. Plant Biol.* **28**: 154-162.

Mustilli AC, Merlot S, Vavasseur A, et al. 2002. Arabidopsis OST1 protein kinase mediates the regulation of stomatal aperture by abscisic acid and acts upstream of reactive oxygen species production. *Plant Cell* **14**(12): 3089-3099.

Negi J, Matsuda O, Nagasawa T, et al. 2008. CO_2 regulator SLAC1 and its homologues are essential for anion homeostasis in plant cells. *Nature* **452**(7186): 483-486.

Ng LM, Soon FF, Zhou XE, et al. 2011. Structural basis for basal activity and autoactivation of abscisic acid (ABA) signaling SnRK2 kinases. *Proc. Natl. Acad. Sci. U. S. A.* **108**(52): 21259-21264.

Nieves-Cordones M, Caballero F, Martinez V, et al. 2012. Disruption of the Arabidopsis thaliana inward-rectifier K^+ channel AKT1 improves plant responses to water stress. *Plant Cell Physiol.* **53**(2): 423-432.

Niittyla T, Fuglsang AT, Palmgren MG, et al. 2007. Temporal analysis of sucrose-induced phosphorylation changes in plasma membrane proteins of Arabidopsis. *Mol. Cell. Proteomics* **6**(10): 1711-1726.

Nishimura N, Hitomi K, Arvai AS, et al. 2009. Structural mechanism of abscisic acid binding and signaling by dimeric PYR1. *Science* **326**(5958): 1373-1379.

Nishimura N, Sarkeshik A, Nito K, et al. 2010. PYR/PYL/RCAR family members are major in-vivo ABI1 protein phosphatase 2C-interacting proteins in Arabidopsis. *Plant J.* **61**(2): 290-299.

Nour-Eldin HH, Hansen BG, Norholm MH, et al. 2006. Advancing uracil-excision based cloning towards an ideal technique for cloning PCR fragments. *Nucleic Acids Res.* **34**(18): e122.

Ohta M, Guo Y, Halfter U, et al. 2003. A novel domain in the protein kinase SOS2 mediates interaction with the protein phosphatase 2C ABI2. *Proc. Natl. Acad. Sci. U. S. A.* **100**(20): 11771-11776.

Okamoto M, Peterson FC, Defries A, et al. 2013. Activation of dimeric ABA receptors elicits guard cell closure, ABA-regulated gene expression, and drought tolerance. *Proc. Natl. Acad. Sci. U. S. A.* **110**(29): 12132-12137.

Palmgren MG, Sommarin M, Serrano R, et al. 1991. Identification of an autoinhibitory domain in the C-terminal region of the plant plasma membrane H^+-ATPase. *J. Biol. Chem.* **266**(30): 20470-20475.

Pandey GK, Grant JJ, Cheong YH, et al. 2008. Calcineurin-B-like protein CBL9 interacts with target kinase CIPK3 in the regulation of ABA response in seed germination. *Mol Plant* **1**(2): 238-248.

Park SY, Fung P, Nishimura N, et al. 2009. Abscisic acid inhibits type 2C protein phosphatases via the PYR/PYL family of START proteins. *Science* **324**(5930): 1068-1071.

Park SY, Peterson FC, Mosquna A, et al. 2015. Agrochemical control of plant water use using engineered abscisic acid receptors. *Nature* **520**(7548): 545-548.

Pei ZM, Kuchitsu K, Ward JM, et al. 1997. Differential abscisic acid regulation of guard cell slow anion channels in Arabidopsis wild-type and *abi1* and *abi2* mutants. *Plant Cell* **9**(3): 409-423.

Pei ZM, Murata Y, Benning G, et al. 2000. Calcium channels activated by hydrogen peroxide mediate abscisic acid signalling in guard cells. *Nature* **406**(6797): 731-734.

Pilot G, Lacombe B, Gaymard F, et al. 2001. Guard cell inward K^+ channel activity in Arabidopsis involves expression of the twin channel subunits KAT1 and KAT2. *J. Biol. Chem.* **276**(5): 3215-3221.

Qi G-N, Yao F-Y, Ren H-M, et al. 2018. Constitutive activation of calcium-dependent protein kinase 3 confers a drought tolerance by inhibiting inward K^+ channel KAT1 and stomatal opening in Arabidopsis. *Sci. Bull.* **63**(16): 1037-1039.

Raschke K, Humble G. 1973. No uptake of anions required by opening stomata of Vicia faba: guard cells release hydrogen ions. *Planta* **115**(1): 47-57.

Raschke K, Schnabl H. 1978. Availability of chloride affects the balance between potassium chloride and potassium malate in guard cells of *Vicia faba L*. *Plant Physiol.* **62**(1): 84-87.

Reintanz B, Szyroki A, Ivashikina N, et al. 2002. AtKC1, a silent Arabidopsis potassium channel alpha -subunit modulates root hair K^+ influx. *Proc. Natl. Acad. Sci. U. S. A.* **99**(6): 4079-4084.

Rodriguez PL. 1998. Protein phosphatase 2C (PP2C) function in higher plants. *Plant Mol. Biol.* **38**(6): 919-927.

Roelfsema MR, Hanstein S, Felle HH, et al. 2002. CO_2 provides an intermediate link in the red light response of guard cells. *Plant J.* **32**(1): 65-75.

Roelfsema MR, Hedrich R. 2005. In the light of stomatal opening: new insights into 'the Watergate'. *New Phytol* **167**(3): 665-691.

Roelfsema MR, Hedrich R, Geiger D. 2012. Anion channels: master switches of stress responses. *Trends Plant Sci* **17**(4): 221-229.

Roelfsema MR, Prins HB. 1997. Ion channels in guard cells of *Arabidopsis thaliana (L.)* Heynh. *Planta* **202**(1): 18-27.

Roelfsema MR, Steinmeyer R, Staal M, et al. 2001. Single guard cell recordings in intact plants: light-induced hyperpolarization of the plasma membrane. *Plant J.* **26**(1): 1-13.

Roelfsema MRG, Kollist H. 2013. Tiny pores with a global impact. *New Phytol*. 197(1): 11-15.

Roelfsema MRG, Levchenko V, Hedrich R. 2004. ABA depolarizes guard cells in intact plants, through a transient activation of R- and S-type anion channels. *Plant J.* **37**(4): 578-588.

Roelfsema MRG, Prins HBA. 1995. Effect of abscisic acid on stomatal opening in isolated epidermal strips of abi mutants of Arabidopsis thaliana. *Physiol. Plant.* **95**(3): 373-378.

Roelfsema MRG, Staal M, Prins HBA. 1998. Blue light-induced apoplastic acidification of Arabidopsis thaliana guard cells: Inhibition by ABA is mediated through protein phosphatases. *Physiol. Plant.* **103**(4): 466-474.

Ronzier E, Corratge-Faillie C, Sanchez F, et al. 2014. CPK13, a noncanonical Ca^{2+}-dependent protein kinase, specifically inhibits KAT2 and KAT1 shaker K^+ channels and reduces stomatal opening. *Plant Physiol.* **166**(1): 314-326.

Rubio S, Rodrigues A, Saez A, et al. 2009. Triple loss of function of protein phosphatases type 2C leads to partial constitutive response to endogenous abscisic acid. *Plant Physiol.* **150**(3): 1345-1355.

Ruschhaupt M, Mergner J, Mucha S, et al. 2019. Rebuilding core abscisic acid signaling pathways of Arabidopsis in yeast. *EMBO J.*: e101859.

Sadhukhan A, Enomoto T, Kobayashi Y, et al. 2019. Sensitive to proton rhizotoxicity1 regulates salt and drought tolerance of Arabidopsis thaliana through transcriptional regulation of CIPK23. *Plant Cell Physiol.* **60**(9): 2113-2126.

Saez A, Apostolova N, Gonzalez-Guzman M, et al. 2004. Gain-of-function and loss-of-function phenotypes of the protein phosphatase 2C HAB1 reveal its role as a negative regulator of abscisic acid signalling. *Plant J.* **37**(3): 354-369.

Saito S, Hamamoto S, Moriya K, et al. 2018. N-myristoylation and S-acylation are common modifications of Ca^{2+}-regulated Arabidopsis kinases and are required for activation of the SLAC1 anion channel. *New Phytol* **218**(4): 1504-1521.

Saito S, Uozumi N. 2019. Guard cell membrane anion transport systems and their regulatory components: an elaborate mechanism controlling stress-induced stomatal closure. *Plants* **8**(1).

Sanders D, Pelloux J, Brownlee C, et al. 2002. Calcium at the crossroads of signaling. *Plant Cell* **14**(suppl 1): S401-417.

Sasaki T, Mori IC, Furuichi T, et al. 2010. Closing plant stomata requires a homolog of an aluminum-activated malate transporter. *Plant Cell Physiol.* **51**(3): 354-365.

Sato A, Sato Y, Fukao Y, et al. 2009. Threonine at position 306 of the KAT1 potassium channel is essential for channel activity and is a target site for ABA-activated SnRK2/OST1/SnRK2.6 protein kinase. *Biochem. J.* **424**(3): 439-448.

Schafer N, Maierhofer T, Herrmann J, et al. 2018. A tandem amino acid residue motif in guard cell SLAC1 anion channel of grasses allows for the control of stomatal aperture by nitrate. *Curr. Biol.* **28**(9): 1370-1379 e1375.

Scherzer S, Maierhofer T, Al-Rasheid KA, et al. 2012. Multiple calcium-dependent kinases modulate ABA-activated guard cell anion channels. *Mol Plant* **5**(6): 1409-1412.

Schindelin J, Arganda-Carreras I, Frise E, et al. 2012. Fiji: an open-source platform for biological-image analysis. *Nat Methods* **9**(7): 676-682.

Schmidt C, Schelle I, Liao YJ, et al. 1995. Strong regulation of slow anion channels and abscisic acid signaling in guard cells by phosphorylation and dephosphorylation events. *Proc. Natl. Acad. Sci. U. S. A.* **92**(21): 9535-9539.

Schroeder JI, Allen GJ, Hugouvieux V, et al. 2001. Guard cell signal transduction. *Annu. Rev. Plant Physiol. Plant Mol. Biol.* **52**: 627-658.

Schroeder JI, Hagiwara S. 1989. Cytosolic calcium regulates ion channels in the plasma membrane of *Vicia faba* guard cells. *Nature* **338**(6214): 427-430.

Schroeder JI, Hedrich R, Fernandez JM. 1984. Potassium-selective single channels in guard cell protoplasts of *Vicia faba*. *Nature* **312**(5992): 361-362.

Schroeder JI, Keller BU. 1992. Two types of anion channel currents in guard cells with distinct voltage regulation. *Proc. Natl. Acad. Sci. U. S. A.* **89**(11): 5025-5029.

Schwartz A, Wu WH, Tucker EB, et al. 1994. Inhibition of inward K^+ channels and stomatal response by abscisic acid: an intracellular locus of phytohormone action. *Proc. Natl. Acad. Sci. U. S. A.* **91**(9): 4019-4023.

Sentenac H, Bonneaud N, Minet M, et al. 1992. Cloning and expression in yeast of a plant potassium ion transport system. *Science* **256**(5057): 663-665.

Sharkey TD, Raschke K. 1981. Separation and measurement of direct and indirect effects of light on stomata. *Plant Physiol.* **68**(1): 33-40.

Shimazaki K, Iino M, Zeiger E. 1986. Blue light-dependent proton extrusion by guard-cell protoplasts of Vicia faba. *Nature* **319**(6051): 324-326.

Siegel RS, Xue SW, Murata Y, et al. 2009. Calcium elevation-dependent and attenuated resting calcium-dependent abscisic acid induction of stomatal closure and abscisic acid-induced enhancement of calcium sensitivities of S-type anion and inward-rectifying K^+ channels in Arabidopsis guard cells. *Plant J.* **59**(2): 207-220.

Sierla M, Horak H, Overmyer K, et al. 2018. The receptor-like pseudokinase GHR1 is required for stomatal closure. *Plant Cell* **30**(11): 2813-2837.

Song SJ, Feng QN, Li CL, et al. 2018. A tonoplast-associated calcium-signaling module dampens ABA signaling during stomatal movement. *Plant Physiol.* **177**(4): 1666-1678.

Spalding EP, Harper JF. 2011. The ins and outs of cellular Ca^{2+} transport. *Curr. Opin. Plant Biol.* **14**(6): 715-720.

Stadler R, Buttner M, Ache P, et al. 2003. Diurnal and light-regulated expression of AtSTP1 in guard cells of Arabidopsis. *Plant Physiol.* **133**(2): 528-537.

Stange A, Hedrich R, Roelfsema MRG. 2010. Ca^{2+}-dependent activation of guard cell anion channels, triggered by hyperpolarization, is promoted by prolonged depolarization. *Plant J.* **62**(2): 265-276.

Staxen I, Pical C, Montgomery LT, et al. 1999. Abscisic acid induces oscillations in guard-cell cytosolic free calcium that involve phosphoinositide-specific phospholipase C. *Proc. Natl. Acad. Sci. U. S. A.* **96**(4): 1779-1784.

Steward FC. 1967. Plants at work. a summary of plant physiology.

Stewart WW. 1978. Functional connections between cells as revealed by dye-coupling with a highly fluorescent naphthalimide tracer. *Cell* **14**(3): 741-759.

Sun Y, Harpazi B, Wijerathna-Yapa A, et al. 2019. A ligand-independent origin of abscisic acid perception. *Proc. Natl. Acad. Sci. U. S. A.* **116**(49), 24892-24899.

Svennelid F, Olsson A, Piotrowski M, et al. 1999. Phosphorylation of Thr-948 at the C terminus of the plasma membrane H^+-ATPase creates a binding site for the regulatory 14-3-3 protein. *The Plant Cell* **11**(12): 2379-2391.

Szyroki A, Ivashikina N, Dietrich P, et al. 2001. KAT1 is not essential for stomatal opening. *Proc. Natl. Acad. Sci. U. S. A.* **98**(5): 2917-2921.

Takemiya A, Sugiyama N, Fujimoto H, et al. 2013. Phosphorylation of BLUS1 kinase by phototropins is a primary step in stomatal opening. *Nat. Commun.* **4**.

Takeuchi J, Okamoto M, Akiyama T, et al. 2014. Designed abscisic acid analogs as antagonists of PYL-PP2C receptor interactions. *Nat. Chem. Biol.* **10**(6): 477-482.

Thor K, Peiter E. 2014. Cytosolic calcium signals elicited by the pathogen-associated molecular pattern flg22 in stomatal guard cells are of an oscillatory nature. *New Phytol* **204**(4): 873-881.

Tian W, Hou C, Ren Z, et al. 2015a. A molecular pathway for CO_2 response in Arabidopsis guard cells. *Nat Commun* **6**: 6057.

Tian W, Hou C, Ren Z, et al. 2019. A calmodulin-gated calcium channel links pathogen patterns to plant immunity. *Nature* **572**(7767): 131-135.

Tian X, Wang Z, Li X, et al. 2015b. Characterization and functional analysis of pyrabactin resistance-like abscisic acid receptor family in Rice. *Rice* **8**(1): 28.

Tong S-M, Xi H-X, Ai K-J, et al. 2017. Overexpression of wheat TaNCED gene in Arabidopsis enhances tolerance to drought stress and delays seed germination. *Biol. Plant.* **61**(1): 64-72.

Ueno K, Kinoshita T, Inoue S, et al. 2005. Biochemical characterization of plasma membrane H^+-ATPase activation in guard cell protoplasts of Arabidopsis thaliana in response to blue light. *Plant Cell Physiol.* **46**(6): 955-963.

Umezawa T, Sugiyama N, Mizoguchi M, et al. 2009. Type 2C protein phosphatases directly regulate abscisic acid-activated protein kinases in Arabidopsis. *Proc. Natl. Acad. Sci. U. S. A.* **106**(41): 17588-17593.

Umezawa T, Yoshida R, Maruyama K, et al. 2004. SRK2C, a SNF1-related protein kinase 2, improves drought tolerance by controlling stress-responsive gene expression in Arabidopsis thaliana. *Proc. Natl. Acad. Sci. U. S. A.* **101**(49): 17306-17311.

Vahisalu T, Kollist H, Wang YF, et al. 2008. SLAC1 is required for plant guard cell S-type anion channel function in stomatal signalling. *Nature* **452**(7186): 487-491.

Vahisalu T, Puzorjova I, Brosche M, et al. 2010. Ozone-triggered rapid stomatal response involves the production of reactive oxygen species, and is controlled by SLAC1 and OST1. *Plant J.* **62**(3): 442-453.

van Kleeff PJM, Gao J, Mol S, et al. 2018. The Arabidopsis GORK K^+-channel is phosphorylated by calcium-dependent protein kinase 21 (CPK21), which in turn is activated by 14-3-3 proteins. *Plant Physiol. Biochem.* **125**: 219-231.

Venema K, Palmgren MG. 1995. Metabolic modulation of transport coupling ratio in yeast plasma membrane H^+-ATPase. *J. Biol. Chem.* **270**(33): 19659-19667.

Verma RK, Santosh Kumar V, Yadav SK, et al. 2019. Overexpression of ABA receptor PYL10 gene confers drought and cold tolerance to indica rice. *Front. Plant Sci.* **10**: 1488.

Very AA, Sentenac H. 2002. Cation channels in the Arabidopsis plasma membrane. *Trends Plant Sci* **7**(4): 168-175.

Vlad F, Rubio S, Rodrigues A, et al. 2009. Protein phosphatases 2C regulate the activation of the Snf1-related kinase OST1 by abscisic acid in Arabidopsis. *Plant Cell* **21**(10): 3170-3184.

Voss LJ, Hedrich R, Roelfsema MRG. 2016. Current injection provokes rapid expansion of the guard cell cytosolic volume and triggers Ca^{2+} signals. *Mol Plant* **9**(3): 471-480.

Voss LJ, McAdam SAM, Knoblauch M, et al. 2018. Guard cells in fern stomata are connected by plasmodesmata, but control cytosolic Ca^{2+} levels autonomously. *New Phytol* **219**(1): 206-215.

Waadt R, Krebs M, Kudla J, et al. 2017. Multiparameter imaging of calcium and abscisic acid and high-resolution quantitative calcium measurements using R-GECO1-mTurquoise in Arabidopsis. *New Phytol.* **216**(1): 303-320.

Wang K, He J, Zhao Y, et al. 2018. EAR1 negatively regulates ABA signaling by enhancing 2C protein phosphatase activity. *Plant Cell* **30**(4): 815-834.

Wang XP, Chen LM, Liu WX, et al. 2016. AtKC1 and CIPK23 synergistically modulate AKT1-mediated low-potassium stress responses in Arabidopsis. *Plant Physiol.* **170**(4): 2264-2277.

Wang Y, Chen ZH, Zhang B, et al. 2013a. PYR/PYL/RCAR abscisic acid receptors regulate K^+ and Cl^- channels through reactive oxygen species-mediated activation of Ca^{2+} channels at the plasma membrane of intact Arabidopsis guard cells. *Plant Physiol.* **163**(2): 566-577.

Wang Y, Dindas J, Rienmuller F, et al. 2015. Cytosolic Ca^{2+} signals enhance the vacuolar ion conductivity of bulging Arabidopsis root hair cells. *Mol Plant* **8**(11): 1665-1674.

Wang Y, Noguchi K, Ono N, et al. 2014. Overexpression of plasma membrane H^+-ATPase in guard cells promotes light-induced stomatal opening and enhances plant growth. *Proc. Natl. Acad. Sci. U. S. A.* **111**(1): 533-538.

Wang YF, Munemasa S, Nishimura N, et al. 2013b. Identification of cyclic GMP-activated nonselective Ca^{2+}-permeable cation channels and associated CNGC5 and CNGC6 genes in Arabidopsis guard cells. *Plant Physiol.* **163**(2): 578-590.

Wernimont AK, Amani M, Qiu W, et al. 2011. Structures of parasitic CDPK domains point to a common mechanism of activation. *Proteins* **79**(3): 803-820.

Westlake TJ, Ricci WA, Popescu GV, et al. 2015. Dimerization and thiol sensitivity of the salicylic acid binding thimet oligopeptidases TOP1 and TOP2 define their functions in redox-sensitive cellular pathways. *Front Plant Sci* **6**: 327.

Wheeler GL, Brownlee C. 2008. Ca^{2+} signalling in plants and green algae-changing channels. *Trends Plant Sci* **13**(9): 506-514.

Wille AC, Lucas WJ. 1984. Ultrastructural and histochemical studies on guard cells. *Planta* **160**(2): 129-142.

Willmer C, Fricker M. 1996. *Stomata*: Springer Netherlands.

Xu J, Li HD, Chen LQ, et al. 2006. A protein kinase, interacting with two calcineurin B-like proteins, regulates K^+ transporter AKT1 in Arabidopsis. *Cell* **125**(7): 1347-1360.

Xue S, Hu H, Ries A, et al. 2011. Central functions of bicarbonate in S-type anion channel activation and OST1 protein kinase in CO_2 signal transduction in guard cell. *EMBO J.* **30**(8): 1645-1658.

Yadav AK, Jha SK, Sanyal SK, et al. 2018. Arabidopsis calcineurin B-like proteins differentially regulate phosphorylation activity of CBL-interacting protein kinase 9. *Biochem. J.* **475**(16): 2621-2636.

Yang Y, Costa A, Leonhardt N, et al. 2008. Isolation of a strong Arabidopsis guard cell promoter and its potential as a research tool. *Plant Methods* **4**: 6.

Ye W, Adachi Y, Munemasa S, et al. 2015. Open Stomata 1 kinase is essential for yeast elicitor-induced stomatal closure in Arabidopsis. *Plant Cell Physiol.* **56**(6): 1239-1248.

Ye Y, Zhou L, Liu X, et al. 2017. A novel chemical inhibitor of ABA signaling targets all ABA receptors. *Plant Physiol.* **173**(4): 2356-2369.

Yin P, Fan H, Hao Q, et al. 2009. Structural insights into the mechanism of abscisic acid signaling by PYL proteins. *Nat. Struct. Mol. Biol.* **16**(12): 1230-U1242.

Yoshida R, Hobo T, Ichimura K, et al. 2002. ABA-activated SnRK2 protein kinase is required for dehydration stress signaling in Arabidopsis. *Plant Cell Physiol.* **43**(12): 1473-1483.

Yoshida R, Umezawa T, Mizoguchi T, et al. 2006. The regulatory domain of SRK2E/OST1/SnRK2.6 interacts with ABI1 and integrates abscisic acid (ABA) and osmotic stress signals controlling stomatal closure in Arabidopsis. *J. Biol. Chem.* **281**(8): 5310-5318.

Yoshida T, Fujita Y, Sayama H, et al. 2010. AREB1, AREB2, and ABF3 are master transcription factors that cooperatively regulate ABRE-dependent ABA signaling involved in drought stress tolerance and require ABA for full activation. *Plant J.* **61**(4): 672-685.

Young JJ, Mehta S, Israelsson M, et al. 2006. CO_2 signaling in guard cells: Calcium sensitivity response modulation, a Ca^{2+}-independent phase, and CO_2 insensitivity of the gca2 mutant. *Proc. Natl. Acad. Sci. U. S. A.* **103**(19): 7506-7511.

Yuan F, Wang M, Hao H, et al. 2013. Negative regulation of abscisic acid signaling by the Brassica oleracea ABI1 ortholog. *Biochem. Biophys. Res. Commun.* **442**(3-4): 202-208.

Yuan F, Yang H, Xue Y, et al. 2014. OSCA1 mediates osmotic-stress-evoked Ca^{2+} increases vital for osmosensing in Arabidopsis. *Nature* **514**(7522): 367-371.

Yunta C, Martinez-Ripoll M, Zhu JK, et al. 2011. The structure of Arabidopsis thaliana OST1 provides insights into the kinase regulation mechanism in response to osmotic stress. *J. Mol. Biol.* **414**(1): 135-144.

Zelitch I. 1963. The control and mechanism of stomatal movement. In: Stomata and Water Relations in Plants. *Conn. Agr. Expt. Sta. Bull.*: 664.

Zelitch I, Walker DA. 1964. The role of glycolic acid metabolism in opening of leaf stomata. *Plant Physiol.* **39**(5): 856-862.

Zhang A, Ren HM, Tan YQ, et al. 2016. S-type anion channels SLAC1 and SLAH3 function as essential negative regulators of inward K^+ channels and stomatal opening in Arabidopsis. *Plant Cell* **28**(4): 949-955.

Zhang J, Wang N, Miao Y, et al. 2018a. Identification of SLAC1 anion channel residues required for CO_2/bicarbonate sensing and regulation of stomatal movements. *Proc. Natl. Acad. Sci. U. S. A.* ***115****(44), 11129-11137.*

Zhang M, Wang D, Kang Y, et al. 2018b. Structure of the mechanosensitive OSCA channels. *Nat. Struct. Mol. Biol.* **25**(9): 850-858.

Zhang X, Wang H, Takemiya A, et al. 2004. Inhibition of blue light-dependent H^+ pumping by abscisic acid through hydrogen peroxide-induced dephosphorylation of the plasma membrane H^+-ATPase in guard cell protoplasts. *Plant Physiol.* **136**(4): 4150-4158.

Zhang XR, Henriques R, Lin SS, et al. 2006. Agrobacterium-mediated transformation of Arabidopsis thaliana using the floral dip method. *Nat. Protoc.* **1**(2): 641-646.

Zhang Z, Liu X, Wang X, et al. 2012. An R2R3 MYB transcription factor in wheat, TaPIMP1, mediates host resistance to Bipolaris sorokiniana and drought stresses through regulation of defense- and stress-related genes. *New Phytol* **196**(4): 1155-1170.

Zhao R, Sun HL, Mei C, et al. 2011a. The Arabidopsis Ca^{2+}-dependent protein kinase CPK12 negatively regulates abscisic acid signaling in seed germination and post-germination growth. *New Phytologist* **192**(1): 61-73.

Zhao Y, Araki S, Wu J, et al. 2011b. An expanded palette of genetically encoded Ca^{2+} indicators. *Science* **333**(6051): 1888-1891.

Zhao YX, Araki S, Jiahui WH, et al. 2011c. An expanded palette of genetically encoded Ca^{2+} indicators. *Science* **333**(6051): 1888-1891.

Zhu J-K. 2016. Abiotic stress signaling and responses in plants. *Cell* **167**(2): 313-324.

Zhu SY, Yu XC, Wang XJ, et al. 2007. Two calcium-dependent protein kinases, CPK4 and CPK11, regulate abscisic acid signal transduction in Arabidopsis. *Plant Cell* **19**(10): 3019-3036.

Zou JJ, Li XD, Ratnasekera D, et al. 2015. Arabidopsis calcium-dependent protein kinase 8 and catalase 3 function in abscisic acid-mediated signaling and H_2O_2 homeostasis in stomatal guard cells under drought stress. *Plant Cell* **27**(5): 1445-1460.

Zou JJ, Wei FJ, Wang C, et al. 2010. Arabidopsis Calcium-Dependent Protein Kinase CPK10 functions in abscisic acid- and Ca^{2+}-mediated stomatal regulation in response to drought stress. *Plant Physiol.* **154**(3): 1232-1243.

6. Acknowledgments

In the past four years of Ph.D. study, I sincerely feel that I am a lucky guy, because I was luckily supervised by PD Dr. M. Rob. G Roelfsema. He guided me step by step to the wonderful world of science. There is no doubt that every progress I achieved is indispensable with his contribution and support. I thank him for his professional competence and good care for my Ph.D. study and thesis writing. I also appreciate his kind, compatibility, trust, and patience. I enjoy the time working with him. He is an excellent supervisor.

My special thank goes to the pioneering scientist in plant electrophysiology, Prof. Dr. Rainer Hedrich, my second supervisor, who put forward the fantastic ideas and provided construct discussion for my study. As the head of the institute, he not only provides the art of state platform but also creates a very nice scientific atmosphere for us.

I would like to deliver my thanks to my third supervisor Prof. Dr. Wolfgang Dröge-Laser (Department of Pharmaceutical Biology, University of Wuerzburg). I gained fresh thinking from him in the annual meeting. I would also like to thank Prof. Dr. Dietmar Geiger, who is an indispensable collaborator/supervisor for the CIPK23 study. I got the training of the molecular biology and heterologous expression system from him.

Besides, my study also got lots of the advice and support from my colleagues and collaborators: Sohail Karimi (qPCR), Dr. Tobias Maierhofer (CIPK23 experiment design, data analysis), Michael Geringer (protein interaction), Prof. Dr. Jörg Kudla (University of Münster, Germany. CIPK23 data analysis and discussion, provided CBL1-OST1 construct), Prof. Dr. Yi Wang (SKLPPB, China Agricultural University, China. provided *lks1-3*, LKS,OE and CBL seeds). Dr. Rainer Waadt (COS, Heidelberg University, Germany. provided the R-GECO1-mTurquoise construct and seed). Dr. Mark D. Curtis (Cell & Gene Technologies at Lonza, Switzerland, provided the original estrogen-induced constructs). I would also like to thank other colleagues in the Department of Molecular Plant Physiology and Biophysics.

I am gratitude China Scholarship Council (CSC) for providing me the stipend, which makes it possible for me to study in Germany.

My great appreciation goes to my wife, Miss Yu Xia, and also our parents. Thank their endless support for my Ph.D. study and take care of my son, DeWei. Thank for our luck which makes us meet here.

Shouguang Huang

01.01.2020, Würzburg, Germany

7. Appendix

7.1 Primers

	For pLB12 construct modification
pLB12 fwd1	GGCTTAAUCGCAAACTAGGATAA
pLB12 rev1	ATTTAAATGGAUCCATTTAAATCGCCTCAGCCAGGTATATATCTCCTTCTTAAAGTT
pLB12 fwd2	ATCCATTTAAAUGACCTCAGCTGTACAAAGTGGTTGATAATTCC
pLB12 rev1	GGTTAAUTCGGAAATGACAATC
pGC1 fwd	GGGGACAAGTTTGTACAAAAAAGCAGGCTATGGTTGCAACAGAGAGGATGA
pGC1 rev	GGGGACCACTTTGTACAAGAAAGCTGGGTATTTCTTGAGTAGTGATTTTGAA
CIPK23 user fwd	GGCTTAAUATGGCTTCTCGAACAACGCCTTC
CIPK23 user oS rev	GGTTTAAUTTATGTCGACTGTTTTGCAATTG
CIPK23 user rev	GGTTTAAUTTATGTCGACTGTTTTGCAATTG
CIPK23 SwaI fwd	GGCGATTUCGATGGCTTCTCGAACAACGCC
YFP/mCh SwaI rev	GGTCATTUTTACTTGTACAGCTCGTCCATGC
YFP SwaI fwd	GGCGATTUCGATGGTGAGCAAGGGCGAGGA
	For creating CIPK23$^{T190+V182K}$ ΔC
CIPK23 V182K user fwd	AGCAAAAACGUGAGGATGGGTTACTTCACACAAC
CIPK23 V182K user rev	ACGTTTTTGCUGAGGTAGAGCGCTCA
CIPK23 T332* user rev	GGTTTAAUTCATACTGGTGTTTTGAGTCCTTCTTC
	For RT-qPCR
CIPK23 fwd	GGACATTGTTTGGAAAACC
CIPK23 red	TTAATCGATTCAAGCCAAG
Venus fwd	CTTCTTCAAGGACGACGG
Venus rev	GATGTTGTGGCGGATCT
AKT1 fwd	ACCTATACTCAAAACCG
AKT1 rev	GAACCCAATTCTAGCA
SLAC1 fwd	CCGGGCTCTAGCACTCA
SLAC1 rev	TCAGTGATGCGACTCTT
SLAH3 fwd	GGTCCTATGTGCCATTG
SLAH3 rev	ATCATTACTCTGACTGC
actin2/8 fwd	GGTGATGGTGTGTCT
actin2/8 rev	ACTGAGCACAATGTTAC

7.2 Publications

Publications that have arisen during this work

Huang S, Waadt R, Nuhkat M, Kollist H, Hedrich R, Roelfsema MRG. 2019. Calcium Signals in Guard Cells Enhance the Efficiency by Which Abscisic Acid Triggers Stomatal Closure. *New Phytologist* **224** (1): 177-187.

Publications not associated with this doctoral thesis

Nguyen TH, Huang S, Meynard D, Chaine C, Michel R, Roelfsema MRG, Guiderdoni E, Sentenac H, Very AA. 2017. A Dual Role for the OsK5.2 Ion Channel in Stomatal Movements and K^+ Loading into Xylem Sap. *Plant Physiology* **174**(4): 2409-2418.

Forster S, Schmidt LK, Kopic E, Anschutz U, Huang S, Schlucking K, Koster P, Waadt R, Larrieu A, Batistic O, Rodriguez PL, Grill E, Kudla J, Becker D. 2019. Wounding-Induced Stomatal Closure Requires Jasmonate-Mediated Activation of GORK K^+ Channels by a Ca^{2+} Sensor-Kinase CBL1-CIPK5 Complex. *Developmental Cell* **48**(1): 87-99 e86.

Liu Y, Maierhofer T, Rybak K, Sklenar J, Breakspear A, Johnston MG, Fliegmann J, Huang S, Roelfsema MRG, Felix G, Faulkner C, Menke F, Geiger D, Hedrich R, Robatzek S. 2019. Anion Channel SLAH3 is A Regulatory Target of Chitin Receptor-Associated Kinase PBL27 in Microbial Stomatal Closure. *eLife* **8**: e44474. DOI: 10.7554/eLife.44474

Conference/poster

Huang S, Hedrich R, Roelfsema MRG. 2019. ABA-Induced Ca^{2+} Signals in Guard Cells Enhance the Stomatal Closure. 18th International Workshop on Plant Membrane Biology, Glasgow 7th – 12th July. **Awarded the Poster prize**.

7.3 Affidavit

I hereby declare that my thesis entitled: „Role of ABA-induced Ca^{2+} signals, and the Ca^{2+}-controlled protein kinase CIPK23, in regulation of stomatal movements" is the result of my own work. I did not receive any help or support from commercial consultants. All sources and/or materials applied are listed and specified in the thesis.

Furthermore, I verify that the thesis has not been submitted as part of another examination process neither in identical nor in similar form.

Besides I declare that if I do not hold the copyright for figures and paragraphs, I obtained it from the rights holder and that paragraphs and figures have been marked according to law or for figures taken from the internet the hyperlink has been added accordingly

Eidesstattliche Erklärung

Hiermit erkläre ich an Eides statt, die Dissertation: „Rolle von ABA-abhängigen Ca^{2+} Signalen, und der Ca^{2+}-gesteuerten Proteinkinase CIPK23, bei der Regulation der Spaltöffnungsbewegungen", eigenständig, d. h. insbesondere selbständig und ohne Hilfe eines kommerziellen Promotionsberaters, angefertigt und keine anderen, als die von mir angegebenen Quellen und Hilfsmittel verwendet zu haben.

Ich erkläre außerdem, dass die Dissertation weder in gleicher noch in ähnlicher Form bereits in einem anderen Prüfungsverfahren vorgelegen hat.

Weiterhin erkläre ich, dass bei allen Abbildungen und Texten bei denen die Verwer-tungsrechte (Copyright) nicht bei mir liegen, diese von den Rechtsinhabern eingeholt wurden und die Textstellen bzw. Abbildungen entsprechend den rechtlichen Vorgaben gekennzeichnet sind sowie bei Abbbildungen, die dem Internet entnommen wurden, der entsprechende Hypertextlink angegeben wurde

Würzburg, _____

_____

Unterschrift/Signature